**Prolonging the Useful Lifetime of Artificial Lungs**

Submitted in partial fulfillment of the requirements for

the degree of

Doctor of Philosophy

in

Biomedical Engineering

Caitlin T. Demarest

B.S., Biophysics, The University of Scranton
M.D., New York Medical College

Carnegie Mellon University
Pittsburgh, PA

May, 2017

**Acknowledgments**

This dissertation and the research it encompasses could not have been completed without the guidance and support of many people. I would like to thank my doctoral committee members for their guidance over the years: Dr. James F. Antaki, Dr. Matthew D. Bacchetta, Dr. Keith E. Cook, and Dr. Conrad M. Zapanta. A great deal of thanks goes to my advisor, and chair of this committee, Dr. Keith E. Cook, whose guidance and encouragement over the past three years have been instrumental to the completion of this work. An additional thanks goes to Dr. Bacchetta, who encouraged me to come to Carnegie Mellon University and pursue this Ph.D.

I would also like to thank all the undergraduate students, graduate students, and laboratory technicians at Carnegie Mellon University and Allegheny General Hospital who spent countless hours manufacturing devices and assisting with experiments over the years. I have truly enjoyed working with all of my fellow graduate students and lab mates; without your assistance I never could have completed this work. Additionally, this research could not have been completed without the financial support of the American Heart Association (14PRE20380061) and the National Institutes of Health (2R01HL089043).

Lastly, I would like to thank my friends and family for your unwavering support throughout the past 10 years of post-graduate training, especially these past three years while I pursued this research.

**Abstract**

Over 26 million Americans suffer from pulmonary disease, resulting in more than 150,000 deaths annually. Lung transplantation remains the only definitive treatment for many patients, but has meager survival rates and only approximately 1,700 of the 2,200 patients added to the lung transplant wait list each year are transplanted. Extracorporeal gas exchangers have been used as an alternative to mechanical ventilation in acute respiratory failure and as a bridge to transplantation in chronic respiratory failure. Current gas exchangers are limited by their high resistance and low biocompatibility that lead to patient complications and device clot formation. Therefore, there exists a dire need for improved devices that can act as destination therapy.

To accomplish the goal of destination therapy, this dissertation discusses three studies that were performed to pave the way. First, I examined clot formation and failure patterns of two common clinical devices (Maquet's CardioHelp (CH) and Quadrox (Qx)) to further our understanding of their limitations with respect to long-term support. Overall, it was demonstrated that the Qx devices fail earlier and more frequently than CH devices and result in a significantly greater reduction in platelet count, and that a four-inlet approach is beneficial. Next, I determined the optimal sweep gas nitric oxide (NO) concentration that minimizes platelet binding and activation while ensuring that blood methemoglobin (metHb) concentrations increase less than 5%. Miniature artificial lungs were attached to rabbits in a pumped veno-venous configuration and run for 4 h with NO added to the sweep gases in concentrations of 0, 100, 250, and 500 ppm (n=8 ea.). 100 ppm significantly reduced the amount of platelet consumption ($p < 0.05$), reduced platelet activation as measured by soluble p-selectin ($p < 0.05$), and had negligible increases in metHb and will thus be used in future experiments. Last, I tested the Pulmonary Assist Device (PAD) which was designed for long term use as a bridge to transplantation and destination therapy. Benchtop

experiments were performed that confirmed that it meets our design and performance goals. From here, we are equipped to commence with 30-day PAD testing in sheep.

**Table of Contents**

**List of Tables**

**List of Figures and Illustrations**

## Chapter 1: Background

Over 26 million Americans suffer from various forms of pulmonary disease including chronic obstructive pulmonary disease (COPD), cystic fibrosis (CF), idiopathic pulmonary fibrosis (IPF), and adult respiratory distress syndrome (ARDS).[1] This results in $173 billion in health-care expenditures and more than 150,000 deaths annually.[2] Lung transplantation remains the only definitive treatment for many patients, but only approximately 1,700 of the 2,200 patients added to the lung transplant wait list each year are transplanted.[2,4] Furthermore, 3- and 5-year survival rates are 70% and 55%, the worst of any transplanted organ.[5] Extracorporeal membrane oxygenation (ECMO) may serve as a temporary bridge to recovery or transplant but is not suitable for routine support beyond a few months due to a multitude of progressive complications, most commonly related to clotting and thromboembolic complications leading to device failure.[6] Ultimately, hundreds of thousands of patients have severe, end-stage lung disease but are not transplant candidates and continue to be burdened by continuous home oxygen requirements, frequent and costly hospitalizations, and no restorative therapies. If clot formation could be prevented and device longevity improved, with less frequent device-related complications, disease exacerbations, and hospitalizations, this would improve patients' quality of life and decrease healthcare expenditures.

### 1.1 Respiratory failure: Epidemiology and Pathophysiology

#### *1.1.1 Respiratory failure*

The lungs provide a wide variety of functions ranging from immunogenic to air filtration and gas exchange. Respiratory failure is typically due to a failure of the gas exchange capabilities of the lungs, characterized by an inability to add oxygen ($O_2$) to or remove carbon dioxide ($CO_2$)

from the blood.[7] Respiratory failure may be chronic, such as in COPD, or acute, such as in ARDS, but both are characterized by inadequate alveolar ventilation due to airway collapse or obstruction, insufficient alveolar gas exchange due to edema, inflammation with exudates or atelectasis, impeded perfusion, or a combination of the above.[7] Type I respiratory failure describes significant hypoxemia without much $CO_2$ retention, whereas Type II is defined as hypoxemia with substantial hypercapnia.[8] IPF and ARDS are Type I (hypoxemic) respiratory failure, whereas COPD is Type II (hypercapnic) respiratory failure, although all diseases have some degree of both hypoxia and hypercapnea. Regardless of the etiology, the treatment goals for all types of respiratory failure are the same: 1) ensure adequate alveolar ventilation and oxygenation, and 2) treat the primary condition, if possible.[8]

### *1.1.2 Acute Respiratory failure*

Acute respiratory failure is the most common organ failure diagnosed in the intensive care unit (ICU) and includes acute lung injury (ALI) and, its more severe form, ARDS. ALI is characterized by the acute onset of dyspnea with hypoxia, bilateral pulmonary infiltrates, and lack of left heart failure. ARDS is characterized by diffuse alveolar damage with profuse exudates causing severe hypoxemia that is unresponsive to oxygen therapy.[9,10] There are 50,000 cases of ARDS per year in the United States[11] and a mortality rate of up to 45%.[12] ARDS is caused by an acute inflammatory lung injury due to a wide variety of insults to the lung, such as toxic inhalation, sepsis, or trauma, with sepsis causing the greatest mortality.[7] Mechanical ventilation is insufficient in ARDS management because the high fraction of inspired oxygen ($FiO_2$) and airway pressures needed to adequately ventilate these patients may exacerbate lung injury and cause oxygen toxicity, barotrauma, and other complications.[7,13]

The only type of ventilation that has been proven in a randomized controlled trial to improve outcomes in adults with ARDS is the use of low tidal volume and low-pressure lung protective ventilation (LPV), which is the current standard of care for ARDS patients.[14,15] LPV reduces inflammation, ventilator induced lung injury, and duration of non-pulmonary organ failure in the ICU.[16,17] The benefits of LPV were first recognized in 2000 when a low tidal volume of 6mL/kg was utilized in patients with ARDS in the landmark ARDS Network trial,[16] with LPV providing an 8.8% absolute reduction in short term mortality, and subsequent trials confirmed this benefit.[18,19] Evidence is emerging regarding the same protective benefits of LPV in all ICU patients,[20] but the first multicenter randomized controlled trial (RCT) evaluating tidal volumes from 4-6 mL/kg in patients without ARDS is underway.[15] One of the primary limitations of LPV is respiratory acidosis; traditionally, ventilation goals were to normalize pH and $PaCO_2$ regardless of pulmonary pressures, but with LPV, the opposite is true, and the primary focus is on decreasing injurious lung stretch with permissive hypercapnia.[16,21] However, patients with severe respiratory failure have such poor gas exchange that they are unable to maintain adequate ventilation with LPV, although they are the ones who would benefit from it the most.[14] As such, there has been increasing interest in and evidence for the use of ECMO in ARDS. ECMO can allow for LPV by providing a degree of gas transfer and decreasing the burden on the native lung, mitigating ventilator associated lung injury and allowing the lungs to rest and recover (see section 1.2.3).[13,22-25] Recent studies are even investigating the application "ultra"-protective tidal volumes <4 mL/mg facilitated by ECMO and their combined benefits.[26]

### *1.1.3 Chronic Respiratory failure*

Over 144,000 patients die every year in the United States from chronic respiratory failure due to chronic obstructive pulmonary disease (COPD), cystic fibrosis (CF), and idiopathic

pulmonary fibrosis (IPF).[1] Each is characterized by a progressive decline in respiratory function with right heart dysfunction from pulmonary hypertension (PH). These patients can be maintained with $O_2$ therapy and pulmonary vasodilators, but not without frequent exacerbations requiring costly hospitalizations. The only long-term treatment is lung transplantation, but with only 1,700 transplants/year[4], most patients decompensate and die without access to a donor lung or means of long-term respiratory support.

*Chronic Obstructive Pulmonary Disease (COPD)*

COPD causes a significant social and economic burden, afflicting 14.8 million Americans and is the third most common cause of death in the United States.[2,9,27] COPD is an umbrella term that includes both chronic bronchitis and emphysema, although the two typically coexist.[10] Emphysema is characterized by abnormal enlargement of terminal airspaces with destruction of their walls, and chronic bronchitis results in mucus hypersecretion and bronchiolar wall inflammation and fibrosis.[10] Together, they are characterized by chronic respiratory insufficiency due to an irreversible airflow obstruction resulting in airflow limitations and air trapping, gas exchange abnormalities, and pulmonary hypertension.[27] Patients suffer from progressive dyspnea, often with cough and copious sputum production, and gas exchange insufficiency causing hypoxemia and hypercapnia.[27] The disease is most widespread in smokers and those with chronic pollution exposure, and its prevalence is increasing.[28] Treatment for COPD patients includes smoking cessation, chronic home oxygen therapy, inhaled bronchodilators and corticosteroids, and oral mucolytics, anti-inflammatories, and steroids.[27] Despite treatment, COPD results in significant chronic morbidity and patients are burdened by recurring exacerbations and complications, necessitating costly medications and hospitalizations. In the United States alone, the cost of COPD is estimated to be $52.4 billion, with the majority of expenditures occurring during frequent

exacerbations.[29] During exacerbations, stable patients are typically treated with noninvasive ventilation (NIV), but mortality during COPD exacerbations is reported to be as high 16%.[8]

Surgical options for the symptomatic treatment of COPD include lung volume reduction surgery (LVRS), bullectomy, and lung transplantation.[30] Removing diseased and nonfunctioning lung tissue through LVRS improves exercise performance and quality of life, but thoughtful patient selection is critical because LVRS can increase mortality in certain patients.[30] Bullectomy is reserved for patients with localized disease and empty airspace occupying at least 40-50% of one hemithorax; in these cases, the remaining functional lung is compressed by the bulla, so their removal provides benefit, but operative mortality rate is as high as 10%.[11] In the end, though, all of these treatments, including transplantation, are not curative and serve only to relieve symptoms and lessen the frequency and severity of disease exacerbations and progression, while supporting the best quality of life possible for patients and their families.

*Cystic Fibrosis (CF)*

CF is the most common lethal genetic disease that affects Caucasians; with an incidence of 1 in 3200 births in the United States and a median life expectancy of 30 years, CF results in an annual death toll of 491 persons. [2,10] CF is a disorder of epithelial transport affecting fluid secretion characterized by airway obstruction and recurrent and chronic pulmonary infections caused by the secretion of abnormally viscid mucus.[10]

The lives of CF patients are punctuated by repeated pulmonary exacerbations, which are very common and linked to reduced quality of life,[31] pulmonary decline, increased healthcare costs,[32] and decreased survival.[33,34] Despite improvements in pulmonary function and nutritional status of CF patients, there has been no reduction in the proportion of individuals with CF who experience pulmonary exacerbations; in fact, the CF Foundation National Patient Registry reported

more than 25,000 CF exacerbations in 2015, affecting more than 40% of patients with CF at least once.[35] During an exacerbation, patients present with increased cough and sputum production, dyspnea, weight loss, decrease in energy, and worsening spirometry performance.[33] The exact pathophysiology and cause of these exacerbations is not well understood, but is due to a complex interaction between the host defense and its inflammatory response with airway microbiology, viral infections, and bacterial colonization.[33] During exacerbations, CF patients have profound difficulty maintaining effective airway clearance and require ventilator support. However, endotracheal intubation with mechanical ventilation during an exacerbation has been shown to be a significant independent risk factor for death with a mortality rate of 59% (HR = 16.8, 95% CI 4.93 to 57.38, p = 0.001),[36] and only 6% of intubated patients survive to 12 months without transplantation. Alternatively, NIV can be used during acute exacerbations to correct hypoxemia,[37] bridge to lung transplantation,[38] and has been demonstrated to improve lung function and fatigue upon discharge.[39] Furthermore, survival to discharge after NIV treatment in the ICU is reported to be as high as 75%.[36,40]

Although CF affects many organ systems, the most common cause of death is cardiopulmonary complications from persistent lung infections, obstructive pulmonary disease, and pulmonary hypertension with right heart failure.[10] Despite more than 25 years of intensive research, there is not yet a cure for CF.[41] Most treatment options focus on ameliorating organ-specific sequelae of the disease, such as optimizing nutrition, thinning airway secretions, and reducing pulmonary bacterial load.[42] Most recently, cystic fibrosis transmembrane conductance regulator gene (the mutation of which is the root cause of CF) modulators have emerged which show promise, but none yet have proven to increase life expectancy and, ultimately, many patients die while awaiting a donor lung.[41,42]

*Interstitial Lung Disease (ILD)*

ILD is a heterogeneous group of disorders characterized by diffuse and chronic involvement of the pulmonary connective tissue.[10] These disorders, such as sarcoidosis and idiopathic pulmonary fibrosis (IPF), are characterized by reduced pulmonary compliance with subsequent dyspnea, hypoxia, and pulmonary hypertension and result in over 6,000 deaths per year. [2,10] All forms of ILD have poor prognosis; IPF, for example, has a mean survival of 3 years or less from the time of diagnosis.[10,43] ILD patients admitted to the ICU have a very poor prognosis, and those who develop acute respiratory failure are unlikely to benefit from extended ICU admissions.[44,45] Additionally, right heart dysfunction is common and ventilation increases the intrathoracic pressure, thereby increasing afterload on the already-strained RV.[44] Treating ILD is challenging and clinicians aim to avoid intubation with mechanical ventilation; due to severe gas exchange impairment and decreased lung compliance necessitating high $FiO_2$ and high peak pressures, the lungs are at further risk for additional damage from ventilator-associated lung injury and oxygen toxicity.[13,46] Noninvasive treatment options include high-flow $O_2$ through a nasal cannula and NIV.[47] ECMO can be utilized in ILD to reduce the oxygenation burden on the native lungs and allow for lung-protective ventilation, but still patients' native lungs do not recover and the only definitive treatment for refractory ILD remains lung transplantation.[44,48] As such, ECMO seems to be an acceptable rescue tool in bridge to lung transplantation (BTT),[44] but acute respiratory failure in ILD is devastating in patients without the option of a lung transplant.

*Pulmonary Hypertension (PH)*

The pulmonary circulation is typically low in pressure and resistance, and PH (pulmonary arterial pressure (PAP) >25 mmHg) can be devastating. Although PH can be a primary vascular disease, the vast majority of cases are secondary, caused by COPD, CF, ILD, and recurrent

pulmonary emboli.[10] The increased pulmonary pressures increase the afterload of the right ventricle, causing overload, hypertrophy, and eventual failure.[7] Pulmonary hypertensive heart failure, or *cor pulmonale* is defined as right ventricular hypertrophy and dilation due to pulmonary hypertension caused by primary diseases of the lung parenchyma or pulmonary vasculature, unrelated to the left heart, and is the leading cause of disability and death in many primary lung diseases.[10,49,50] The five-year survival rate of COPD patients with PAP >20 mmHg is approximately 50% and COPD is likely responsible for 80% of all cor pulmonale cases.[50,51]

## 1.2 Current Treatment Modalities and Their Limitations

### *1.2.1 Mechanical Ventilation*

*Indications*

The general indications for mechanical ventilation include: 1) inadequate oxygenation despite increasing oxygen supplementation, 2) increased $Pa_{CO2}$ associated with decreased mental status, and 3) failure to control secretions.[8] Traditionally, most patients in the ICU were intubated and mechanically ventilated, but as increasing evidence emerges regarding diminished outcomes with mechanical ventilation, centers worldwide have adjusted their ventilator management algorithms accordingly.

*Complications and Limitations*

Complications of mechanical ventilation include muscle atrophy, respiratory and systemic inflammation, multi-organ failure, barotrauma, oxygen toxicity, gastric ulcers with gastrointestinal bleeding, nosocomial pneumonia, and poor outcomes after transplantation.[8,13,52-55]

The primary goal in most forms of respiratory failure is to provide oxygenation, but there is a limit to how much $O_2$ can be delivered before $O_2$ toxicity develops. The amount of $O_2$ delivered

by the ventilator is measured as fraction of inspired oxygen ($FiO_2$), and prolonged high $FiO_2$ results in diminished gas exchange, decreased ciliary activity, bronchitis, and atelectasis, oftentimes worsening lung injury.[46,56]

Mechanical ventilation may result in repetitive overstretching of lung tissue, which causes disruption of the pulmonary endothelium, lung inflammation, atelectasis, and the release of inflammatory mediators.[15,16,57] Pulmonary barotrauma occurs when rupture of the alveolar walls adjacent to pulmonary vessels results in the development of extra-alveolar air. Barotrauma is associated with greatly increased morbidity and mortality, particularly in patients with severe underlying lung disease, specifically ARDS and ILD.[13,58] The incidence of barotrauma increases with disease severity, occurring up to 87% of the time in patients with ARDS.[59] While inadequate PEEP leads to further decreases in pulmonary compliance, high PEEP is an independent predictor for mortality, with mechanical ventilation-induced barotrauma contributing to high mortality (70-90%).[60]

Lastly, ventilator-associated pneumonia (VAP) is the most common infection in critically ill patients receiving mechanical ventilation, developing in approximately 20% of patients due to the presence of an endotracheal tube (ETT).[61] The ETT allows access to the lower respiratory tract, impairing the cough reflex and mucociliary reflex with resultant microaspiration and biofilm formation.[53,55,62] ICU patients who develop VAP have increased morbidity and hospitalization length (ICU stay 11.7 days vs. 5.6 days, $p < 0.001$) and cost (>$40,000 increase in charges, $p < 0.001$) compared to those without.[52,54,62] Furthermore, a large meta-analysis of 24 trials of VAP reported the overall attributable mortality due to VAP in the ICU is 13%, although it was as high as 69% in surgical patients.[63]

### *1.2.2 Noninvasive Ventilation*

Noninvasive ventilation (NIV) refers to the delivery of ventilator support or positive pressure into the lungs without an endotracheal tube, typically through a mask.[64] There are two primary NIV modes: continuous positive airway pressure (CPAP) and noninvasive positive pressure ventilation (NIPPV). CPAP applies a continuous positive pressure, increasing the amount of air in the lungs on expiration. NIPPV, the most common form of which is BiPAP, is used more often clinically; it provides both inspiratory and expiratory support and requires a ventilator.[65] NIV has demonstrated improved outcomes in respiratory failure with decreased complications as compared to mechanical ventilation, including barotrauma and VAP, and is currently the first-line management option for respiratory failure in many settings.[65] Indications include acute exacerbations of COPD, acute cardiac pulmonary edema, asthma, community-acquired pneumonia, and ARDS.[65]

### *1.2.3 ECMO*

In all of the disease states listed above, ECMO is playing an increasing role. During ECMO, blood is removed, oxygenated, has its $CO_2$ removed, then returned to the body. ECMO was long deemed insufficient as a bridge to lung transplantation due to poor outcomes. [66] However, the success of ECMO is increasing as cannulae and oxygenator technology advances and medical management of ECMO patients improves.

Furthermore, a change in Lung Allocation Scores has shortened wait list times, reducing the period of support required by a ECMO bridge to transplantation. However, median wait list times while on ECMO are thus typically 3-12 days, and 15% of patients still die while waiting.[6,67-69] As such, there exists a great need for an artificial lung that could successfully bridge patients to transplantation who otherwise would die awaiting transplant, support a patient post-transplantation

until recovery, or, ideally, function as a destination therapy device. Obstacles to artificial lung development include designing a device small enough to be worn at the patient's belt that 1) has no more surface area than currently available oxygenators ($1.8m^2$), 2) provides sufficient gas exchange, 3) is low in resistance to decrease pump speed in peripheral venovenous ECMO and therefore reduce blood damage, as well as not overload the heart in cases of central ECMO attachment (see below), and 4) has low blood velocities to avoid shear-induced blood damage and activation, but not so low that there is stasis and thrombosis forms.[70]

*History and Evidence for Use*

ECMO for adults with respiratory failure was initially fraught with complications and failure, but recent advancements in technology, evidence, and experience have broadened its applicability and usability.[23] The first randomized controlled trial (RCT) of ECMO was conducted by the National Institutes of Health during the initiation of ECMO in the 1970s,[66] but survival was only 10%, and ECMO provided no survival benefit over conventional management. The next RCT focused on extracorporeal $CO_2$ removal ($ECCO_2R$, see below) and also demonstrated no survival benefit. However, both of these studies employed management strategies vastly different from those in practice today (such as maximum anticoagulation, VA ECMO for purely pulmonary disease, and high pressure ventilation) so their results are no longer relevant and most pertinent data to date is observational. The first large case series to report ECMO success was from 1997 and reported 1000 patients supported on VV ECMO for respiratory failure and there was survival to discharge in 56% of adult patients.[71] As of today, the Extracorporeal Life Support Organization Registry International Summary reports a survival to discharge of 58%.[72]

In 2010, the CESAR (Conventional Ventilation or ECMO for Severe Adult Respiratory Failure) trial, a multicenter RCT was published that compared the rates of death and severe

disability at 6 months following conventional management versus ECMO in ARDS.[14] It is the only RCT evaluating ECMO in ARDS, and its results are promising. Patients were 18-65 years of age with severe, but potentially reversible, respiratory failure. A total of 68 patients underwent ECMO and 87 patients underwent conventional management (CM). Fewer patients in the ECMO arm than in the CM arm had died or were severely disabled 6 months later (36.7% versus 52.9%, $p = 0.030$).

*Cannulation Strategies*

There are two primary modes of ECMO cannulation: venovenous (VV) and venoarterial (VA). VV ECMO is used for pure respiratory failure; blood is drained from the venous system, oxygenated, and returned to the venous system, decreasing the need for native lung oxygenation capability. In VA ECMO, blood is drained from the venous system, oxygenated, and returned to the arterial system, thereby providing pulmonary and cardiac support.[73] If VV or VA ECMO are not providing sufficient oxygenation, a third venous cannula can be inserted for VVV or VAV ECMO; similarly, if there is a new decline in cardiac function, VV ECMO can be converted to VAV ECMO to provide cardiac support.

Cannulae were traditionally inserted into the femoral vessels, but recent improvements have allowed for upper body percutaneous cannulation.[73] For example, a double lumen cannula can be inserted into the right internal jugular vein, where blood is drained from the superior and inferior vena cavae, oxygenated, and reinfused into the right atrium.[70] The benefit of this cannulation is that all blood is pumped through the native circulation following oxygenation, allowing for the important metabolic and filtering functions of the lungs.[74]

In addition to cannulae, synthetic grafts can also be utilized for ECMO attachment. Grafts are typically anastomosed in an end-to-side fashion and attached to the ECMO circuit. This process is more invasive than the percutaneous approach and is generally reserved for central cannulation

directly into the aorta and right atrium. Central cannulation provides the benefits of larger cannulas with better flows and antegrade blood flow to the arch vessels and coronaries, but is far more invasive than percutaneous peripheral cannulation.[73] One peripheral application of grafts that has demonstrated success is during upper body VA ECMO using the subclavian artery.[75] A graft is attached, end-to-side, to the subclavian artery, a counterincision is made, and an arterial cannula is tunneled and inserted into the graft in a sleeve-like fashion. Although more complex, this cannulation strategy allows a patient on VA ECMO to be ambulatory, avoids both short- and long-term complications associated with percutaneous cannulation of the subclavian artery. Furthermore, the patient can be decannulated at the bedside with simple transection of the arterial graft. Such an approach using grafts and tunneling would be particularly useful in a destination therapy device.

*Contemporary Indications*

There are cardiac indications for ECMO, respiratory indications, and those that are mixed. In terms of respiratory failure, the most common indications include ARDS, pneumonia, trauma, or primary graft failure following lung transplantation.[73] When deciding whether to initiate ECMO, the likelihood of organ recovery must be considered. If the organ failure is reversible with treatment and rest on ECMO, then the patient could benefit from ECMO as a bridge to recovery (BTR). If there is no hope of lung recovery, then the patient must be a transplant candidate to be bridged to transplantation (BTT), otherwise initiation of ECMO can only end in patient death and is therefore not indicated.[73] Currently, the most common indication for ECMO is ARDS with severe hypoxemia, and uncompensated hypercapnia with acidemia.[23] During ECMO, ventilator settings can be reduced, allowing for LPV in ARDS patients and resting the lungs to promote recovery. However, the ability of ECMO to remove $CO_2$ at lower blood flow rates with smaller

cannulae has begun to expand ECMO's indications to include mild ARDS, COPD exacerbations, and patients awaiting a lung transplantation as a BTT (see below).[76]

*Early Mobilization*

It is known that critically ill patients who receive early rehabilitation have better outcomes and shorter hospitalizations.[77,78] Until recently, ECMO patients were considered too unstable for ambulation. With improvements in technology and cannulation strategies, though, ECMO patients can now be weaned from mechanical ventilation, extubated, and may participate in physical therapy.[79-81] This early mobilization is extremely beneficial as the length of ECMO treatment continues to increase, particularly for patients being bridged to transplantation. Abrams et al.[79] have been able to initiate intensive physical therapy programs for more than 40% of their ECMO patients, and they have been successful in extubating 66% of them, despite the high severity of illness in their patient population. Hoopes et al.[82] have also been able to wean all patients off sedation after ECMO initiation, with evaluation by a multidisciplinary team involving physical and occupational therapy, respiratory therapy, speech pathology, and a nutritionist, and patients are assisted by the team to begin ambulation. Not only is ambulation in ECMO feasible, one case series out of Duke University[83] compared to patients who did not participate in physical therapy and ambulation during BTT to those that did. Pre-transplant patients receiving rehabilitation and ambulation had short mean duration of posttransplant mechanical ventilation (4 d vs 34 d, P = .01), ICU stay (11 d vs 45 d, P = .01), and hospital stay (26 d vs 80 d, P = .01). Furthermore, no subject who participated in active rehabilitation had post-transplant myopathy, compared to 3 of 4 subjects who did not participate in pre-transplant rehabilitation on ECMO. Additionally, ambulatory ECMO has been shown to have a 22% ($60,204) reduction in total hospital cost, 73% ($104,939) reduction in post-transplant ICU cost, and 11% ($32,133) reduction in total cost compared with

non-ambulatory ECMO subjects. However, there are limitations to these retrospective reviews, including selection bias and confounders, and, although the benefit of active rehabilitation seems intuitive, additional confirmatory studies are needed.

*Extracorporeal $CO_2$ Removal*

Despite widespread acceptance that LPV with low tidal volumes provides improved survival, attempts at LPV are often abandoned due to hypercapnia-induced acidosis. Perhaps more clinicians could fully apply LPV if decarboxylation could be supplemented. As such, extracorporeal $CO_2$ removal ($ECCO_2R$) has been investigated as a means of supplementing the ventilator and allow for better adherence to LPV strategies.[22] The primary difference between $ECCO_2R$ versus oxygenation with ECMO is that $CO_2$ removal can be done at low blood flow rates comparable to hemodialysis rates, lessening blood damage and its complications, and allowing for smaller cannulae that are easier to insert.[12,84] However, $ECCO_2R$ was generally dismissed by the medical community from the 1970s-1990s due to failure to improve patient outcomes and complications, mainly hemorrhage and thrombosis.[85] Since then, extracorporeal technology has undergone significant improvements: centrifugal pumps cause minimal blood damage, biocompatible circuits require less systemic anticoagulation, dual lumen cannulae allow for a single access point, and oxygenators have lower resistance and are significantly more efficient and durable than older generations.[76]

$ECCO_2R$ cannulation can be arteriovenous ($AVCO_2R$) or venovenous ($VVCO_2R$). $AVCO_2R$ has been successfully investigated as a bridge to lung transplantation.[86-89] $AVCO_2R$ is commercially available via the Novalung iLA, which is a low resistance oxygenator that has demonstrated effectiveness in allowing LPV in ARDS and BTT.[12,90] In $AVCO_2R$, blood flows into a compact gas exchanger and is pumpless,[91-93] which is thought to cause significantly less blood

activation than ECMO and may be better suited for long-term support. Cannulas are placed peripherally in the femoral artery and vein, and a patient's own blood pressure is used to drive flow through the device.[90] However, limitations to $AVCO_2R$ include ineffectiveness if a patient is hypotensive, and limb ischemia due to femoral artery cannulation.[12,93] Furthermore, the AV shunt forces the heart to increase cardiac output to maintain peripheral circulation, making $AVCO_2R$ unsuitable for patients with PH and ventricular dysfunction.[89,91]Additionally, although the AV approach allows for effective $CO_2$ transfer, it supplies less than 10% of a patient's oxygen requirements.[94]

$VVCO_2R$, on the other hand, requires a pump to generate blood flow and the circuits are more complex than $AVCO_2R$. Commercially available options include the iLA active with combines the Novalung iLA with a pump, and the Hemolung which is an oxygenator paired with a centrifugal pump.

There is promise in this area as devices become simpler and smaller, and $ECCO_2R$ may even eliminate the need for intubation in patients with primarily hypercarbic respiratory failure. Such a device could sustain patients with end-stage COPD, facilitating their rehabilitation to maintain their adequacy for lung transplantation, and decrease severity of exacerbations. Perhaps, even, a device could be designed for long-term destination therapy. The aforementioned devices, though, are inadequate to this end as they do not provide sufficient oxygenation, and even hypercarbic COPD patients require supplemental oxygen. As such, there is a great need for a low resistance device that can adequately oxygenate and decarboxylate at low flow rates.

*Limitations and Complications*

Despite recent advances, ECMO and $ECCO_2R$ remain burdened by limitations including the need for ICU admission, bleeding, infection, blood damage, thrombosis with embolization, and

hemorrhage.[70,74,76,95] The most common complication is bleeding, which is confounded by medical anticoagulation on top of ECMO-induced coagulopathy and thrombocytopenia.[73,96] All patients on ECMO receive systemic heparinization to prevent clotting in the ECMO circuit as well as end-organ microthrombi and fibrin deposition, although most centers use low-dose anticoagulation, as opposed to the full-dose used in the past.[80,97] On top of that, there is continuous activation of both the intrinsic and extrinsic coagulation cascades, as well as consumption and dilution of clotting factors.[98] Additionally, platelet consumption and acquired von Willebrand's disease lead to bleeding complications.[99,100] Typical red blood cell and platelet consumption remains 450-1125 ml and 150-500 ml per day, respectively.[69,101] Cannulation sites can cause complications, particularly a risk of leg ischemia with femoral artery cannulation.[76] Additional complications include air embolism, hemorrhage due to tubing rupture, thromboembolism, and intracerebral hemorrhage.[102]

Survival to transplantation decreases with length of time on ECMO and common complications, including infections and multi-organ failure, can prohibit transplantation.[6,67-69] Premature initiation of ECMO may lead to progressive complications and reduced survival,[67,103] but if not initiated soon enough, patients may progress to irreversible organ damage. Although a few patients have been supported for 30-50 days, it is critically important to quickly find organs for patients on ECMO waiting for lung ransplantation.[67]

### *1.2.4 Thoracic Artificial Lungs*

Despite improvements in ECMO as a BTT, a device is still needed that can provide respiratory support for months to years without the above complications that limit ECMO. Thoracic artificial lungs (TALs) may be an answer. TALs attach to the pulmonary circulation with blood flowing from the proximal pulmonary artery (PA) and returned to either the left atrium (LA) in PA-LA attachment or to the distal PA in PA-PA attachment. The right ventricle drives blood

through the TAL, obviating the need for a mechanical pump. The TAL has a resistance less than healthy lungs--0.5 mmHg/(L/min) – eliminating PH and improving RV function when attached PA-LA.[104-106] The TAL eliminates the large circuit and team of specialists who are required to run ECMO. The heart adjusts its output as needed to modulate gas exchange, and the TAL can be run with a 5% $CO_2$, 95% $O_2$ gas mixture that allows for a fixed gas flow rate. Most important for long-term use, the TAL's low blood-flow resistance, minimal shear stresses, and the lack of a pump, heat exchanger, and reservoir cause a marked reduction in coagulation, inflammation, and damage to formed elements in blood as compared to ECMO.[99,101,107-111] Thus, unlike ECMO, no blood products need to be given during TAL use.[107,110] The MC3 Biolung TAL and the compliant TAL (cTAL) cause no significant hematological, hemodynamic, or organ function deficits over 14-30 days of testing. As a result, there is no known limit to TAL support duration, but devices will nevertheless need to be replaced due to clot formation.

*Thoracic Artificial Lung as a Bridge to Transplantation*

97% of lung transplant program directors indicated they would support a phase I trial using a TAL as a BTT.[112] The first clinical attempts at this application have proceeded, using the lowest resistance gas exchanger on the market, the Novalung ILA.[113-116] In every case, the patient had primary PH. The main goal was to unload the RV, and the device was implanted in a PA-LA fashion. Six out of the seven patients (87%) were successfully bridged. Although successful, the ILA is not designed for destination therapy as it lacks sufficient $O_2$ transfer to support patients with respiratory failure and provides only marginal unloading of the RV.[114] Thus, when the ILA is used in the ECMO setting, patients remained on mechanical ventilation with high $FIO_2$ (0.5-0.9) and peak pressures (31-47 mmHg).[87] When used in the PA-LA configuration, the Novalung slightly improved RV function, but provided a negligible reduction in PA pressures, necessitating inotropic

support.[114] This is because the Novalung resistance is approximately 5-6 mmHg/(L/min) at blood flows of 2-2.5 L/min, limiting device blood flow and RV unloading.[91,117,118] Perhaps most importantly, Bioline coated ILAs fail due to clot formation after 10-12 days on average.[88,89,115,116,119] Thus, it is not ideally suited as either a bridge to lung transplantation or destination therapy device.

*Compliant Thoracic Artificial Lung (cTAL)*

The cTAL was developed in our lab, and results from preliminary studies suggest that its excellent biocompatibility should allow for longer periods of support than current clinical devices. The cTAL has an elastomeric, Biospan housing and a gas transfer membrane consisting of 210 μm OD polypropylene (PP) fibers wound into a bundle with a void fraction of 0.75 and a surface area of 2.4 $m^2$. The cTAL has a rated flow well over 7 L/min[105], well above that of the Novalung,[86] and a blood flow resistance of 0.5 mmHg/(L/min).[104-106] This is less than half of a healthy natural lung and < 10% of the Novalung ILA.[91,117,118]

The cTAL was implanted, in a PA-LA fashion, for 14 days in normal sheep (n=5). In these studies, heparin anticoagulation was used at an ACT of 180-220s, and the cTAL was uncoated. In normal sheep, arterial $PO_2$, $CO_2$, and mean arterial pressure remained stable and in normal ranges (**Figure 1.1a**). Cardiac output was initially elevated due to post-op stress but stabilized in a normal range after one week (**Figure 1.1b**).

Platelet counts decreased as a result of surgery but were above normal and stable after day 6. There was no laboratory evidence of red blood cell lysis or end-organ dysfunction. Remarkably, these uncoated devices remain nearly completely clot free with no significant change in resistance after 14 days of testing (**Figure 1.1b**). Only one of 5 devices featured an increased resistance, but was paradoxically free from clot (**Figure 1.1c**) and had no decrease in blood flow, suggesting measurement error.

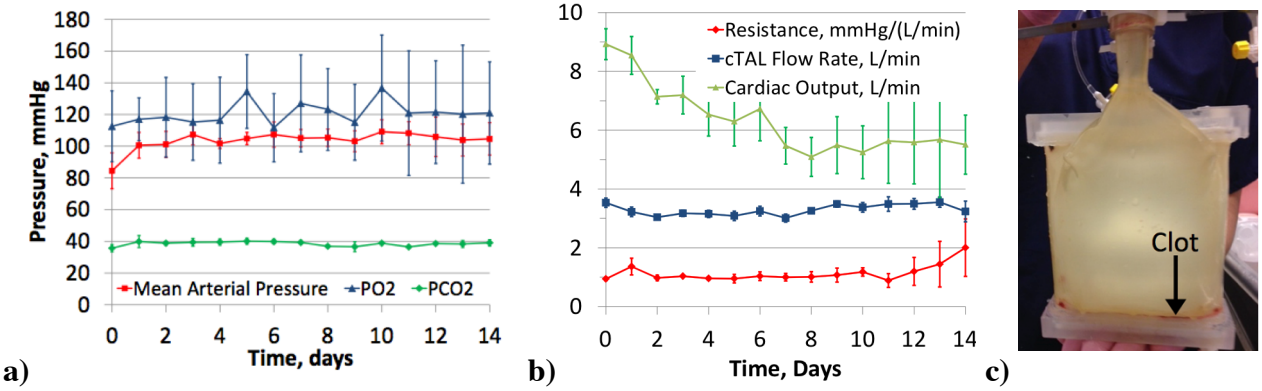


**Figure 1.1**: 14-Day cTAL *in vivo* results (n=5): a) mean arterial blood pressure and arterial $PO_2$ and $PCO_2$, b) cardiac output and cTAL flow rate and resistance, c) Typical cTAL after 14 days of use. There is only a thin layer of clot in the distal end.

*TAL Clinical Application*

TALs would allow for improved lung transplantation outcomes and potentially bridge more patients, improving gas exchange, removing the need for mechanical ventilation, eliminating PH, recovering RV function, and reversing organ failure. Patients would be able to participate in physical therapy, improving their transplant candidacy and survival. Lastly, TAL use in the immediate post-op period might permit the use of injured donor lungs as they recover *in vivo*, thus extending the donor pool. For this application, the TAL would need to last weeks to months. Recent studies of the cTAL suggest that its excellent biocompatibility should allow for support on the order of months and perhaps several years with elective device replacement. Therefore,

transplant ineligible patients might use the TAL as destination therapy with the ability to leave the hospital, similar to patients who receive ventricular assist devices (VADs) for heart failure. Patients with severe pulmonary hypertension and recurrent exacerbations might be supported preventatively, which could delay the need for transplantation, reduce medical expenses, improve quality of life, reduce hospitalizations, and improve survival. Such a technology would revolutionize the management of both acute and chronic respiratory failure, potentially serving a vast cohort of patients with respiratory failure, as either bridge to recovery, bridge to transplantation, or true destination therapy.

### *1.2.5 Lung Transplantation*

As of 2014, there were more than 11,000 people alive with a lung transplant, but 2485 lung transplant candidates remain actively-listed, the longest the list has ever been.[120] As of 2000, it was estimated that more than 122,000 annual deaths in the United States could have been prevented with lung transplantation.[121] Indications for lung transplantation include COPD, alpha-1 antitrypsin deficiency, IPF, primary PH, CF, and bronchiectasis.[11] Candidates must have a chronic disease with significant functional disability for which no further medical or surgical therapy is available, when life expectancy is limited and quality of life is unacceptably poor.[122] Furthermore, they must not have other chronic and debilitating diseases.[11] Implemented in 2005, the Lung Allocation Score (LAS) reflects risk of wait-list mortality and probability of posttransplant survival; as of 2014, transplant patients were sicker than ever with the highest average recorded LAS. The median waiting time in 2012 was 4 months, and 65.3% of transplant candidates underwent transplantation within 1 year of listing.[120] Mortality is 12% at one year and about 50% at 5 years posttransplant, an outcome which has not improved since 2005.[120] As compared to all organ transplantations, lung

recipients have the highest rate of complications and rehospitalization: 43.7% in the first year alone.[120]

Although transplant waitlist mortality has been improving, patients with IPF and PH remain at high risk for acute decompensation and sudden cardiac death.[123] These patients have inadequate treatment options while awaiting a donor lung; medication and ventilator therapies are ineffective and they often die from fulminant respiratory failure before a lung becomes available. Additionally, although lung transplantation can improve functional capacity of patients with a COPD, it has been difficult to demonstrate that patients selected for transplantation truly derive a survival advantage.[122,124,125] The median survival for lung transplantation in COPD patients has been reported to be 5 years in those receiving a single lung transplant and 7 years in those receiving a bilateral lung transplant.[27] One complex statistical model created using the United Network for Organ Sharing (UNOS) database suggests that only 22-45% of COPD patients would gain a survival benefit of at least 1 year.[122,126] Despite the number of potential recipients increasing, lung transplantation remains limited primarily by shortage of donor organs; only 0.37 lungs are recovered per donor and discard rates of recovered lungs are 7.3%. In 2016, 2121 lungs were transplanted. Whereas the use of ECMO used to be a contraindication to lung transplantation,[76,127] in 2014, 5.3% of transplant recipients were on ECMO at the time of transplantation.[120]

### 1.3 Destination Therapy Device Concept

Despite the increasing useful lifetime of ECMO, devices still fail, burdened by clot formation. To further prolong device longevity, we need to i) better design devices, optimizing gas exchange while limiting device size, and ii) employ additional methods of clot prevention, ideally

at the fiber surface. In order to make appropriate design changes, we need to first determine our performance goals to treat our intended target population – those with chronic respiratory failure.

### *1.3.1 Increasing ECMO Lifetime with Bridge to Transplantation*

Recently, utilizing ECMO as BTT has pushed the envelope with respect to the amount of time a patient can spend on ECMO, and clinicians have learned more about the limitations of the systems. Experienced centers have reported satisfactory survival rates, demonstrating that the use of extracorporeal technologies to salvage, rehabilitate, and transplant patients with nonrecoverable lung disease is technically doable and logistically feasible.[82] Hoopes et al. initiated ECMO in 31 patients with respiratory failure and hemodynamic instability and reported a 97% success rate of bridging patients to transplantation with a 1-year survival rate exceeding 90%.[82]

Expanding upon these studies, perhaps low-flow ECMO functioning as $ECCO_2R$ could also serve as a BTT for patients with hypercapnic respiratory failure. Such a technique has already proven to be successful in ARDS,[24,76] and might even obviate the need for invasive mechanical ventilation in purely hypercapnic patients altogether and prevent complications of mechanical ventilation including ventilator-associated lung injury, VAP, patient discomfort, deconditioning, and resulting high mortality rates.[76] Additionally, mechanical ventilation is a relative contraindication to lung transplantation because it results in poor outcomes, with a reduction in overall 1 year posttransplant survival rate by 20%.[83,128] If ECMO provided enough gas exchange to replace the ventilator, then transplant candidacy would be optimized. ECMO has even been shown to improve post-transplant survival in high-risk patients.[127,129] Furthermore, upper body cannulation allows for early mobilization, ambulation, participation in physical therapy, and continued oral intake, reducing ICU-related complications.[75,130] All of these factors combined make

ECMO a promising means of reliable BTT, and perhaps ECMO can become for lung transplantation what ventricular assist devices have become for cardiac transplantation.

### *1.3.2 Columbia Experience with Minimal Long-Term ECMO Support*

Columbia University Medical Center's ECMO program has completed more than 600 cases of adult ECMO over the last 5 years, building one of the largest contemporary experiences, as well as tackling the most complicated indications for use. The etiologies of the pulmonary failure include ARDS, CF, ILD and PH, and indications for ECMO range from acute hypoxemia failure to hypercapnic failure from COPD exacerbations, to combined hypoxemic and hypercapnic failure, and chronic respiratory failure requiring BTT.

From this clinical experience, they have learned to tailor their approaches to a patient's specific pathophysiologic derangement, which led to a critical insight: only partial support is needed to improve patients' clinical status and allow them to become ambulatory.[79] When comparing a patient's calculated cardiac output to the ECMO flow necessary to attain significant physiological improvement and even ambulation, they learned that full support, which current devices are designed to provide, is not necessary (**Table 1.1**). With only partial support, patients' performance improvement is remarkable; they participate in physical therapy and eat independently. Despite initial severe physiologic derangement, all patients have a rapid and profound response to the application of device therapy, and all patients are able to participate in some form of physical therapy, with more than 50% ambulating by day 2 after cannulation.[79]

**Table 1.1**: Comparison of calculated cardiac output (CO Calc, liters per minute) versus actual device support (Device Flow) provided. (LPM = liters per minute)

| **Type of disease** | **CO Calc (LPM)** | **Device Flow (LPM)** | **%Device flow/CO calc** |
|---|---|---|---|
| Hypercapnic | 3.9 | 1.7 | **44.6%** |
| Hypoxemic | 4.2 | 3.1 | **75.5%** |
| Pulm. HTN | 4.3 | 3.0 | **71.5%** |

### *1.3.3 Pulmonary Assist Device*

As explained above, we have recently recognized that many patients with chronic lung disease require only partial ECMO support of 50-70% of their cardiac output, depending on their particular pathological derangement, to attain acceptable RV unloading, oxygen delivery, and $CO_2$ transfer. With the need for less support, this can allow us to develop novel cannulation approaches and device designs that would be smaller, more convenient, and more durable for long-term support. As a result, the goal of this work is to create a smaller ECMO oxygenator based on design concepts from the cTAL, but with smaller size and surface area for our partial support goals, and develop this device as a means of destination therapy. When combined with our endothelial-like biocompatibility strategy, this device should allow for support on the order of months and perhaps several years with elective device replacement.

## 1.4 Coagulation in Artificial Lungs

Clot formation presents a challenge with all blood-contacting biomaterials, but is particularly problematic in oxygenators due to their large surface area. In fact, surface-induced thrombosis is the primary challenge faced by the scientific community in the development of long-term artificial devices.[131]

### *1.4.1 Mechanisms of Clot Formation*

Coagulation is initiated at a blood-biomaterial interface due to protein adsorption and platelet adhesion and activation, with initiation of the coagulation cascade and subsequent thrombus formation.[131,132] Fibrinogen undergoes a conformational change upon adsorption, allowing the unactivated form of platelet receptor GpIIb/IIIa to bind, inducing platelet immobilization, activation, and aggregation.[131] Similarly, FXII adsorption initiates the intrinsic

branch of the coagulation cascade, thrombin formation, and platelet activation.[131] Ultimately, both of these reactions lead to surface-induced clot formation which is particularly problematic in oxygenators due to their large surface area.

### *1.4.2 Methods of Clot Reduction and Prevention*

Clot formation can be prevented or mitigated through careful device design, as well as through chemical and enzymatic means. Currently, all patients on ECMO require systemic anticoagulation, typically via heparin. However, systemic anticoagulation causes hemorrhagic complications in 15-25% of cases, including intracranial hemorrhage and bleeding at surgical and cannula sites which are associated with diminished survival.[96,133] Ideally, anticoagulation in an artificial lung should occur only at the biomaterial surfaces, allowing for normal coagulation systemically within the patient. Currently, local clot-prevention measures being used include various coatings of the artificial surfaces. Another promising means is surface release of nitric oxide, an extremely short-acting platelet inhibitor.

*Clot Prevention Through Engineering and Design*

Engineers can slow cot formation in oxygenators through device design considerations. Typical design techniques to improve blood gas exchanger biocompatibility include i) eliminating recirculation and stagnation regions to avoid focused build-up of procoagulant molecules, ii) reducing shear stresses < 10-15 dyne/cm$^2$ to avoid platelet activation and iii) reducing overall surface area.

*Coatings Currently Available*

Heparin-coated surfaces are currently widely used in artificial devices, ranging from tubing to oxygenators. Heparin sulfate is a naturally occurring proteoglycan found on the native endothelium and it is a crucial part of the complex natural anticoagulant surface activity of the

vascular endothelium.[134] Heparin binds antithrombin (AT) III and causes a conformational change that enhances its antithrombotic action.[135] Surface heparin coatings were first demonstrated by Gott et al.[136] in 1963 when they were testing graphite as an antithrombotic coating for valves and serendipitously determined that heparin became bound to the graphite, which thereby reduced clot formation. Since that time, multiple commercialized heparin coating technologies have emerged over the past three decades.[137] Most coatings employ immobilized heparin via ionic or covalent linkage.[137] For example, ASTUTE™ Advanced Heparin Coating, used to coat CPB devices and hemodialysis catheters, covalently binds heparin to a hydrophilic binding layer; BIOLINE® Coating, used to coat ECMO devices and vascular grafts, ionically and covalently binds heparin to an albumin priming layer; and the CARMEDA® BioActive Surface coating utilizes covalently bonded heparin, as well.[137] DURAFLO® II, also used in ECMO devices, on the other hand, ionically binds heparin to the surface. However, this is the extent of available information in many cases, as there is very limited published data on the technologies and their efficacies.

Heparin coatings have limitations. One downside is the possibility of causing heparin-induced thrombocytopenia (HIT), which is a rare but potentially lethal hypercoagulable state caused by antibodies generated through heparin adminstration.[137,138] Also, notably, the reaction kinetics for immobilized surface heparin differs from systemically administered heparin. For example, blood flow rate over the surface affects the uptake of AT by the surface.[139] Furthermore, its activity may diminish over time. Thus, i) not all binding methods may provide effective or long-term anticoagulation and ii) current devices that have heparin coatings still experience clot formation and failure over a few weeks. Therefore, improved coating methods are needed.

*Poly(carboxybetaine) (pCB) Surface Coating*

Recent research has focused largely on "non-fouling" coatings that resist nonspecific protein adsorption. In general, these coatings rely on surface-grafted molecules to create a hydration layer on the surface that is very similar to the normal physiological environment. This layer prevents proteins from reaching the hydrophobic artificial surface where they can undergo conformational change and activation, thereby preventing nonspecific protein adsorption and reducing local procoagulant concentrations. In theory, if protein adsorption was completely eliminated, so would surface-induced coagulation.

Poly-2-(methoxyethylacrylate) or PMEA is one such biocompatible coating. PMEA has a polyethylene backbone with polarity which forms a hydration layer at the artificial surface that resists protein and cell adsorption.[140] It has been commercially available since 2000 by Terumo as Xcoating™, stated to reduce both protein denaturation and platelet adhesion. Xcoating™ is indicated in heparin-sensitive patients, such as those who have, or who have had, HIT. A recent study compared patients undergoing CPB with either heparin- or PMEA-coated devices and determined that PMEA-coated circuits result in less platelet, total protein, and albumin loss ($p < 0.05$; note: the study was funded by Terumo).[140] Similarly, Gupta et al.[141] demonstrated that PMEA provides modest reduction in platelet surface adhesion by 15-25%.

Poly(carboxybetaine) (pCB) is a novel non-fouling coating under investigation that has demonstrated superior results as compared to PMEA. Dr. Shaoyi Jiang's group at University of Washington has developed a variety of zwitterionic coatings utilizing pCB (**Figure 1.2**). Zwitterionic ions have an equal number of positive and negative charges, resulting in a net neutral charge. pCB coatings are ultra-low fouling because they tightly bind water to create a super-hydrophilic surface, and, importantly, pCB coating thickness (10-30nm) is small enough as to not

hinder gas diffusion. Jiang's group has demonstrated that pCB can

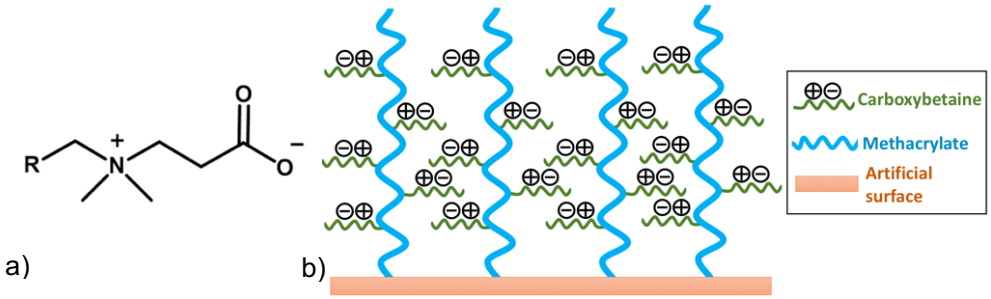


**Figure 1.2**: a) Carboxybetaine b) pCB on methacrylate backbone

decrease fibrinogen fouling on hydrophobic surfaces by 90% compared to an uncoated control.[142] Collaborative work between our lab and Jiang's group has showed 75% reduction in platelet deposition for pCB-coated surface versus uncoated, when they were exposed to PRP for 8 hours, compared to the <25% provided by PMEA above.[143] Unlike other previous coatings, pCB-coated surfaces are highly resistant to protein adsorption.[143] In cooperation with Dr. Jiang's lab, these coatings are currently undergoing long-term testing on artificial lungs in the Cook lab.

*Nitric Oxide*

Surface nitric oxide (NO) flux has also been investigated in the hope of reducing thrombosis in oxygenators. Among its many properties, NO is a short acting (half-life 0.05-1.8 ms in blood),[144,145] potent platelet inhibitor that is produced by endothelial cells.[146] Freely diffusing into platelets, NO increases platelet cGMP levels, decreasing expression of the surface receptors including GPIIb/IIIa, P-selectin, and CD63, and reducing platelet affinity for agonists (**Figure 1.3**).[3] Platelet-derived NO

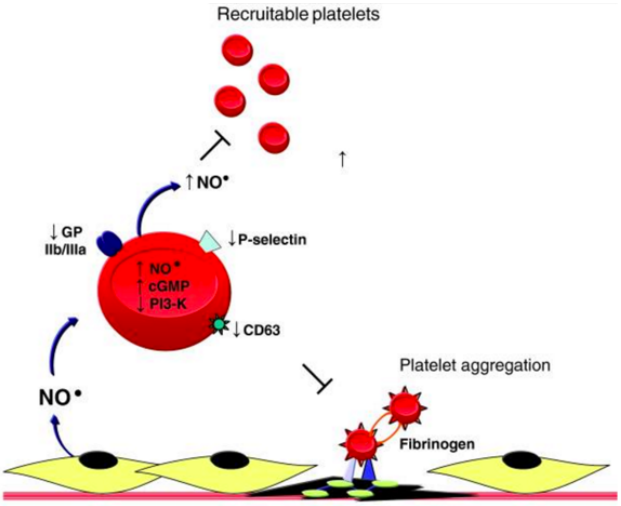


**Figure 1.3**: NO effects on platelets[3]

is also generated and inhibits the recruitment of circulating platelets to sites of vascular injury. Additionally, NO blocks the release of platelet granules, which would otherwise induce further activation and aggregation. The NO flux can be created by adding it to the sweep gas[147] or by generating it at the oxygenator surface, primarily through the use of copper-containing polymers which decompose NO donors to release NO, with reduction in platelet adhesion ranging from 20-40%.[141,147-151] There have been previous *in vitro*, *in vivo,* and clinical studies investigating sweep gas NO and its effects on platelet activation and adhesion; results have varied, but most demonstrate a modest difference in platelet counts or platelet activation.[147,152,153] It has been demonstrated that NO production at the fiber surface can prevent platelets from adhering to the fiber surface of artificial lungs.[149]

However, NO can combine with hemoglobin (Hb) to form nitrosylhemoglobin, which is rapidly oxidized to methemoglobin (metHb).[154] Not only does metHb have reduced oxygen carrying capacity, but it also has such an extremely high affinity for $O_2$ that bound $O_2$ is unable to dissociate to tissues, causing tissue hypoxia.[154] Methemoglobinemia causes cyanosis with levels as low as 10%, symptoms (i.e. shortness of breath and fatigue) when 35%, and fatality when greater than 70%.[154,155]

When using NO surface flux in oxygenators, our goal is to generate less than 5% metHb to allow for a cushion of safety. However, it is unknown what NO flux can be used before a patient develops significant metHb. This has been answered clinically when using inhaled NO as a pulmonary vasodilator in patients with pulmonary hypertension. At doses below 100ppm NO, metHb levels are typically insignificant, and the risk of significant metHb is generally outweighed by the benefits.[154] However, given the small surface area of gas exchangers in comparison to the native lung, it is possible that higher doses of NO will be tolerated without toxicity. Tevaearai et

al.[147] administered 80 ppm in a bovine CPB model and found no increase in metHb, whereas Sly et al.[152] administered 500 and 1000 ppm NO in a porcine CPB model, which resulted in a metHb increase of 4% and 8.6%, respectively. It is unclear, however, what dose between 80 and 500 would be tolerated.

*Combined Approaches*

The endothelium is the only truly non-thrombogenic surface. It utilizes a variety of anticoagulation methods, including a non-fouling surface, $PGI_2$ and NO release, and surface expression of heparin, thrombomodulin, and ADP-ase.[156] Artificial surfaces would be greatly improved by mimicking this approach, but this has not yet been fully and successfully duplicated synthetically. We have demonstrated that the anti-fouling, endothelial-like, zwitterionic pCB coating being studied in our lab will prevent protein adsorption, reducing local procoagulant concentrations, amplifying the effect of NO, and allowing for marked anticoagulation at lower NO flux rates (**Figure 1.4**).[143] Alone, NO flux and pCB may not be sufficient to prevent device failure, but *in vitro*, their combination has been shown to decrease platelet adsorption by 92%.[151] Therefore, our goal is to couple pCB with NO to obtain synergistic prevention of clot formation at the fiber surface *in vivo*.

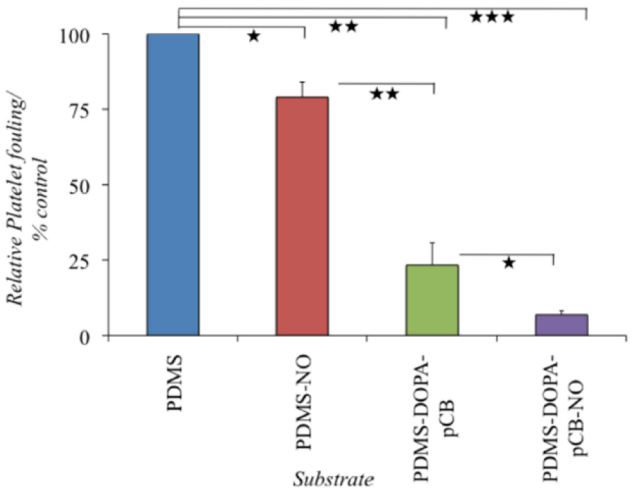


**Figure 1.4:** The synergistic effect of DOPApCB-coating and NO release on platelet adsorption is compared with the effects of coating alone, NO release alone, and plain PDMS surface.. * ($p < 0.05$), ** ($p < 0.01$), and *** ($p < 0.001$)

### 1.5 Approaching Destination Therapy

As outlined above, despite recent advances in technologies, the use of artificial lungs remains limited to a couple of weeks and there is a tremendous need for improved oxygenator design allowing for longer usable duration. The primary mechanism of device failure and functional deterioration is clot formation, and thrombosis prevention is the main obstacle prohibiting the development of a long-term artificial lung. Although most oxygenators employ a heparin coating, the effects are modest and devices still clot. NO release at the fiber surface is being investigated for local clot prevention in artificial lungs, and when combined with the non-fouling coating pCB, the two may have a synergistic effect. In addition to improved clot prevention strategies, there are also design considerations necessary to progress to long-term artificial lung support. Such a device must be small, low in resistance, uncomplicated to electively replace, and as stated in section 1.3.2, the device can be designed to provide only partial support.

To this end, I performed a number of studies that were necessary to pave the way. First, I examined clot formation and failure patterns of clinical devices to further our understanding of their limitations with respect to long-term support. Next, before proceeding to *in vivo* experiments with pCB, the ideal flux of NO that will prevent platelet activation while not resulting in significant metHb was determined. Last, I tested our PAD design to confirm that it meets our design goals and allow for appropriate alterations prior to proceeding to long-term sheep experiments. From here, we are equipped to commence with 30-day testing in sheep.

## Chapter 2: The Time Course of Clinical Oxygenator Failure Due to Clot Formation

### 2.1 Introduction

Extracorporeal membrane oxygenation (ECMO) is being used with increasing frequency and duration for both respiratory and cardiac support. In both cases, it is used as a bridge to recovery, bridge to durable device support, or bridge to transplantation (BTT).[82] Despite increased usage and protocolized anticoagulation, ECMO oxygenators remain plagued by progressive performance deterioration and biocompatibility issues that limit the effectiveness of long-term ECMO, including bleeding, clotting and thromboembolic complications.[6,157] Thus, the durability of the oxygenators is limited and the requisite anticoagulation increases the risk for bleeding. The limitations of current oxygenators restrict their effectiveness for lung term BTT support and preclude their use as durable support devices for patients who are ineligible for lung transplantation. These patients continue to live with chronic lung disease, burdened by continuous home oxygen requirements, frequent and costly hospitalizations, and no restorative therapies.

The main factor preventing the long-term use of these devices in chronic lung disease patients is clot formation. As clot propagates, oxygenator gas exchange declines, blood flow resistance increases progressively and an injurious cycle of hemolysis can occur. Clotting is initiated at the artificial surface with protein adsorption, which then causes platelet adhesion and activation, initiation of the coagulation cascade, and subsequent thrombus formation.[131,132] Although there is a breadth of research focused on improving anticoagulation and antithrombotic coatings, there are limited publications that track the time course of clot formation and device functional deterioration within the most commonly used clinical oxygenators. A few investigators have evaluated D-dimer, computed tomography, and pressure drop as a means to evaluate clot formation and determine if a device is failing,[158-160] but none has sought to connect these strategies

to average device performance. Broader understanding of the location and time course of clot formation within these devices will allow engineers to analyze failure mechanisms and improve the design of future devices, while also giving clinicians important feedback into their current ECMO decision-making.

To analyze patterns of clot formation and device functional deterioration, clinical information was collected from all ECMO cases over a three-month period at Columbia University Medical Center. Every oxygenator was examined for physical and functional patterns indicating clot formation, whether removal was for device failure or patient weaning. The time course of functional deterioration in each device was determined using longitudinal changes in blood flow resistance and oxygen transfer. The probability of clot formation at each location in the gas exchanger inlet and outlet was also determined as a function of time using digital image processing, and the extent of clot was compared to the observed functional deterioration. Patient demographics and laboratory values were compared to assess their effects on the rate of deterioration. Results suggest significant differences in long-term performance between the Qx and CH systems.

## 2.2 Methods

### *2.2.1 Data Collection*

All ECMO cases were evaluated over a three-month period, regardless of the indication, length of ECMO course, or reason for discontinuation (i.e. weaning due to patient recovery, patient transplant, or device failure). Common ECMO indications during this period included acute hypoxemic failure most commonly due to acute respiratory distress syndrome, hypercapnic failure from chronic obstructive pulmonary disease exacerbations, combined hypoxemic and hypercapnic failure, cardiac failure, and chronic respiratory failure requiring bridge to lung transplantation. The

majority of patients were on venovenous (VV) or venoarterial (VA) ECMO, with a few veno-arterial-venous (VAV) cases. All patients received a bolus of 5,000u heparin at the time of ECMO cannulation, and then were maintained on a heparin drip thereafter with a targeted and activated partial thromboplastin time (aPTT) of 40-60s. Patients were given packed red blood cells when their hemoglobin fell below 7, and a platelet count less than 50 was tolerated in absence of bleeding.

The ECMO systems at Columbia are either Maquet's CardioHelp (CH) or a Quadrox (Qx) oxygenator (**Figure 2.1**) coupled with either a Rotoflow or CentriMag pump. These two oxygenators have a similar overall design; they both consist of polymethylpentene hollow fibers with Bioline heparin coating and a 1.8m$^2$ gas exchange surface area. However, CH is an integrated pump-oxygenator with four inlets, whereas the Qx is a stand-alone oxygenator with one inlet that is paired with a pump. These subtle variances lead to different flow patterns within the devices, which might produce different patterns of clot formation. The type of device used on a patient was at the clinician's discretion. However, a Qx was typically used if the patient was immobile and likely to remain so whereas a CH was used if the patient was expected to be ambulatory or be transported from an outside hospital to Columbia; this decision was based on the less expensive cost of the Qx versus the smaller size and fewer independent components of the CH system.

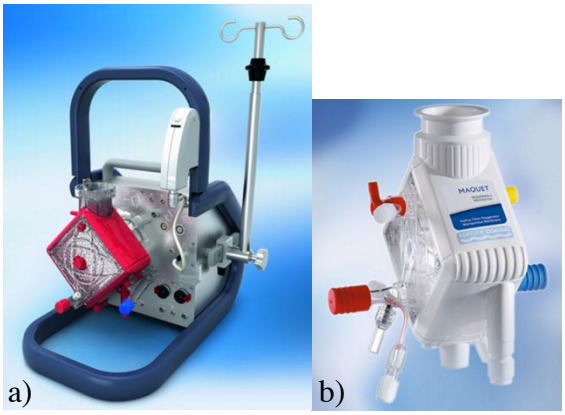


**Figure 2.1**: Columbia University's ECMO oxygenators: a) CardioHelp, b) Quadrox

Patient demographics collected included age, indication for ECMO, and type of cannulation. Clinical parameters measured included arterial blood gases (ABG), hemoglobin (Hgb), platelet count (PLT), and aPTT. Circuit data was collected daily throughout the ECMO course, including device flow (Q), inlet and outlet pressures, inlet and outlet blood gases, and sweep gas flow rate.

### *2.2.2 Data Analysis*

Statistical analyses comparing the Qx and CH groups were performed using SPSS software (SPSS, Chicago, IL). All data are presented as mean and standard deviation. The statistical significance of most variables was determined by the two-sample t-test assuming unequal variances. A p-value of $< 0.05$ was required for statistical significance. When comparing PLT counts between groups, patients that received platelet transfusions were excluded. Device failure was defined as an increase in blood flow resistance ((inlet pressure – outlet pressure)/device flow) greater than 1 mmHg/(L/min)/day for more than one day; survival analysis using this failure criterion was performed using the Kaplan Meier method. As a measure of device performance, the inlet-outlet oxygen content difference ($\Delta C_{O2}$) was determined. $O_2$ content is defined as the amount of $O_2$ bound to hemoglobin plus $O_2$ dissolved in plasma, and is calculated as follows:

$$O_2\ Content\ (mL\ O_2/L\ blood)$$

$$= \left( \frac{g\ Hgb}{100\ mL\ blood} \times 1.34 \frac{mL\ O_2}{1g\ Hgb} \times \left( \frac{\%O_2\ Saturation}{100} \right) \right.$$

$$\left. + \left( PO_2\ mmHg \times 0.00314\ \frac{mL\ O_2}{100mL\ blood} \right) \right) \times \frac{1000mL\ blood}{1L\ blood}$$

### *2.2.3 Heat-Map Generation*

Following detachment from the ECMO circuit, the oxygenators were gently rinsed with saline until the effluent was clear and photographed. A program was developed to process these

photographs and generate a probability density map of clot formation. To do this, the images were first converted to grayscale, and a darkness threshold value between 129 and 255 was used to identify clot. This threshold range was determined by evaluating five randomly chosen oxygenators and finding a range that accurately identified the clot seen in the original photo; thereafter, the same darkness threshold was used to evaluate every photo. By applying this threshold, the images were converted to binary using ImageJ, where a clot is depicted as white (RGB value of 255), and the remaining image is black (RGB value of 0). These binary images were then aligned in ImageJ and imported as a stack into MATLAB. Refer to **Appendix A** for the MATLAB code. The program evaluated each individual pixel (x.y position) in each image to generate a matrix of 0s and 1s. If the pixel is black, with an RGB value of 0, then the equivalent position in the matrix is left as 0, and if the pixel is white, with an RGB value of 255, then the equivalent position is assigned a 1. The program then sums each matrix and averages them. More specifically, it sums the values at each pixel and divides by the total number of images, resulting in a scale from 0 to 1 at each pixel. The resulting image depicts the probability of clot formation on an absolute color scale, where 0 is blue (0% clot frequency), and 1 is red (100% clot frequency).

## 2.3 Results

### *2.3.1 Patient Demographic and Hematological Data*

A total of 28 CH and 14 Qx cases were evaluated. **Table 2.1** summarizes selected pertinent data. There were no statistically significant differences in patient age or total number of days on ECMO. The CH patients were used most commonly in pure respiratory failure needing VV cannulation, whereas the Qx group had a higher percentage of patients needing cardiopulmonary support with VA cannulation. There were no statistically significant differences between groups

in the mean platelet count prior to ECMO initiation or mean aPTT throughout the ECMO course, indicating similar coagulation profiles between the two patient populations. Additionally, there was no statistically significant difference in initial device resistance between the two groups, and there was no difference in average device blood flow rate throughout the ECMO course, indicating a similar amount of support delivered in each group.

**Table 2.1**: Clinical data, presented as mean ± standard error of the mean.

| **Parameter** | **Oxygenator** | | **p-value** |
|---|---|---|---|
| | CardioHelp | Quadrox | |
| Patients (*n*) | 28 | 14 | |
| Age (average years) | 37.43 ± 3.74 | 49.07 ± 6.82 | 0.149 |
| Days on ECMO | 12.14 ± 1.09 | 10.07 ± 1.67 | 0.308 |
| Circuit:<br>VV *n* (%)<br>VA *n* (%)<br>VAV *n* (%) | <br>17 (61%)<br>10 (36%)<br>1 (3%) | <br>6 (43%)<br>6 (43%)<br>2 (14%) | |
| ECMO indication[1]<br>1 *n* (%)<br>2 *n* (%)<br>3 *n* (%)<br>4 *n* (%) | <br>2 (7%)<br>12 (43%)<br>7 (25%)<br>7 (25%) | <br>1 (7%)<br>4 (29%)<br>2 (14%)<br>7 (50%) | |
| Mean platelet count before ECMO | 227.73 ± 20.50 | 227 ± 41.77 | 0.997 |
| Average aPTT throughout ECMO course | 51.41 ± 2.40 | 54.99 ± 3.38 | 0.395 |
| Average Initial Device Resistance | 4.78 ± 0.28 | 4.74 ± 0.45 | 0.94 |
| Average Flow throughout ECMO course (L/min) | 3.44 ± 0.18 | 3.6 ± 0.35 | 0.686 |

[1]ECMO indications: 1 primary respiratory failure (viral/bacterial/aspiration pneumonia, flu), 2 acute respiratory distress syndrome (ARDS), 3 other pathologies (idiopathic pulmonary fibrosis, pulmonary hypertension, pulmonary embolism, cystic fibrosis, tracheal injury), 4 cardiac

Although there were no differences in their initial platelet count, the CH group had an average percent change in platelet count of 7.19 ± 15.45%, whereas the Qx group had a percent change of -33.87 ± 10.26% ($p<0.05$) by the end of the ECMO run (**Figure 2.2**). Patients that received platelet transfusions throughout the ECMO course were excluded from platelet trends (CH n=5, Qx n=5) to remove it as a confounding factor.

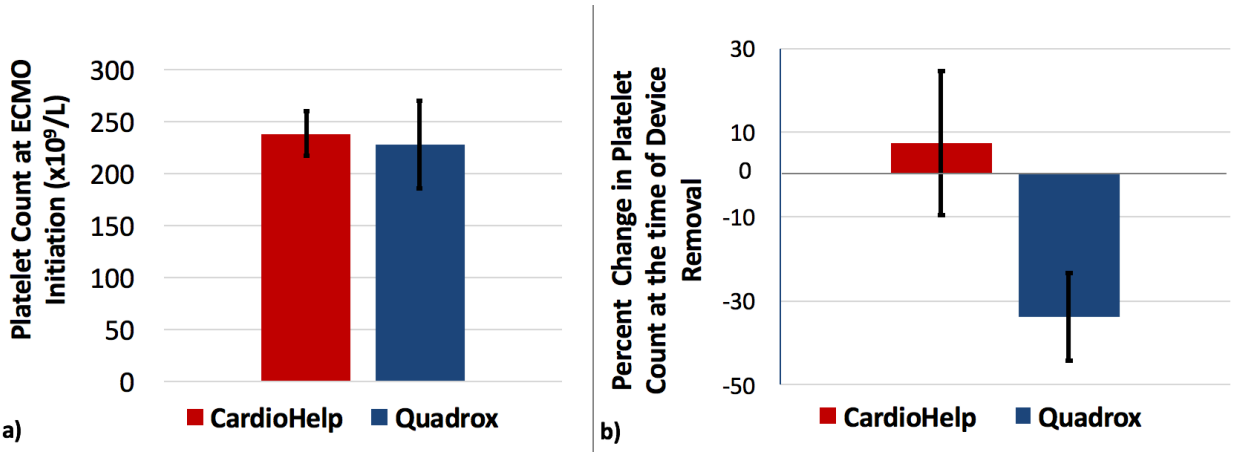


**Figure 2.2**: a) Average platelet count at time of ECMO initiation, b) Average percent change in platelet count at the time of ECMO discontinuation.

### *2.3.2 Device Resistance and Performance Data*

Resistance data are shown in **Figures 2.3 and 2.4**. As seen in **Fig. 2.3**, the Qx oxygenators have a more prominent early increase in resistance, whereas there is little change in resistance of the CH devices over the first 4 days. Around day 11, the average resistance of the Qx devices decreases, but this observation is due to 4 failed devices being removed, leaving behind only the most well-functioning devices and resulting in a selection bias. **Figure 2.4** shows that when devices fail, they do so acutely with a sudden, exponential increase in resistance.

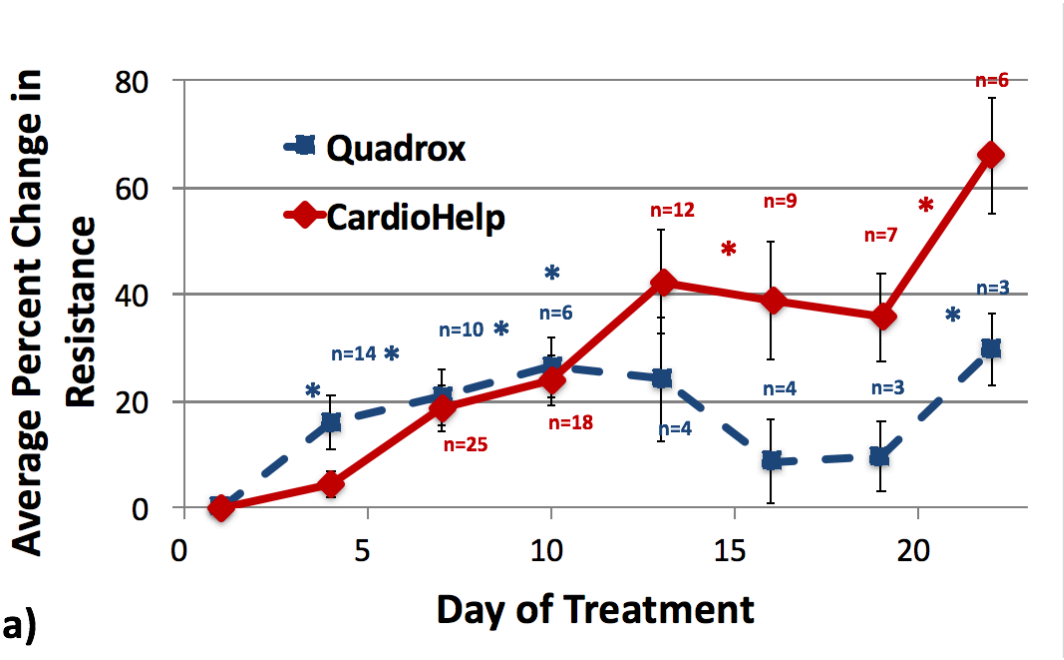


**Figure 2.3**: Percent change in resistance averaged over three days versus time. n = number of devices remaining. Asterisks (*) indicate device removal due to failure.

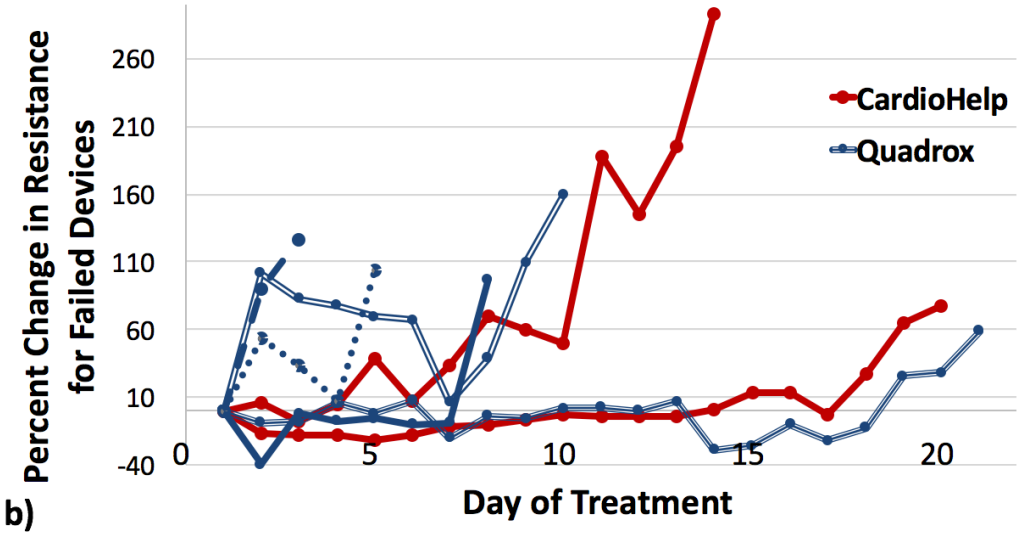


**Figure 2.4**: Percent change in resistance over time for failed individual devices.

Device survival data is depicted in **Figure 2.5**, which indicates that Qx devices meet the blood flow resistance failure criteria more quickly than CH oxygenators ($p < 0.05$).

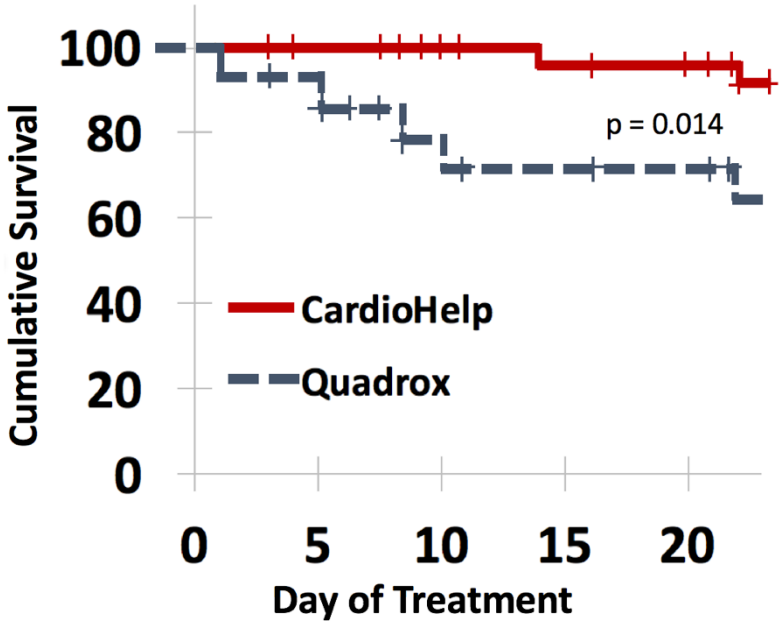


**Figure 2.5**: Device survival versus day on ECMO based on resistance failure criteria. Log-Rank, $p = 0.014$. Plus signs (+) indicate device removal due to weaning.

**Figure 2.6** shows the percent change in $\Delta C_{O2}$, with a greater decrease seen in the Qx group. These results parallel the resistance trends, with the CH maintaining performance for over 7 days, while the Qx devices experience a statistically significant decline in gas exchange by day 2 ($p < 0.05$) and a statistically significant increase in resistance by day 3 ($p < 0.05$).

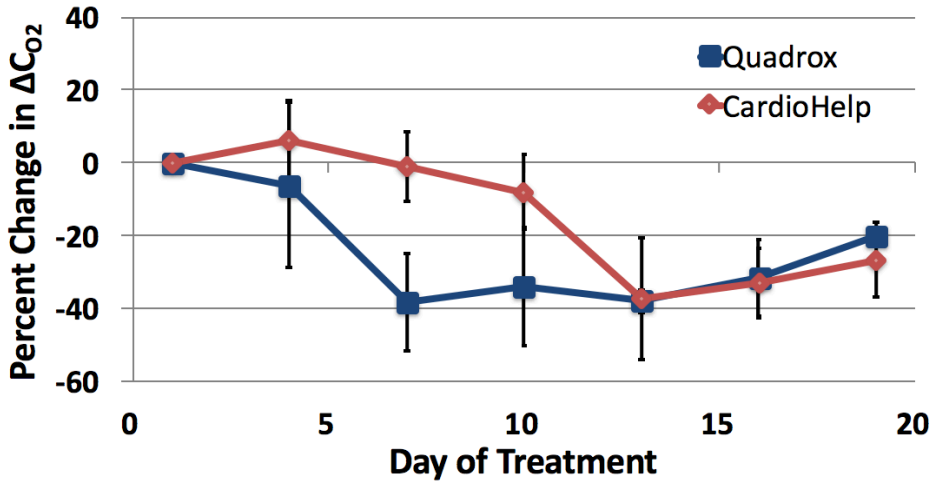


**Figure 2.6**: Percent change in inlet-outlet oxygen content difference ($\Delta C_{O2}$).

### *2.3.3 Heat Maps*

Probability densities of clot formation at the device inlets are seen in **Figure 2.7a**. Viewing the figure from left to right shows the average clot formation in all CH and Ox devices, followed by surviving devices within each group, failed devices, and then by number of days attached. As expected, clot formation is most significant at points most distal from the inlets. For the Qx group, there is increased clot at the inlet in the failed devices, coming predominantly from one corner, but also diffusely spread across the inlet face. In contrast, the two CH devices that failed had hardly any visible surface clot at the inlet. The final two images are averages of all devices removed from days 10-14 and 19-22 for CH, and days 8-11 and 15-21 for Qx, regardless of whether the patient was taken off ECMO or the device failed. The progressive thrombus propagation over time is clearly evident. With the CH devices, clot burden is strictly at the center of the device, farthest from all inlets, whereas in Qx devices, there is a more diffuse pattern of clot formation. **Figure 2.7b** shows probability densities of clot formation at the outlets. Unlike the inlet, clot formation at the CH outlet is indicative of failure, with failed devices showing a diffuse pattern of outlet clot

formation. Similar to its inlet pattern, clot formation in the Qx outlet is more diffuse. Although surviving Qx devices had more clot formation at the corners, it likely didn't affect performance significantly because those areas initially had reduced blood flow. Failed Qx devices, however, have a more diffuse clot pattern, indicating clot formation in the middle of the bundle. As expected, oxygenators associated with longer ECMO runs had increased clot burden at the device inlets. Unlike the Qx outlets which had increasing clot formation over time, the CH did not demonstrate substantial clot formation at its outlets.

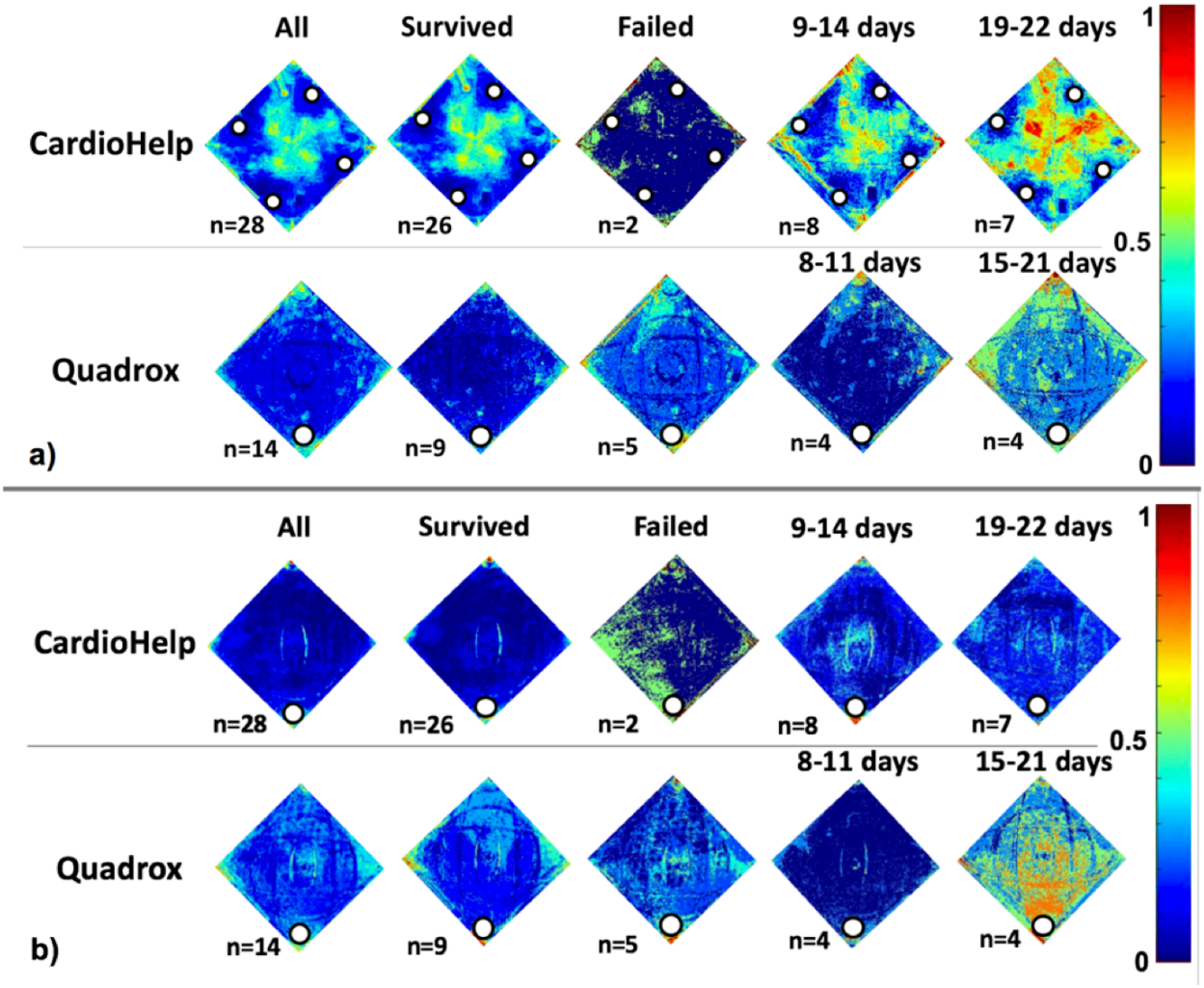


**Figure 2.7**: Probability density of clot formation. a) Device inlets. White circles indicate inlets. b) Device outlets. White circles indicate outlets. Color scale pictured: 0 (dark blue) indicates 0% clot frequency, 1 (dark red) indicates 100% clot frequency.

**Discussion**

The pathway to developing an artificial lung as destination therapy for end stage lung disease patients is currently limited by inadequate device longevity, primarily related to clot formation. The ability to prolong device lifetime would provide the basis for destination therapy, but in order to do so, we must first understand patterns of clot formation. To this end, we evaluated the time-course of thrombus development in two of the most commonly used clinical oxygenators.

Although the two patient populations were similar with regard to their coagulation profiles, with similar starting platelet counts, aPTTs throughout the ECMO course, and no statistically significant difference in flow rates, they had distinct differences in various hematological and device characteristics over time. Overall, the Qx devices fail earlier and more frequently than CH devices, and when they fail, it is with a sudden, exponential increase in resistance. There was an early increase in resistance of the Qx oxygenators, with 4 out of 14 devices failing by day 11. After this, the resistance has a downward trend, but this is due to survival bias of the remaining well-functioning devices. Over the first 4 days, there was no change in resistance of the CH oxygenators, and it was not until day 15 that the first of two devices failed. We observed a distinct increase in resistance at day 22, which was due to the failure of the second device.

Platelet counts decreased significantly more in the Quadrox patients during the course of ECMO, likely due to deposition or destruction. Interestingly, this difference was seen even when sorting the patient populations into finer groups, such as indication for ECMO (**Table 2.2**). The only difference seen between the two groups that may be related is that the Qx patients required higher overall pump speed in revolutions per minute (RPM; CH 3020 ± 62, Qx 3413 ± 95, $p = 0.013$) to maintain similar average device flow between the two groups, ($p = 0.69$). All patients had a centrifugal pump. The Qx was paired with a Rotoflow or Centrimag in all cases, whereas

the CH has an integrated centrifugal pump. The difference in RPMs between the CH and Qx devices persisted regardless of pump type. The relationship between pump speed and pump shear stresses are likely to be different between the pumps, but this suggests that there may be more shear-induced platelet activation and loss in the Qx circuits than the CH circuits. Because these platelets travel directly from the pump to the oxygenator, this may contribute to the accelerated failure in the Qx oxygenators, however this would need be confirmed with further study.

**Table 2.2**: Percent change in platelet count, presented as mean ± standard error of the mean.

| Parameter | Oxygenator | |
|---|---|---|
| | CardioHelp | Quadrox |
| ECMO Indication[1] | | |
| 1 | 7.21 ± 19.80 (n=2) | -60.36 (n=1) |
| 2 | 19.68 ± 27.53 (n=12) | -16.25 ± 28.42 (n=3) |
| 3 | -31.02 ± 20.20 (n=4) | -59.45 (n=1) |
| 4 | 14.39 ± 24.95 (n=5) | -34.08 ± 6.11 (n=4) |
| Cannulation | | |
| VV | 7.29 ± 19.14% (n=15) | -42.23 ± 5.72% (n=4) |
| VA | 8.11 ± 9.62% (n=8) | -27.71 ± 10.09% (n=5) |
| Failed Devices | 31.5 ± 5.03% (n=2) | -29.88 ± 18.13% (n=5) |
| Survived Devices | 5.97 ± 18.86% (n=21) | -38.86 ± 8.30% (n=4) |

[1]ECMO indications: 1 primary respiratory failure (viral/bacterial/aspiration pneumonia, flu), 2 acute respiratory distress syndrome (ARDS), 3 other pathologies (idiopathic

As a measure of gas transfer performance, we calculated the inlet-outlet oxygen content difference ($\Delta C_{O2}$). This metric was chosen, rather than oxygen transfer, to eliminate some of the effect of device weaning since oxygen transfer is nearly linearly related with oxygenator blood flow rate. We identified an immediate decrease in $\Delta C_{O2}$ of the Qx oxygenators, which correlates with the increase in resistance seen in this group. Together, these suggest an increased early clot burden in the Qx oxygenators. On approximately day 13, the CH $\Delta C_{O2}$ declines substantially, which is around the same time the average resistance of this group exceeds that of the Qx group. After approximately 13 days, the remaining Qx devices and the CH devices show similar gas exchange function. Together, these results suggest that Qx devices are more prone to early failures in the first 10 days, but surviving devices function well thereafter relative to the CH devices.

The program used to analyze the images was able to clearly demonstrate clot formation patterns. In the CH devices, thrombus grows with time from the center of the device, farthest from the four inlets. It is likely, therefore, that the higher blood velocity at each of the four device inlets washes away clotting factors and thus maintains an open blood path, whereas the central region away from the inlets suffers from a mix of recirculation and stagnation, leading to rapid clot formation. Interestingly, the two CH devices that failed did not have substantial visible clot burden at the inlets, but had significantly more clot formation at the device outlet. It appears that the clot formation in the CH inlet does not interfere significantly with the normal blood flow path in this oxygenator, and thus little change in resistance is seen. However, CH devices with increasing resistance likely have more diffuse clot formation throughout the fiber bundle that grows from the inlet side toward the outlet with increasing concentrations of activated platelets and clotting factors. Notably, there were no differences found between the two patients with failed CH oxygenators, demographically or hematologically, that could explain why these devices failed more quickly.

In the Qx oxygenators, clot formation is more diffuse, although there is a general trend towards more clot formation at the point in the inlet manifold farthest from the blood inlet connector. This diffuse pattern of clot formation is likely the cause of the early failures in these devices. Moreover, unlike the CH oxygenators, the Qx outlets had a significant amount of diffuse clot that grew over time.

Overall, we were able to demonstrate differences in patterns of clot formation, platelet consumption, resistance increases, and diminishing gas exchange efficiencies between the two oxygenators. The greater longevity of the CH oxygenators suggests that a more distributed, four-inlet approach is better than a single-inlet. Furthermore, although visual inspection is one of the

considerations when deciding to switch out a device, our heat maps show that for the CH, only clot burden at the outlet correlates with device failure, which may be a subtle indicator given its understated visual manifestation. Additionally, percent increase in resistance appears to correlate with loss in gas exchange capabilities; for example, as the average resistance of CH increases around day 10, the $\Delta C_{O2}$ decreases accordingly. Lastly, CH devices seem to provide more durable gas exchange than the Qx. Although not part of our study, the increased durability of CH may make it more cost effective than the Qx if a long ECMO run is anticipated due to less frequent need for oxygenator switch-outs. Although an economic analysis was not included in this study, it could form the basis for a breakeven financial analysis that includes anticipated duration of ECMO support.

One limitation of this study is that our images only evaluate the inlets and outlets of the device and do not indicate the clot formation patterns on the interior. Future studies should consider performing similar assessment of the internal aspects of the fiber bundle, either by cutting devices open or using non-invasive imaging techniques. Other useful future studies to help explain the observed differences would include analysis of the relative rates of platelet activation by the pumps when isolated from their oxygenators and more detailed analysis of platelet coagulation, including both extent of platelet activation and function, and concentration of activated coagulation factors. One final limitation is that all information came from a single institution. Patient and circuit management differs based on institutional and clinician preference, which could influence the functional durability of the oxygenators.

## Chapter 3: Determination of the Optimal Safe *in vivo* Dose of NO in the Sweep Gas

### 3.1 Introduction

Coagulation at a blood-biomaterial interface is largely attributable to two synergistic mechanisms: protein adsorption and platelet adhesion. Fibrinogen adsorption causes a conformational change, allowing the unactivated form of platelet receptor GpIIb/IIIa to bind, inducing platelet immobilization, activation, and aggregation.[131] Similarly, FXII adsorption initiates the intrinsic branch of the coagulation cascade, thrombin formation, and platelet activation.[131] Platelet activation then accelerates progression of the coagulation cascade, resulting in thrombus formation. To limit this, both of these processes should optimally be inhibited simultaneously and ideally only at the biomaterial surface to allow for normal clotting in the patient. A promising means of doing this would be to combine surface coatings that eliminate protein adsorption and surface release of nitric oxide (NO), an extremely short-acting platelet inhibitor.

Among its many properties, NO is a short acting (half-life 0.05-5s in blood),[144,161] potent platelet inhibitor that is produced by endothelial cells.[146] Freely diffusing into platelets, NO increases platelet cGMP levels, decreasing expression of the surface receptors including GPIIb/IIIa, P-selectin, and CD63, and reducing platelet affinity for agonists.[3] Surface NO flux has been previously investigated as a means to reduce thrombosis in oxygenators by adding it to the sweep gas or generating it at the oxygenator surface, resulting in a 20-40% reduction in platelet adhesion.[141,147-151] Additionally, anti-fouling, endothelial-like, zwitterionic polycarboxybetaine (pCB) coatings prevent protein adsorption, reducing local procoagulant concentrations, amplifying the effect of NO, and allowing for marked anticoagulation at lower NO flux rates.[151] It has been previously demonstrated that pCB can result in a 75% reduction in platelet deposition on flat

PDMS sheets. Alone, either NO flux or pCB may not be sufficient to prevent device failure, but *in vitro*, their combination has been shown to decrease platelet adsorption by 90%.[151]

The following study aims to determine the optimal NO concentration that should be used in the sweep gas of artificial lungs. Previous studies have examined similar phenomena, albeit in a cardiopulmonary bypass setting. These studies include significant platelet activation and losses due to tissue trauma and variable NO doses with the same experimental preparation. Although informative, the results are of limited application in the setting of long-term artificial lung support. In theory, increased NO flux should result in less platelet deposition and activation; however, NO results in methemoglobin (metHb) formation, which reduces blood's oxygen carrying capacity and hinders oxygen delivery to tissues.[154] Methemoglobinemia causes cyanosis with levels as low as 10%,[154,155] so our goal is to determine what NO dose will keep metHb <5% while providing the desired anti-platelet effects. To determine this, 0-500 ppm of NO was delivered to rabbits via artificial lung sweep gas in short term *in vivo* experiments, while measuring platelet activation, platelet losses, and metHb generation with resulting blood chemistry changes. The optimal NO dose determined through this study will be used for future experiments that will evaluate the synergistic anti-clotting effects of NO in addition to the pCB coating to prolong the lifetime of artificial lungs.

## 3.2 Methods

### *3.2.1 Device Manufacturing*

Miniature artificial lung (MAL) devices were constructed with siloxane-coated polypropylene hollow fibers. Fiber (Celgard X30-150) was fabricated at 3M Membranes (Charlotte, NC), coated with siloxane by Applied Membrane Technology (Minnetonka, MN), and

knit into fibers mats (43 fibers per inch with a 30-degree crossing angle) by 3M Membranes. The hollow fibers had an average inner and outer diameter of 150 and 203 μm. Each fiber bundle had a path length and frontal area of 1.5 cm and 6 $cm^2$, respectively. The fiber bundle's packing density (solid volume/total volume) was 27%, the same as prototype artificial lungs in development,[104-106,162] compared to a typical value of 50-58% in commercial oxygenators. The prime volume and surface area were 47 mL and 0.1 $m^2$. The surface area was chosen to approximate the surface area:body weight ratio of a CardioHelp or Quadrox oxygenator in an average 70kg person (0.026 $m^2$/kg).

A total of 32 devices were fabricated for *in vivo* testing. A detailed list of fabrication steps can be found in **Appendix B**, but a basic description is as follows. A fiber bundle is created by wrapping the length of fiber around a laser-cut core until its dimensions match specifications, then secured. The bundle is secured inside the housing by encasing both together in PDMS using a centrifuge. The potted region is then cut to expose the lumen of the gas exchange fibers, and a gas cap applied. A completed device can be seen in **Figure 3.1h**.

### *3.2.2 Acute Rabbit ECMO Studies*

*Circuit Components:*

The test circuit (**Figure 3.1**) was a pumped veno-venous (VV) shunt to mimic support in pure respiratory failure. The device inlet circuit components included the following: a 6 cm piece of pressure tubing with 4 side-holes serving as the inflow cannula, 3/16" luer lock polycarbonate tubing connector, 28" long 3/16" inner diameter (ID) Tygon ND 100-65 medical tubing (US Plastic, Lima, OH), 3/16" to 1/4" polycarbonate reducer connector, 3.5" long 1/4" ID Tygon tubing, another 3/16" to 1/4" polycarbonate reducer connector, 2" long 3/16" ID Tygon tubing, and a 3/16"-3/16" luer lock straight polycarbonate connector which attached to the device. The

outlet circuit consisted of one 3/16"-3/16" luer lock straight polycarbonate connector followed by an 8" long 3/16" ID Tygon tubing, and a 3/16" luer lock polycarbonate tubing connector which

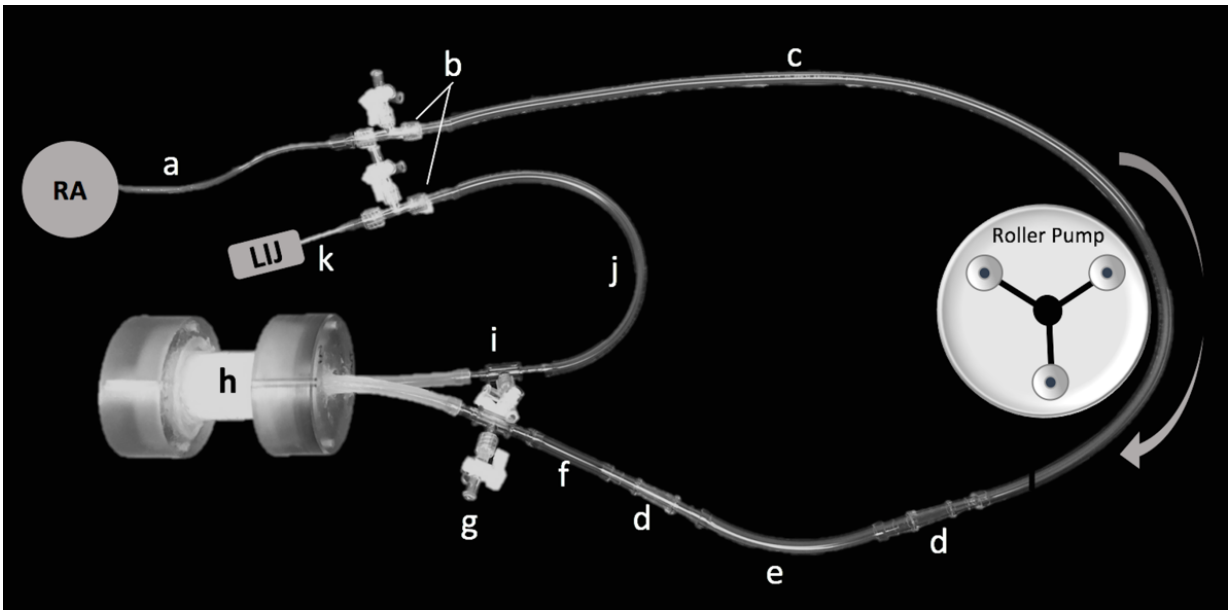


**Figure 3.1**: Extracorporeal circulation circuits. (RA: right atrium, a: 6 cm pressure tubing with 4 side-holes serving as the inflow cannula, b: 3/16" luer lock polycarbonate tubing connector, c: 28" long 3/16" inner diameter Tygon tubing, d: 3/16" to 1/4" polycarbonate reducer connector, e: 3.5" long 1/4" ID Tygon tubing, f: 2" long 3/16" ID Tygon tubing, g: blood inlet pressure port, h: silicone hollow fiber oxygenator (surface area = 0.1m$^2$), i: blood outlet pressure port, j: 8" long 3/16" ID Tygon tubing, k: 14 gauge angiocatheter with 3 side-holes, LIJ: left internal jugular vein.

was attached to a 14 gauge angiocatheter with 3 side-holes that served as the outlet cannula.

*Rabbit Model for Testing:*

The animal housing and surgical procedures were approved by the Allegheny-Singer Research Institute's Institutional Animal Care and Use Committee in accordance with institution and federal regulations. A total of 32 MAL circuits (N = 8/group) were tested to determine NO's antiplatelet effects and toxicity using 32 adult New Zealand rabbits (4.24±0.36kg, Covance, Princeton, NJ) with NO doses of 0, 100, 250, and 500 ppm. All rabbits were initially anesthetized with intramuscular injections of ketamine (35 mg/kg) and xylazine (3 mg/kg). Rabbits were endotracheally intubated and attached to the ventilator, and anesthesia was maintained via

isoflurane gas inhalation at a rate of 1-5%. In order to aid in maintenance of blood pressure stability, Lactated Ringer's (LR) was given intravenously at a rate of 20 mL/(kg/hr) through an aural vein and a phenylephrine infusion (0.5-5µg/(kg/min)) was administered as needed. For monitoring blood pressure and collecting blood samples, the rabbit's left carotid artery was dissected and cannulated with a 16 gauge angiocatheter (Becton Dickinson, Franklin Lakes, NJ).

Blood pressure and heart rate were monitored with a data acquisition system (Biopac Systems, Aero Camino Goleta, CA). Body temperature was monitored with a rectal probe and normothermia (38-40°C) was maintained using warm air circulation via a Bair Hugger (3M, St. Paul, MN). Prior to placement of the VV custom-built extracorporeal circuits, the rabbit left and right internal jugular (IJ) veins were isolated and baseline hemodynamics and blood samples were taken: activated clotting time (ACT) was measured using a Hemochron Response Blood Coagulation System (Accriva Diagnostics, Piscataway, NJ), arterial blood gases (ABG) were measured with an ABL800 FLEX blood gas analyzer (Radiometer, Copenhagen, Denmark), platelet and total white blood cell (WBC) counts were measured with a Coulter Counter Z1 (Beckman Coulter, Brea, CA) according to manufacturer specifications, and hematocrit (HCT) using a micro-hematocrit centrifuge (Damon/IEC Division, Needham Heights, MA). Blood samples for metHb, and platelet surface and soluble P-selectin were taken for later processing (see methods below).

After baseline blood measurements, the circuit was placed into position after being primed with saline solution and 10mg/kg of methylprednisolone to dampen the inflammatory response to device attachment. The circuit was attached by cannulating the left IJ for the circuit outflow and the right IJ for circuit inflow, with the tip of the cannula in the right atrium. The outlet cannula was inserted first, and intravenous heparin was administered at 1 U/min through the cannula to

prevent clotting for approximately four minutes while the right IJ cannula was being inserted. Heparin was then turned off, and remained off for the duration of the experiment to hasten coagulation. The circuit was unclamped and the roller pump (Cobe, Arvada, CO) was turned on and adjusted to a flow rate of 35.7mL/kg/min, to mimic a clinical ECMO flow rate. Blood flow was monitored with an ultrasonic flow probe and flow meter (T402, Transonic Systems Inc., Ithaca, NY). Ten thousand ppm NO in a balance of nitrogen (Matheson Gas, Basking Ridge, NJ) was blended into 100% oxygen to form the mini-lung sweep gas at a rate of double the blood flow rate. The NO-$N_2$ flow rate was adjusted between 3-15 mL/min to achieve total sweep gas NO concentrations of 0, 100, 250, or 500 ppm.

Mini-lung inlet and outlet pressures were measured using pressure transducers (Edwards Lifesciences, Irvine, CA) and a data acquisition system (Biopac Systems, Aero Camino Goleta, CA). Pressures and flow were recorded at the onset of blood flow and every 30 minutes thereafter. In addition, blood samples were collected every hour for measurement of ACT, ABG, platelet and WBC counts, HCT, and metHb. At 30 minutes, 2 hours, and 4 hours, blood samples for soluble and platelet bound P-selectin were also collected.

After 4 hours, the rabbits were euthanized with intravenous potassium (2 mEq/kg). The devices were gently rinsed with saline until the effluent was clear, fixed with 2% glutaraldehyde, and imaged for clot formation on their gas exchange fibers using scanning electron microscopy.

### *3.2.3 Blood Sampling*

Rabbit whole blood samples were collected in non-anticoagulated syringes for HCT, ACT, WBC, metHb, ELISA, and flow cytometry; heparinized syringes for ABG; and citrated syringes for platelet counts.

*P-selectin ELISA:*

An anti-rabbit P-selectin enzyme-linked immunosorbent assay (ELISA) kit was used to determine soluble P-selectin concentration as a measure of platelet activation per manufacturers specifications (MBS011457, MyBioSource, San Diego, CA).

*Methemoglobin:*

The metHb concentration was determined using previously published methods employing cyanide.[163] In brief, 0.1 mL of whole blood is diluted in 10 mL of water to lyse the red blood cells and release hemoglobin. The absorbance is read with the Novaspec Plus spectrophotometer at 645 nm ($Abs_{sample}$). One mL of 10 mg/mL potassium ferricyanide is then added to the sample to convert all free hemoglobin to metHb. Fifteen minutes later, the absorbance is read again at 645 nm, which correlated to a 100% metHb concentration $Abs_{cyanide}$ and a calibration curve was generated by graphing $Abs_{cyanide}$ versus HCT using a total of 103 blood samples from these experiments. The equation from this calibration was then used to calculate, for any HCT, the absorbance of the sample if 100% of the hemoglobin was metHb. To determine metHb%, background absorbance was subtracted out and the $Abs_{sample}$ was divided by the absorbance value determined by the calibration equation for that sample's HCT, then multiplied by 100. Graphical representation below will indicate difference in metHb versus the control.

*Flow Cytometry for P-selectin Expression:*

To determine platelet-bound P-selectin (CD62P) expression, 100 mL diluted whole blood aliquots (1:100 dilution of blood to Hank's Balanced Salt Solution (HBSS) without $CaCl_2$ and $MgCl_2$) were directly prepared for cell surface staining of P-selectin. In three polystyrene tubes containing 100 mL of diluted blood, 4 µL of 1µg/µL collagen in isotonic glucose solution was added to one tube (Chrono-Log, Havertown, PA) for platelet activation, and 4 µL saline was added

to the other two tubes. Next, saturating concentrations (10 μL) of monoclonal anti-rabbit CD62P phycoerythrin (PE) antibody (CD62P antibody (orb303374, Biorbyt, Berkeley, CA) conjugated with PE (LNK021RPE, AbD Serotec, Raleigh, NC)) was added to one collagen and one saline treated tube and incubated for 15 min at room temperature (RT) in the dark. In the other tube containing saline, 10 μL of saline was added as control and also incubated for 15 min at RT in the dark. After the antibody incubation, each tube received 700 mL of freshly prepared 1% formaldehyde buffer (in dPBS) and stored at 4°C until ready for flow cytometric analysis. A BD LSRFortessa cell analyzer (Becton Dickinson, Franklin Lakes, NJ) was used for flow cytometry analysis. Platelet cell populations were identified for data collection by their forward scatter and side scatter light profiles. For each sample, 10,000 total events were collected. Fluorescence intensity of immunostaining is quantified by integrating the area under the curve to determine percent of maximum p-selectin expression.

*Scanning Electron Microscopy:*

The mini-lung was fixed in 2% glutaraldehyde in 0.2 M phosphate buffer for at least 24 hours. The mid-sections of the inlet, middle, and outlet of the fiber bundles were excised and progressively dehydrated by bathing them with 25%, 50%, 75%, and then 100% ethanol solutions for 10 minutes each, and then drying in air for 30 minutes. Dried fibers were sputter-coated with platinum, and imaged with a Philips XL-30 scanning electron microscope at 5 kV accelerating voltage.

### *3.2.4 Data Processing and Statistical Analysis:*

Platelet count and P-selectin data are corrected for the hemodilution caused by circuit attachment using the formula $x_{cor} = x_{raw}(HCT_{pre}/HCT_{post})$, which $x_{cor}$ is the corrected data, $x_{raw}$ is the data prior to correction, and $HCT_{pre}$ and $HCT_{post}$ are the hematocrit before and after circuit

attachment. Data are expressed as mean ± SEM (standard error of the mean). The statistical program SPSS was used to perform all statistical tests. Mixed model analysis with repeated measures was used to compare dependent variables (platelet count, P-selectin, metHb, serum bicarbonate, and serum lactate) between subjects. Analysis of variance (ANOVA) in Excel was used to analyze the differences among group means for ACT and device resistance. A p-value < 0.05 is considered statistically significant for all tests.

### 3.3 Results

#### 3.3.1 *Effect of NO on Coagulation*

The percent increase in ACT from baseline did not differ significantly between groups (average percent change: 0ppm 31.44±3.15%, 100ppm 30.14±5.19%, 250ppm 38.02±3.24%, 500ppm 39.03±3.92%; p = 0.18). In all groups, there was an initial sharp decrease in platelet count, which plateaus around 60 minutes (**Figure 3.2**) in the 0, 250, and 500 ppm groups. The 100 ppm group platelet counts decreased the least and were significantly greater than the control ($p < 0.05$), whereas the 250 and 500 ppm groups did not differ significantly from the control (p = 0.99 and 0.754, respectively). The main effect of the 100 ppm group was to reduce the early marked loss in platelets that occurs within 60 minutes in all other groups.

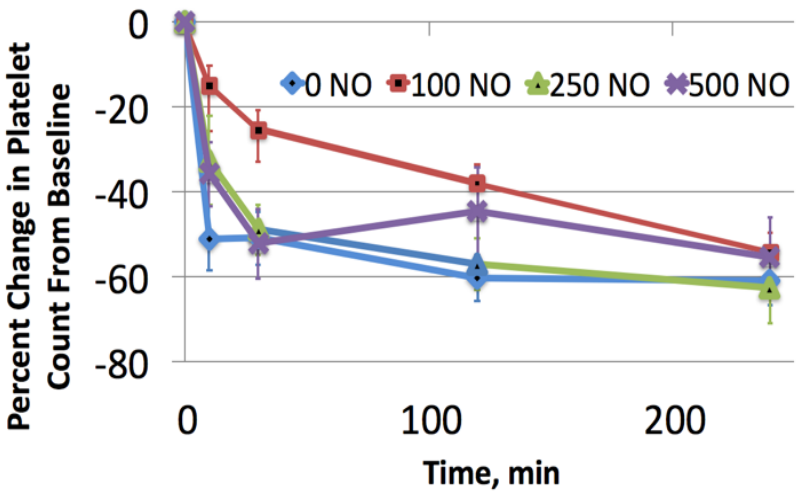


**Figure 3.2**: Percent change in platelet count from baseline.

The concentration of soluble p-selectin increases substantially in the first 30 minutes of each experiment, after which it tends to stabilize. However, NO reduces the initial increase (**Figure**

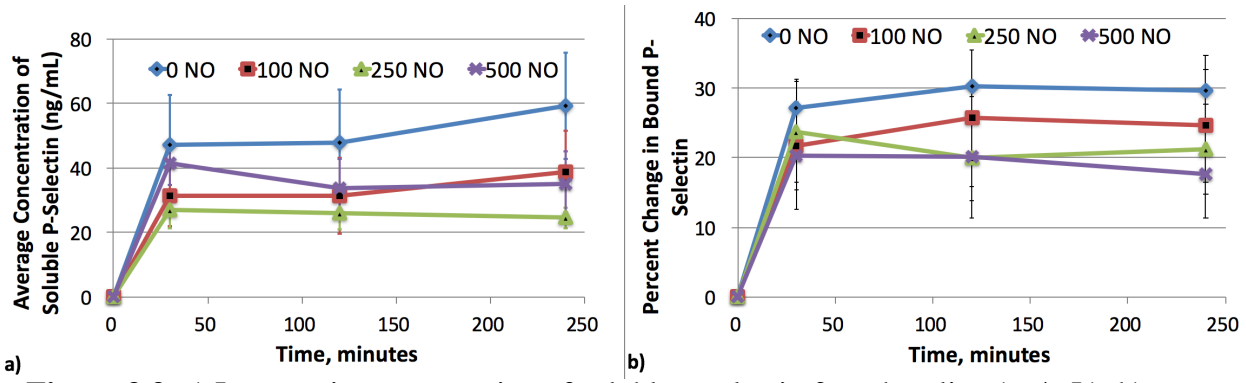


**Figure 3.3**: a) Increase in concentration of soluble p-selectin from baseline (ng/mL), b) Percent change in bound p-selectin concentration from baseline.

**3.3a**, $p < 0.05$). Soluble p-selectin concentrations in the 100 and 500 ppm groups did not differ significantly from the control ($p = 0.33$ and 0.71, respectively), but the 250 ppm group did ($p < 0.05$). Bound p-selectin, measured using flow cytometry, showed the same trend, but the difference was not statistically significant (**Figure 3.3b**, $p = 0.41$). Taken as a whole, this data indicates that NO has a limited effect on platelet surface binding in this setting, but does decrease platelet activation.

There was little visible clot formation on any of the devices given the short duration of the experiments. There is a trend suggesting NO may prevent an increase in device resistance, with the smallest increase in resistance in the 100 ppm group (**Figure 3.4**), however, there was no statistically significant difference ($p = 0.48$). SEM images (**Figure 3.5**) reveal clot formation on the vertical

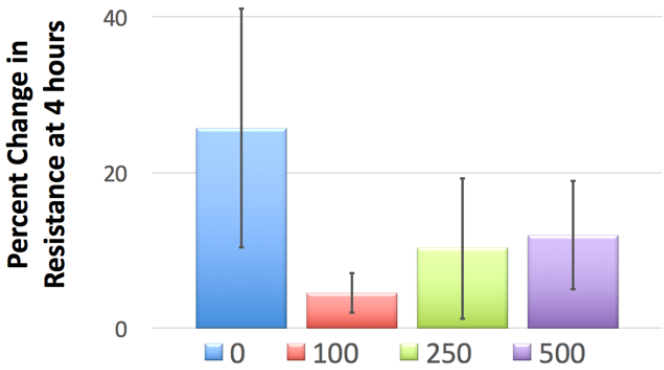


**Figure 3.4**: Percent increase in resistance at 4 hours.

gas exchange fibers, with the most significant amount on the 0 ppm fibers, and much less on all NO fibers. All groups had clot formation on the horizontal weaving fibers, however, which do not release NO.

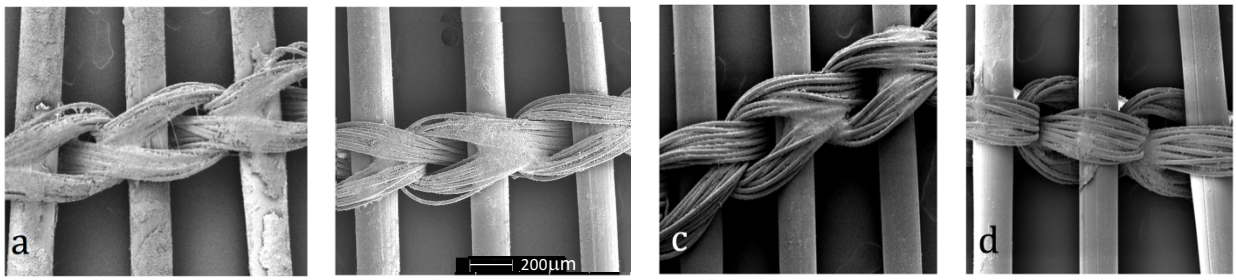


**Figure 3.5**: Representative scanning electron micrographs of gas exchange fibers post-experiment for a) 0 ppm, b) 100 ppm, c) 250 ppm, and d) 500 ppm of nitric oxide. Samples taken from the center of the fiber on the inlet side of the device.

### 3.3.2 *Effect of NO on Methemoglobin Formation and Acidosis*

The metHb concentrations in the 100 and 250 ppm groups did not increase significantly vs. the control ($p = 0.99$ for both), with less than a 0.1% difference with the 0 ppm group. In contrast, the 500 ppm group had an initial sharp increase in metHb that stabilized at an increase around 5% after about 30 minutes (**Figure 3.6**). Accordingly, the 500 ppm group was the only group to result in a statistically significant increase in metHb ($p < 0.01$).

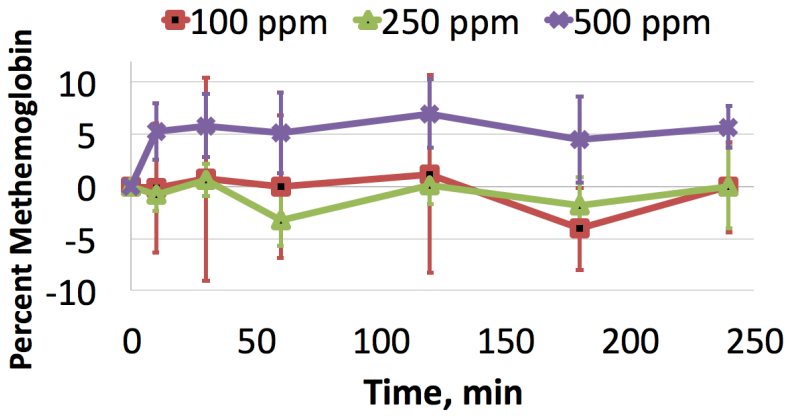


**Figure 3.6**: Change in average methemoglobin relative to the control group.

As a result of increasing metHb concentration, the 500 ppm group demonstrated decreasing oxygen carrying capacity and thus significantly increasing serum lactate ($p < 10^{-9}$) and decreasing serum bicarbonate concentration ($p < 10^{-5}$) (**Figure 3.7**). As a result, the 500 ppm group had 18%

less bicarbonate and 473% more lactate than the control group after 4 hours. There was no significant difference between the control group and the 100 and 250 ppm groups (p = 0.99).

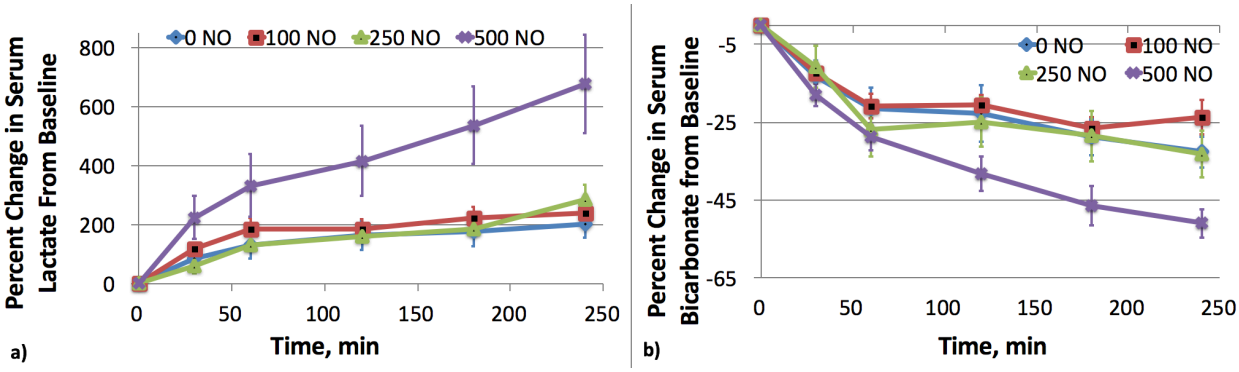


**Figure 3.7**: Percent change in a) serum lactate and b) bicarbonate from baseline.

### 3.4 Discussion

This study aimed to determine the optimal NO concentration that can be used in the sweep gas of artificial lungs. This concentration is defined as the one that minimizes platelet binding and activation while ensuring that metHb increases less than 5%. This same question has been answered clinically when using inhaled NO as a pulmonary vasodilator in patients with pulmonary hypertension. In this setting, metHb levels are typically insignificant when inhaled NO is less than 100ppm, and the risk of significant metHb is generally outweighed by the benefits.[154] However, the 1-2 $m^2$ surface area of artificial lungs is small in comparison to the 50-100 $m^2$ surface area of the native lung, and the mass transfer efficiency is different. Thus, it is possible that higher NO doses in the artificial lung sweep gas could be tolerated without toxicity.

The study results demonstrate that NO in the sweep gas reduces platelet activation, with platelet activation decreasing with increasing NO concentration, but with limitations beyond 250 ppm, perhaps due to NO toxicity as speculated by Sly et al.[164] However, the results also indicate that systemic platelet counts and activation are not correlated when using NO. Systemic platelet losses were significantly reduced at 100 ppm, but in contrast to our hypothesis, platelet losses were

not inhibited significantly at 250 and 500 ppm. Although not expected, this could potentially be due to NO's ability to increase fibrinogen adsorption on artificial materials,[148,165,166] leading to a more complete layer of adsorbed fibrinogen for the 250 and 500 ppm groups.[167] Lantvit et al.[165] hypothesized that NO facilitates fibrinogen adsorption in an altered conformation that doesn't participate in coagulation. This study's results, however, suggest that it is more likely that platelets still bind to this adsorbed fibrinogen, but the presence of NO keeps those adsorbed platelets from activating, as evidenced by the lower p-selectin levels for the 250 ppm group. The 100 ppm group appears to limit this effect, limiting platelet adhesion while providing a modest level of inhibition.

Previous investigations into NO's effects on platelet counts during ECMO and cardiopulmonary bypass (CPB) have been positive but not conclusive. Mellgren et al.[168] administered 40 ppm NO into the sweep gas in 10 patients. Higher platelet counts were observed postoperatively in the NO group, though this difference was not statistically significant. Two years later, Tevaearai at al.[147] delivered 80 ppm NO in the sweep gas to calves on ECMO. NO prevented an increase in device resistance. Platelet counts stabilized after 2 hours, with no difference between the NO and control groups, but the initial decrease in platelet count during the first hour was far more pronounced in the control group than the NO group (-23.1±13.6% NO vs. -41.4±10% control, $p = 0.05$).

The present study had similar results. Focusing on the 100 ppm group, the initial drop in platelet count seen at 30 minutes was significantly less profound than the control group (-25.2±7.7% NO vs -50.8.2±6.3% control). This benefit continued through 2 hours (-38.0±5.8% NO vs -60.1±5.4% control), before diminishing to an insignificant benefit at 4 hours (-54.1±4.9% NO vs -60.7±5.8% control). During short-term rabbit ECMO, Amoako et al.[148] demonstrated that NO flux via NO-generating-fibers in an ECMO setting resulted in markedly less surface clot formation

compared to control groups, with hardly any visible platelets on electron micrographs and no increase in device resistance. However, there was no difference in platelet counts between groups. Similar findings were seen by Sly et al.[152] during CPB. Amoako et al. speculated that although NO prevented platelet binding on the surface, platelets were still becoming activated downstream by surface-generated procoagulant molecules. These results parallel the current study, which revealed minimal platelet binding on 250 and 500 ppm NO fibers as seen on SEM, but no difference in circulating platelet counts between these two groups and the control. This may be explained in part by the surface generation of procoagulant molecules, and it may also be due to platelet binding to weaving fibers and remainder of the circuit, which do not release NO. All groups had some degree of platelet binding to these weaving fibers, although it was less in the NO groups.

The above studies used NO doses of 40, 80, 500, and 1000 ppm. It is also possible that 40 ppm is not high enough to have significant effects on platelet counts, but 500 and 1000 ppm are too high, resulting in a fibrinogen layer as discussed above or a degree of NO toxicity that affects platelet function. Our results at 100 ppm look similar to those of Tevaearai at al.[147] at 80 ppm, with an initial beneficial effect on platelet counts that dissipates thereafter. Our test dose of 100 ppm may then represent an ideal dose. Conclusions are confounded, however, by the use of polypropylene fibers in previous studies and PDMS-coated polypropylene fibers in this study, which could result in different degrees of NO flux, as well as the mixture of ECMO and CPB studies, which will have different degrees of surgical trauma.

Although the results indicate that NO flux is capable of reducing platelet binding and activation, the results also demonstrate some limitations. The SEM images clearly show that the beneficial effects of the NO flux are markedly less effective at limiting platelet adhesion and activation on the horizontal weaving fibers used to connect the gas exchanger fibers into a fiber

mat for manufacturing. These weaving fibers are densely packed, contain areas of stasis, and do not carry and release NO. In standard mats, these areas typically occur every 0.5-1 cm, should be minimized if possible, and may, in particular, benefit from anti-adsorptive coatings.

The addition of an anti-adsorptive pCB coating should also temper, if not negate, NO's limitations on platelet activation and binding. Without coatings, high concentrations of platelet agonists due to protein adsorption likely blunt inhibition by NO, requiring larger NO fluxes to prevent coagulation and thus higher metHb levels. The addition of pCB, however, will decrease fibrinogen and FXII adsorption, resulting in less generation of platelet agonists and decreased platelet binding.[151] Together, pCB and NO should work synergistically to improve each other's effectiveness.

With respect to toxicity, results demonstrate that 100 and 250 ppm are safe, leading to no significant increase in metHb and no metabolic acidosis from reduced tissue oxygen delivery. On the other hand, 500 ppm is not safe, leading to a significant increase in metHb with concomitant acidosis. The optimal NO sweep gas concentration then depends on whether it is ideal to have less platelet binding using 100 ppm or less platelet activation using 250 ppm. Ultimately, the 100 ppm group has a smaller increase in blood flow resistance over time than all of the groups, indicating that 100 ppm is optimal and, moreover, provides an additional margin of safety should the dose deviate from the intended dose.

In conclusion, 100 ppm NO does not increase metHb concentrations significantly, appears to reduce platelet consumption more than 250 or 500 ppm, and will thus be used in all future experiments. When used in conjunction with anti-adsorptive zwitterionic pCB coatings, we expect a synergistic relationship that will further prevent platelet activation and clotting of artificial lung devices. The question remains, however, as to their effectiveness over longer periods of time

beyond four hours; as such, future studies will extend experiment length to eight, if not more, hours to determine whether the prevention of fouling endures over time.

## Chapter 4: *in vitro* in vitro Gas Exchange and Blood Flow Resistance of the Pulmonary Assist Device (PAD)

### 4.1 Introduction

The PAD is smaller than any device currently available and employs a loosely packed fiber bundle that leads to a marked reduction in resistance and significant improvements in biocompatibility overall. The device will be modular, which has not been attempted in any other device for this purpose, and will allow for routine, minimally invasive and safe device exchange. Modularity will allow for one or two devices in parallel to be used, depending on the needs of the patient. A single device should be sufficient for hypercapnic COPD patients because it will remove ample $CO_2$, and significant $O_2$ transfer is not necessary. Additionally, these patients can tolerate limited time without support during device exchange. On the other hand, hypoxic patients and those with PH will require two devices in parallel. First, together they will provide sufficient gas exchange. Second, and importantly, these patients can suffer cardiac arrest within seconds of device support cessation. Parallel modularity will allow one device to remain functioning while the other is replaced or if it fails. Though compliant housings have demonstrated improved biocompatibility, the PAD will be smaller and utilize solid housings, allowing patients to be ambulatory without fear of device damage. Most importantly, the device will be low in resistance and minimally thrombogenic to allow for months of support without device exchange.

If successful, this would allow for destination therapy, during which patients could leave the hospital while supported with an artificial lung. This would create a change in respiratory care similar to the change in cardiac care caused by ventricular assist devices. We believe our preliminary results warrant the start of this development process and that this is a challenging, yet realistic goal.

### 4.1.1 *Design Goals*

To appropriately model and construct our device, we must first determine what performance and design goals are needed. Clinical need was determined through review of Columbia University's ECMO data and consultation with clinical collaborators. First, the device must process blood flows needed to support all target patient populations; **Table 1.1** states that device flow needed by patients on ECMO ranged from 1.7-3.1 L/min. Additionally, the device should be low in resistance. When attached in a pumped configuration, high device resistance requires higher pump speeds which increases blood damage and activation[169]; when attached centrally, a high resistance device increases the workload on the already-strained heart. Therefore, the PAD should have a resistance approaching that of the native lung with 2 devices in parallel. The surface area and resistance of the commonly used oxygenators Qx and CH are 1.8$m^2$ and 5 mmHg/(L/min). Additionally, one of the primary limitations to patient mobility on ECMO currently is the large size and complexity of ECMO circuits. Thus, the device and its system must be small.

Therefore, our design goals for this device are as follows: 1) receive up to 4 L/min of cardiac output 2) achieve > 95% outlet $O_2$ saturation at 2 L/min blood flow rate, 3) remove 100 mL/min of $CO_2$ at a sweep gas flow of 5 L/min 4) have a resistance less than 2.5 mmHg/(L/min) at 2 L/min per module, much less than any gas exchanger currently on the market, 5) develop less than a 100% increase in resistance over a period of 2 months, and 6) incorporate gas exchange fibers that eliminate plasma and gas leakage to ensure maintenance of gas transfer and exclusion of air emboli. Each module (**Figure 4.1**) has a 0.9 $m^2$ fiber bundle created from PDMS coated polypropylene fibers (Membrana fibers coated by Applied Membrane Technology). Preliminary

computer modeling (see below) indicates that these design specifications can be met, and *in vitro* testing confirmed these predictions.

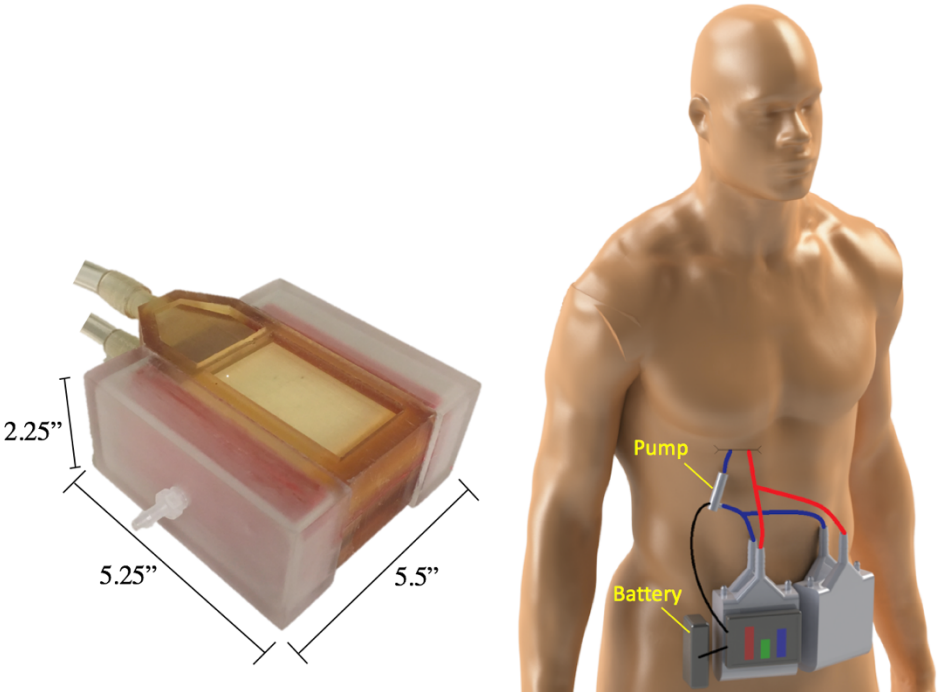


**Figure 4.1**: PAD design and patient with 2 PAD modules at belt

### *4.1.2 Preliminary Data*

Previous work in our lab utilizing computer modeling indicates that our performance goals can be met with our design. The PAD design was guided by mathematical models that estimate bundle resistance[170-174] and $O_2$[175] and $CO_2$ exchange.[176] An estimate for the inlet and outlet resistance was obtained using minor loss coefficients determined from a similar device.[162] Model results were used to choose the appropriate fiber bundle and housing dimensions. Ultimately, the PAD was designed with a fiber bundle frontal area of 70 $cm^2$, a fiber bundle path length of 2.8 cm, and a gas exchange surface area of 0.9 $m^2$, substantially less than 1.8$m^2$ in current ECMO oxygenators. Drawing from the experience of designing the cTAL, the PAD design incorporates a loosely packed fiber bundle and 45 degree tapering inlet and outlet housing sections.[106,170] This results in a device with low resistance and efficient gas exchange, meeting the needs of a variety of chronic lung diseases with one or two modules in parallel. The resistance of the fiber bundle for each

module is estimated to be approximately 0.509 mmHg/(L/min), yielding a total module resistance of 1.5 mmHg/(L/min), which is far less than the resistance of commercially available ECMO oxygenators (5 mmHg/(L/min)). Each module is theoretically capable of increasing blood oxygen saturation from 65% to 95% at 2 L/min of blood flow, allowing for a total allowable blood flow through the system to exceed 4 L/min with two modules in parallel, nearly the 5 L/min current full-size ECMO oxygenators can support. A two-module PAD will also transport approximately 120 ml/min of $CO_2$ using a reasonable sweep gas flow rate of 5 L/min, attainable with at-home oxygenators.

## 4.2 Materials and Methods

### *4.2.1 Device manufacturing*

Six PAD housings were prototyped with rapid-prototyped stereolithography housings using Accura SL 5530. Although less biocompatible, 3-D printing allows for inexpensive, easily prototyped devices for *in vitro* testing prior to arduous and expensive *in vivo* studies. Similar housings have proven sufficient for testing of up to a week in this setting.[110] Once the full PAD was constructed (see **Appendix B** for a detailed list of fabrication steps), the following studies were conducted to confirm performance goals. In each experiment, four single-module devices were tested.

### *4.2.2 Gas Exchange Testing*

*Gas Resistance*

As mentioned in the fabrication steps in **Appendix B**, the devices must be cut after potting to open up the hollow fibers for gas exchange. For quality control, the gas resistance of all devices was tested as a measure of fiber plugging. If the gas resistance of a device was not less than

1.5mmHg/(L/min), it did not proceed to *in vitro* testing. To test gas resistance, one gas cap was

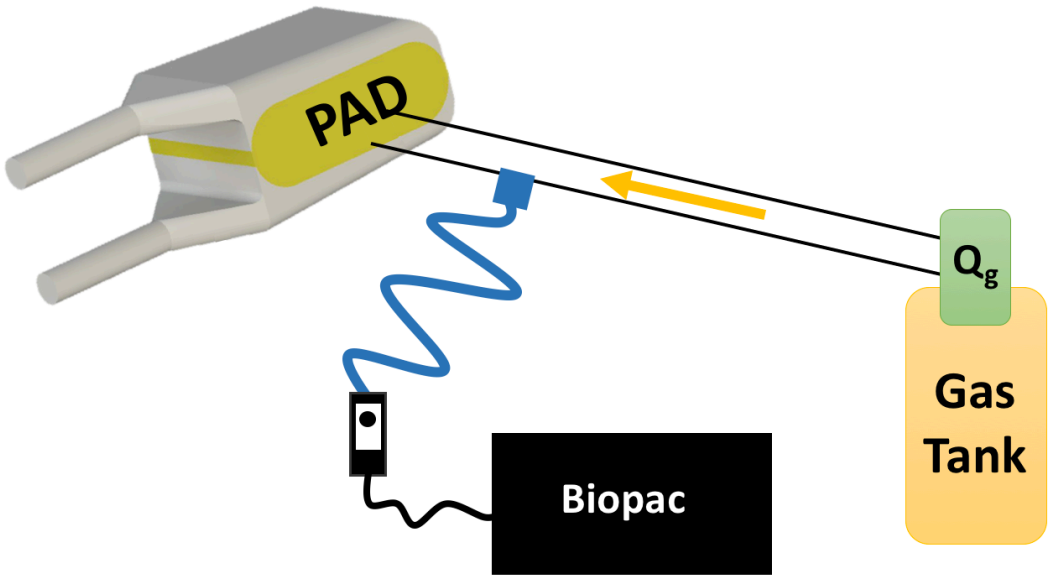


**Figure 4.2**: Gas resistance circuit consisting of gas tank, gas flowmeter ($Q_g$), pressure tubing filled with water (blue line), and pressure transducer connected to Biopac computer.

attached to the PAD using silicone RTV. A tube was connected to the gas cap with a connector with a side luer. A piece of pressure tubing was connected from a pressure transducer to the luer connection, and filled with water until it reached the level of the air tube (**Figure 4.2**). A baseline pressure was measured with a sweep gas flow rate of zero, and this value was subtracted from all subsequent measurements. Sweep gas was then flown at rates of 0.5, 1.0, 1.5, 2.0, 2.5, 3.0, and 3.5 L/min, and the pressure at the pressure transducer was measured. Gas resistance was calculated as follows

$$Resistance = \frac{(P_{gas,in} - P_{gas,out})}{Q_{gas}} = \frac{P_{gas,in}}{Q_{gas}}$$

where $Q_{gas}$ is the sweep gas flow rate, $P_{gas,in}$ is the pressure at the gas inlet, and $P_{gas,out}$ is the pressure at the outlet, but $P_{gas,out}$ can be taken as zero since it is open to the atmosphere.

*Gas Exchange*

The gas transfer performance of four PADs that met gas resistance specifications was tested in an *in vitro* circuit using heparinized and citrated bovine blood conditioned to Association for the Advancement of Medical Instrumentation (AAMI) venous standards (**Table 4.1**).

**Table 4.1**: AAMI blood conditioning specifications

| | |
|---|---|
| Hemoglobin (g/dL) | 12±1 |
| pH | 7.4±0.1 |
| $pCO_2$ (mmHg) | 45±5 |
| Oxygen Saturation (%) | 65±5 |
| Base Excess (mmol/L) | 0±5 |
| Temperature (°C) | 37±2 |

Blood was conditioned using a recirculation circuit consisting of a centrifugal pump, three commercial Quadrox oxygenators (Maquet, Germany) in parallel, and a blood reservoir (**Figure 4.3**). There was a separate water circuit used to warm the blood via the Qx oxygenators' built-in heat exchanger consisting of a hot water bath (Lab-Line Shak-R-Bath, Barnstead Lab Line, Melrose Park, IL) and a roller pump (Cobe, Arvada, CO), and the temperature of the circulating blood was monitored with a temperature probe (YSI, Yellow Springs, OH) and monitor (YSI, Yellow Springs, OH or Seabrook Medical Systems, Inc, Cincinnati, OH). The sweep gas used to condition the blood consisted of varying levels of $O_2$, $N_2$, and $CO_2$. Repeated blood gas samples were taken until AAMI venous blood standards were met through the adjustment of sweep gases, the additional of saline to correct hemoglobin, and/or the addition of sodium bicarbonate to correct base deficit, if needed. After about two hours, once the blood was conditioned, blood flow was rerouted from the conditioning circuit to the PAD. For oxygen exchange, blood was pumped through the PAD at blood flows of 1, 2, and 3 L/min and sweep gas was 100% $O_2$ at flow rates 2x

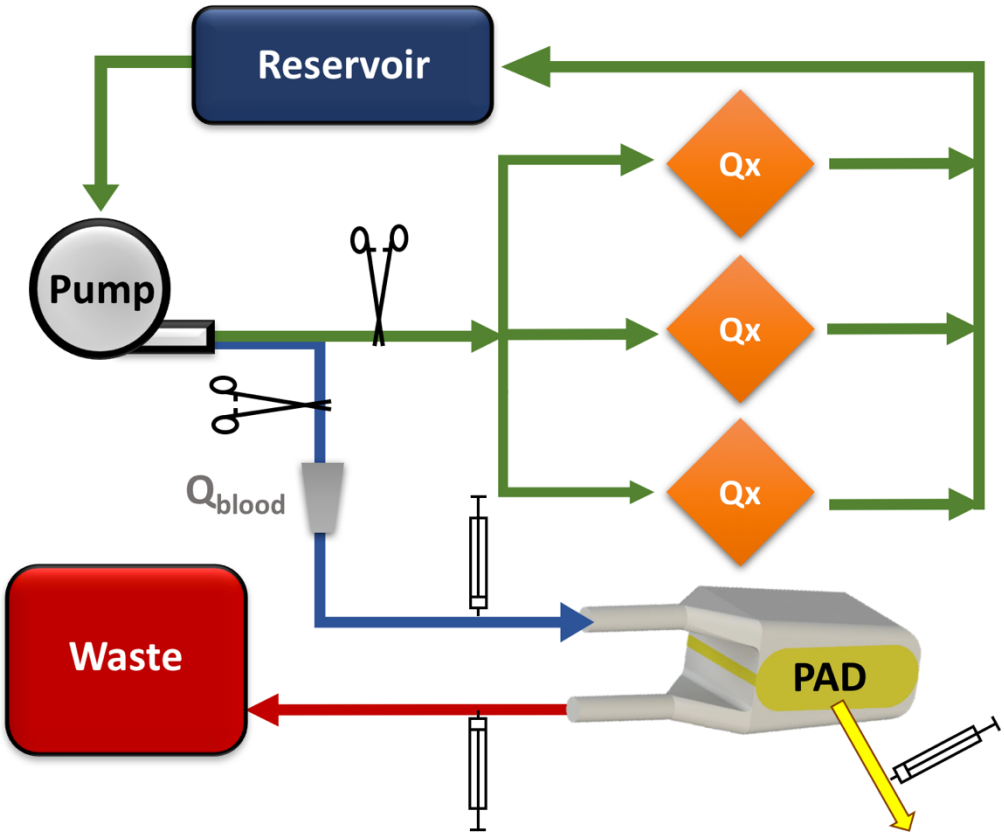


**Figure 4.3**: *In vitro* gas exchange circuit comprised of a conditioning circuit (green arrows) and test circuit (blue and red arrows) separated by tubing clamps, consisting of a centrifugal pump, 3 Quadrox (Qx) oxygenators in parallel, a reservoir filled with bovine blood, a PAD, and a waste bucket.

that of blood. For $CO_2$ exchange, blood was pumped at 2 L/min and the sweep gas was adjusted to 2, 5, and 10 L/min.

At each condition, blood samples were drawn in duplicate from the PAD inlet and outlet and analyzed with an ABL800 FLEX blood gas analyzer (Radiometer, Copenhagen, Denmark) to measure $PO_2$, oxygen saturation, and hemoglobin concentration. Additionally, a sweep gas sample was also drawn in duplicate at each condition and analyzed with the blood gas analyzer to measure the $CO_2$ content to be used in $CO_2$ exchange calculations. All duplicate samples were averaged and PAD gas transfer rates were calculated.

Oxygen transfer rate ($V_{O2}$) was calculated as follows,

$$V_{O2} = Q_b(Content_{O2,out} - Content_{O2,in})$$

where $Content_{O2,out}$ is the oxygen content in the blood from the outlet of the device, and $Content_{O2,in}$ is the oxygen content in the blood from the inlet of the device. To determine $O_2$ content, the following equation was used

$$Content_{O2}\ (mL\ O_2/L\ blood)$$

$$= \left(\left(Hgb\frac{g}{100\ mL\ blood} \times 1.34\frac{mL\ O_2}{1g\ Hgb} \times \left(\frac{sO_2}{100}\right)\right)\right.$$

$$\left. + \left(PO_2 \times 0.00314\ \frac{mL\ O_2}{100mL\ blood}\right)\right) \times \frac{1000mL\ blood}{1L\ blood}$$

which combines the amount of oxygen that is bound to hemoglobin (red part of the equation) with the oxygen that is dissolved (blue part of the equation). *Hgb* is the grams of hemoglobin per 100 mL of blood, 1.34 is how much oxygen a gram of hemoglobin can carry, $sO_2$ is the oxygen saturation, $PO_2$ is the partial pressure of oxygen in blood, and 0.00314 is the amount of oxygen that is dissolved in plasma.

The volume rate of $CO_2$ exchange ($V_{CO2}$) in mL/min was calculated from the sweep gas outlet sample via

$$V_{CO2} = Q_g C_{CO2}$$

where $Q_g$ is the sweep gas flow rate through the device in mL/min and $C_{CO2}$ is the fractional concentration of $CO_2$ in the sweep gas outlet as determined by the gas analyzer.

### *4.2.3 Bloodflow Resistance Testing*

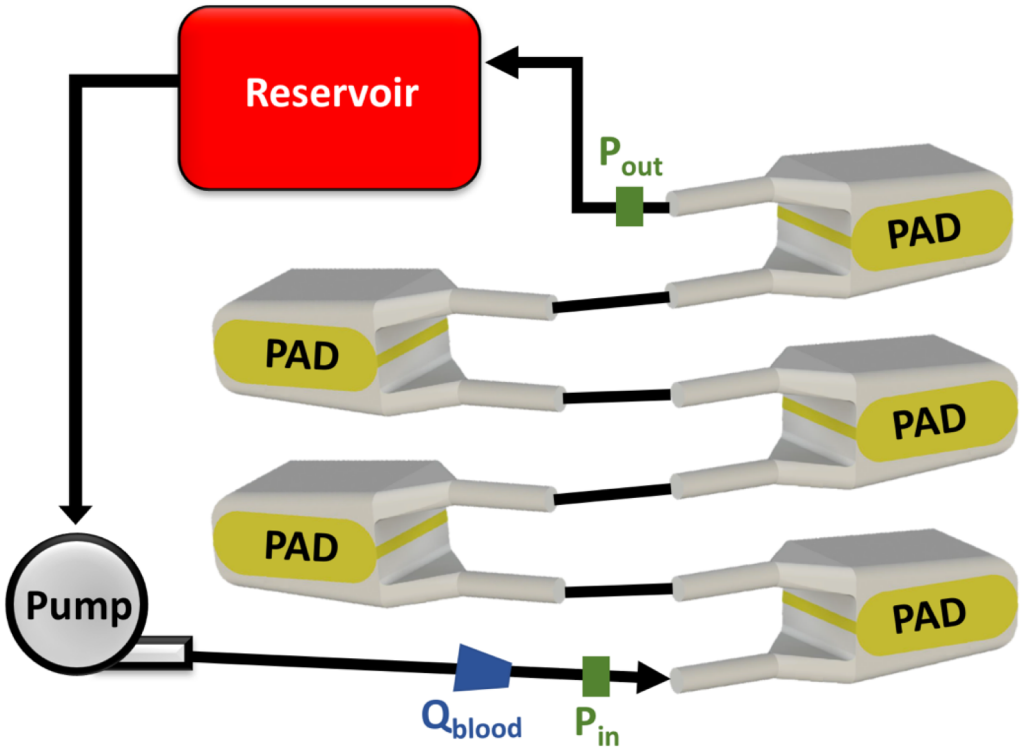


**Figure 4.4**: *In vitro* testing circuit for resistance study, consisting of centrifugal pump, five PADs, and reservoir filled with bovine blood. Flow probe ($Q_{blood}$) in place proximal to PADa and two pressure lines were connected to the device at the inlet ($P_{in}$) and outlet ($P_{out}$).

*In vitro* resistance testing was performed in a circuit consisting of a centrifugal pump (Terumo Cardiovascular, Ann Arbor, MI or Medtronic, Minneapolis, MN)), PAD (n = 5), and reservoir filled with bovine blood that had been heparinized and heated to 37°C (**Figure 4.4**). PAD inlet and outlet pressures were measured using pressure transducers (Edwards Lifesciences, Irvine, CA) and a data acquisition system (Biopac Systems, Aero Camino Goleta, CA). Blood flow was monitored with an ultrasonic flow probe and flow meter (T402, Transonic Systems Inc., Ithaca, NY). Pressure drops were so small that the Biopac was not able to measure accurately; therefore, the devices were tested in series and the total pressure drop of the system was measured and divided by the number of devices in series. The total resistance of the circuit was then measured, the resistance of the tubing was subtracted, and it was divided by five to give an estimated

resistance per device. Blood was pumped through the PAD at flow rates of 0.5, 1, 2, 3, and 4 L/min and device resistance was calculated at each condition using the following equation

$$Resistance\ per\ device = \frac{\left(\frac{(P_{in} - P_{out})}{Q_b}\right)}{Total\ \#\ PADs\ in\ series}$$

where $P_{in}$ and $P_{out}$ are the pressures measured at the PAD inlet and outlet, respectively, and $Q_b$ is the blood flow.

### *4.2.4 Dimensionless analysis*

*Introduction*

Bovine blood was utilized for the *in vitro* experiments, but from the results, one can not only predict device performance in humans under various conditions, but also to predict the performance of differently sized fiber bundles for future bundle modeling. Hollow fiber gas exchangers are similar to tube heat exchangers, but they exchange $O_2$ and $CO_2$ rather than heat and the interactions are far more complex. As such, heat exchange theory has been modified by accounting for uptake of $O_2$ by hemoglobin to apply it to gas exchangers.

*Determination of m and Φ*

According to gas exchange theory, the gas exchange characteristics can be modeled locally for a small differential distance through the fiber bundle using the following equation:[177]

$$\Phi * {N_{Re}}^{-m} = \frac{D_f * por}{4 * (1 - por)} * \left(\frac{\mu}{\rho * Diff_{wb}}\right)^{2/3} * \frac{\left(1 + \lambda\left(P_{O_2}\right)\right)^{2/3}}{\left(P_{O_{2_g}} - P_{O_{2_b}}\right)} * \frac{dP_{O_2}}{dx}$$

Dimensionless gas exchange constants m and Φ can be calculated using the results of *in vitro* gas exchange testing and the following equations. These values can then be fed back into the previous equation to predict oxygen exchange not only for human blood under various flow rates, but also for differently sized fiber bundles.

With the exception of m and Φ, all variables are known (and will be defined in detail below): $N_{Re}$ is Reynolds number, $D_f$ is the outer diameter of the gas exchange fibers, ρ is the density of blood, μ is the dynamic viscosity of blood, por is the porosity of the fiber bundle, $Diff_{wb}$ is the diffusivity of oxygen in whole blood, and $\lambda(P_{O2})$ is a sink term that takes into account oxygen uptake by hemoglobin.

The solution for this equation for the entire blood flow path through the bundle can be obtained through integration and simplification to form,

$$\Phi * {N_{Re}}^{-m} = \frac{D_f * por}{4 * (1 - por)} * \left(\frac{\mu}{\rho * Diff_{wb}}\right)^{2/3} * \frac{1}{PL} \int_{P_{O2_{in}}}^{P_{O2_{out}}} \frac{\left(1 + \lambda\left(P_{O_2}\right)\right)^{2/3}}{\left(P_{O_{2_g}} - P_{O_{2_b}}\right)} dP_{O_2}$$

which utilizes the known inlet and outlet partial pressures of oxygen from experimental data for integration. Known variables can be calculated as follows: The path length (PL) is the distance the blood must travel through the fiber bundle, which is 2.79cm for the PAD, and $P_{O2in}$ and $P_{O2out}$ are the inlet and outlet partial pressures of oxygen in the blood, respectively. $N_{Re}$ is defined as,

$$N_{Re} = \frac{Q_b D_f \rho}{(1 - por) A_f \mu}$$

where $Q_b$ is blood flow, $D_f$ is the outer diameter of the gas exchange fibers, ρ is the density of blood, $A_f$ is the frontal area, μ is the dynamic viscosity of blood in Poise, defined as,

$$\mu = (2.205E - 5) * e^{\left[\frac{1965}{273.15 + T} + (2.31 * HCT)\right]}$$

and por is the porosity of the fiber bundle, which is equivalent to the void fraction of the fiber, or one minus the packing density. In other words, porosity is the amount of open space for blood to travel through compared to the volume taken up by fiber:

$$Por = \frac{Total\ Volume - Fiber\ Volume}{Total\ Volume} \times 100$$

$$; where\ Fiber\ Volume = \pi(radius\ of\ fiber)^2(length\ of\ fiber) \times \#fibers$$

$Diff_{wb}$ is the diffusivity of oxygen in whole blood in $cm^2/sec$ and can be calculated via the following series of equations;

$$Diff_{wb} = \frac{Diff_p * k_p * [1 + (G * \mathcal{X})]}{k_{wb} * (1 - G)}$$

$$Diff_p = (1.62e - 5) * 1.025^{(T-25)}$$

$$Diff_c = (0.76e - 5) * 1.025^{(T-25)}$$

$$k_p = (2.855e - 5) * 1.01^{(37-T)}$$

$$k_c = (4.658e - 5) * 1.01^{(37-T)}$$

$$k_{wb} = (k_c * HCT) + [k_p * (1 - HCT)]$$

$$G = \frac{HCT * (N - 1)}{N + \mathcal{X}}$$

$$N = \frac{k_c * Diff_c}{k_p * Diff_p}$$

$$\mathcal{X} = \frac{1 - [N * (1 - \beta)]}{N - 1 - \beta}$$

$$\beta = \frac{(N - 1)}{3} * \left\{ \frac{2}{1 + \left[(N - 1) * \left(\frac{m_{rbc}}{2}\right)\right]} + \frac{1}{1 + [(N - 1) * (1 - m_{rbc})]} \right\}$$

where $Diff_p$ is the diffusivity of oxygen in the plasma component of blood, $Diff_c$ is the diffusivity of oxygen in the cellular component of blood (both in $cm^2/sec$), T is the temperature in Celsius, $k_p$ is the solubility of oxygen in the plasma component of blood in $mL_{O2}/(mL_{blood}*mmHg)$, $k_c$ is the solubility of oxygen in the cellular component of blood in $mL_{O2}/(mL_{blood}*mmHg)$, $k_{wb}$ is the solubility of oxygen in whole blood in $mL_{O2}/(mL_{blood}*mmHg)$, HCT is the fractional hematocrit, and N, β, G and $\mathcal{X}$ are intermediary constants included for the ease of calculation, and $m_{rbc}$ is the aspect of ratio of a red blood cell, assumed to be 0.283. $\lambda(P_{O2})$ is a sink term that takes into account oxygen uptake by hemoglobin, as follows;

$$\lambda\left(P_{O_2}\right) = 1.34 * \frac{C_{Hb}}{k_{wb}} * \left(\frac{P_{O_2}}{P_{50}}\right)^{n_{rbc}-1} * \frac{n_{rbc}}{P_{50}} * \frac{1}{\left[1+\left(\frac{P_{O_2}}{P_{50}}\right)^{n_{rbc}}\right]^2}$$

where 1.34 is the amount of oxygen that can be dissolved in 1 gram of Hb ($mLO_2/gHb$), $C_{Hb}$ is the Hb concentration, $k_{wb}$ is the solubility of oxygen in whole blood as defined above, $P_{O2}$ is is the partial pressure of oxygen dissolved in the blood, $n_{rbc}$ is the Hill parameter which is 2.85 for bovine blood and 2.7 for human blood, and $P_{50}$ is the partial pressure of oxygen dissolved in blood in mmHg when the Hb is 50% saturated, and is calculated via the following equations, for bovine and human blood, respectively:

$$P_{50_{bovine}} = 29.0 * 10^{\{[0.41*(7.4-pH)]-[0.024*(37-T)]\}}$$

$$P_{50_{human}} = 26.6 * 10^{\{[0.48*(7.4-pH)]-[0.024*(37-T)]\}}$$

Combining the above equations, all variables can be calculated, with the exception of m and Φ:

$$\Phi * N_{Re}{}^{-m} = \frac{D_f * por}{4*(1-por)} * \left(\frac{\mu}{\rho * Diff_{wb}}\right)^{2/3} * \frac{1}{PL}\int_{P_{O2_{in}}}^{P_{O2_{out}}} \frac{\left(1+\lambda\left(P_{O_2}\right)\right)^{2/3}}{\left(P_{O_{2_g}} - P_{O_{2_b}}\right)} dP_{O_2} \qquad \textbf{(Equation 4.1)}$$

After solving for all variables using experimental data, the right hand side of this equation was calculated using a trapezoidal numerical integration with a 0.025 mmHg step size for all flowrates tested with the PAD. Following this, all data was combined into a single data set and plotted on a log-log plot with Reynolds number ($N_{Re}$) on the x-axis and the right hand side on the y-axis. The values of m and Φ were determined by a power law fit performed in excel.

## 4.3 Results

### 4.3.1 Gas exchange Testing

*Gas Resistance*

Gas resistance results of all constructed PADs can be seen in **Figure 4.5**. Only devices 3, 4, 5, and 6 progressed to *in vitro* gas exchange testing because they passed our quality control cut off of a gas resistance of <1.5 mmHg/(L/min) at 2 L/min sweep gas flow rate.

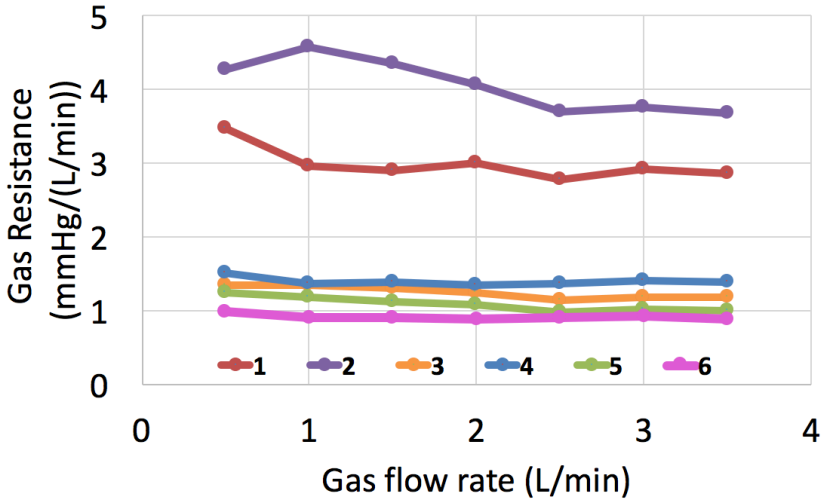


**Figure 4.5**: Gas resistance (mmHg/(L/min) versus sweep gas flow rate (L/min)

*Gas Exchange*

All four devices met our goal of saturating blood to 95% at 2 L/min blood flow rate (**Figure 4.6a**). $VO_2$ can be seen in **Figure 4.6b**, which demonstrates consistent gas exchange with the

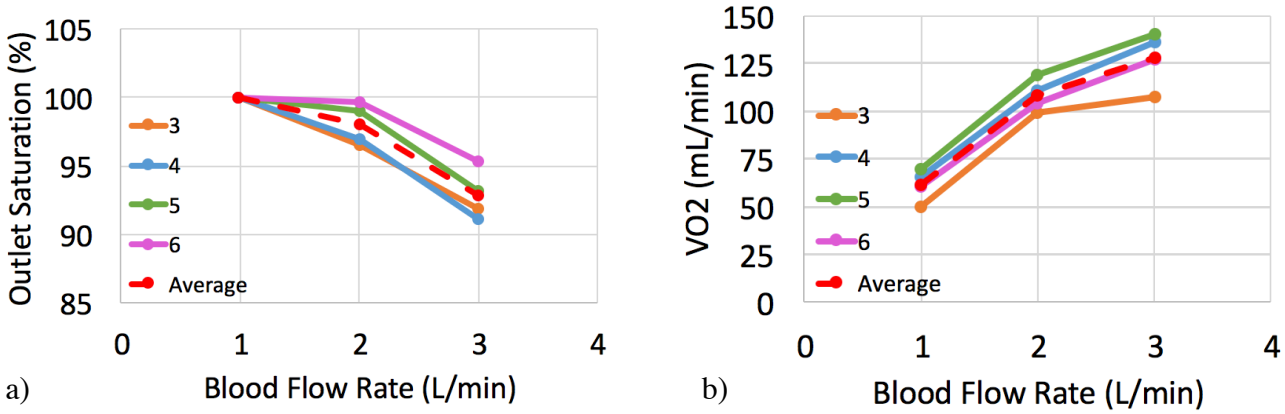


**Figure 4.6**: a) Outlet blood saturation (%) versus blood flow rate (L/min), b) VO2 (mL/min) versus blood flow rate (L/min)

exception of device 3, whose outlet blood samples differed greatly in oxygen content due to visible blood shunting around the fiber bundle. In all cases the saturation decreased and $VO_2$ increased with increasing blood flow rate as would be expected.

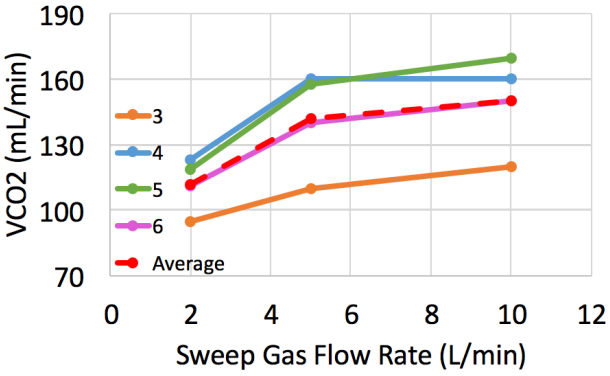


**Figure 4.7**: VCO2 (mL/min) versus sweep gas flow rate (L/min)

As seen in **Figure 4.7**, the $VCO_2$ also met our goal of removing 100 mL/min of $CO_2$ at a sweep gas flow rate of 5 L/min. Similar to the $O_2$ exchange, device 3 had the lowest $VCO_2$, although it still met the goal. As expected, the $CO_2$ exchange increased with increasing sweep gas flowrate.

### 4.3.2 Bloodflow Resistance Testing

As expected, resistance increased with increasing blood flow rate. The average resistance at 2 L/min was 2.06 mmHg/(L/min)), which meets out performance goal of less than 2.5 mmHg/(L/min), but is higher than the computational modeling prediction of 1.5 mmHg/(L/min) (**Figure 4.8**). The y-intercept should approximate the resistance of the fiber bundle; the computationally-predicted bundle resistance was 0.5 mmHg/(L/min) and the y-intercept of our in vitro data is 1.26, also higher than predicted.

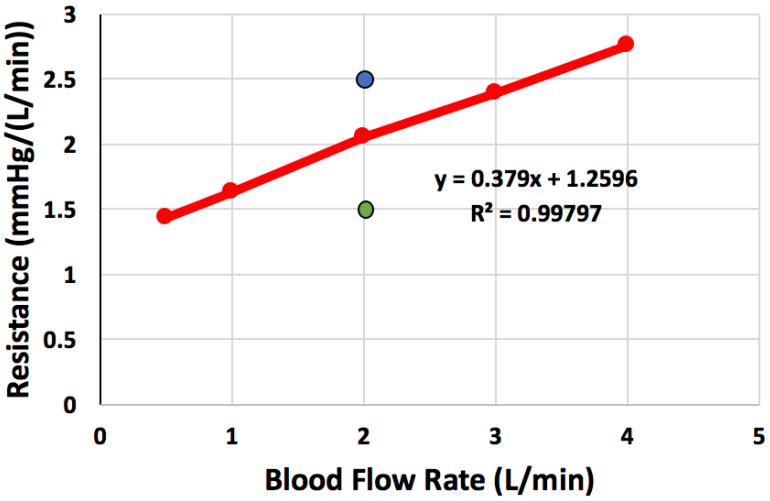


**Figure 4.8**: Blood flow resistance (mmHg/(L/min) versus blood flow rate (L/min). Blue circle indicates performance goal and green circle indicates model prediction.

### 4.3.3 Dimensionless Analysis

To predict the PAD's performance in humans under various conditions, as well as help with future device modeling, the oxygen exchange modeling constants $m$ and $\Phi$ were determined for all PADs grouped together. **Figure 4.9** shows the log-log plot with Reynolds number on the x-axis and the right hand side of **Equation 4.1** on the y-axis. A power law fit determined that $m$ and $\Phi$ are 0.776 and 0.5074, respectively. Previous data using an earlier generation PAD design determined an $m$ and $\Phi$ of 0.718 and 0.46362, respectively.

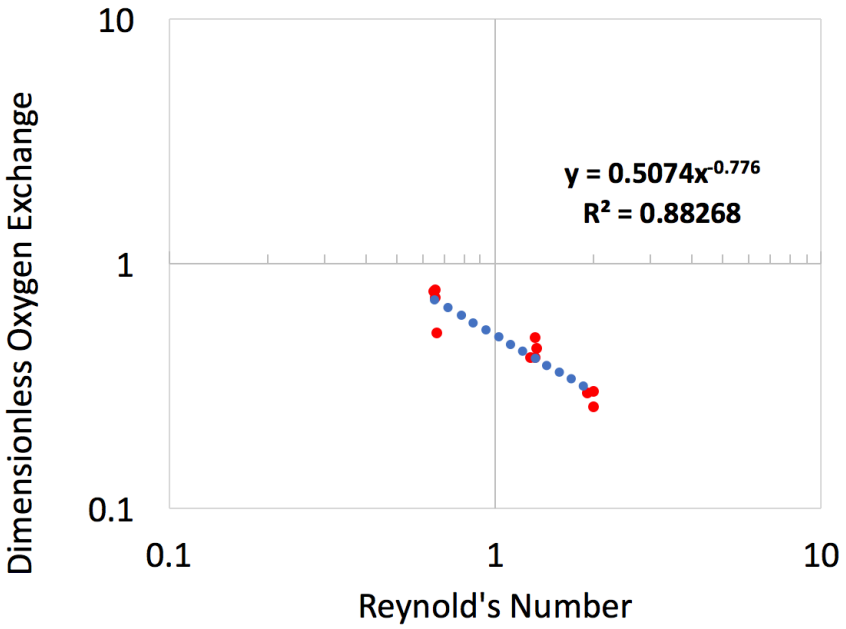


**Figure 4.9**: The dimensionless oxygen exchange as a function of Reynold's number

## 4.4 Discussion

### 4.4.1 Gas exchange Testing

*Gas Resistance*

The first two potted devices had a much higher gas resistance than the others (avg 3.5 vs. 1.2 mmHg/(L/min)). The material used to pot the devices, as described in detail in **Appendix B**, is Wacker Elastosil RT625 PDMS. Following potting, the device is put into the oven to cure. All devices prior to the PAD were much smaller and used a smaller volume of potting material (about 80% less PDMS). These devices were typically cut the next day, as the cure time stated by the manufacturer is 12 hours. However, when the PADs were cut the following day after the first round of potting, the PDMS was not yet cured in the center. This resulted in smearing of the uncured PDMS over the surface of the fibers during the cutting process. Despite our best efforts, we were unable to open up the gas exchange fibers. Our best guess is that, due to the large volume of the

potted region, the deepest areas of PDMS need a longer amount of time to cure. From this point forward, we left the potted devices in oven for at least 5 days before cutting, and we have not had this problem again.

*Gas Exchange*

*In vitro* testing demonstrated that the current PAD design meets our gas exchange performance goals. It has an average saturation of 98.1% at 2 L/min blood flow, above our goal of 95%. In terms of $CO_2$ exchange, the device also meets that goal, averaging 141.9 mL/min when the goal was to exchange 100 mL/min $CO_2$ at 5 L/min sweep gas flow rate. Although the PAD meets our oxygen and carbon dioxide goals, there was visible shunting around the fiber bundles in each of the devices, which will diminish our gas exchange capabilities. This was most apparent in device 3, which had the most visible shunting. In this device, dark red blood was seen coming from the front and back of the device, around the fiber bundle and dark red ribbons of blood were visible in the outlet tubing. As such, device 3's duplicate outlet blood samples varied appreciably in color and $O_2$ and $CO_2$ content. **Figure 4.10a** represents the side-view of the PAD: the blue ovals represent the fiber bundle and the grey line is the core that the fiber is wrapped around. In **Figure 4.10a**, two blue blood streams can be seen shunting around the front and back of the fiber bundle, between the bundle and the housing. Going forward, increased compression on the curvature of the fiber bundles could eliminate shunting, but this must be balanced with not providing so much compression that it results in areas of stasis. Alternatively, the device could be potted in four directions rather than two, which will add two sections of potting material (yellow areas in **Figure 4.10b**) to the areas where the fiber bundle abuts the housing, completely eliminating shunting and thereby increasing our gas exchange even further.

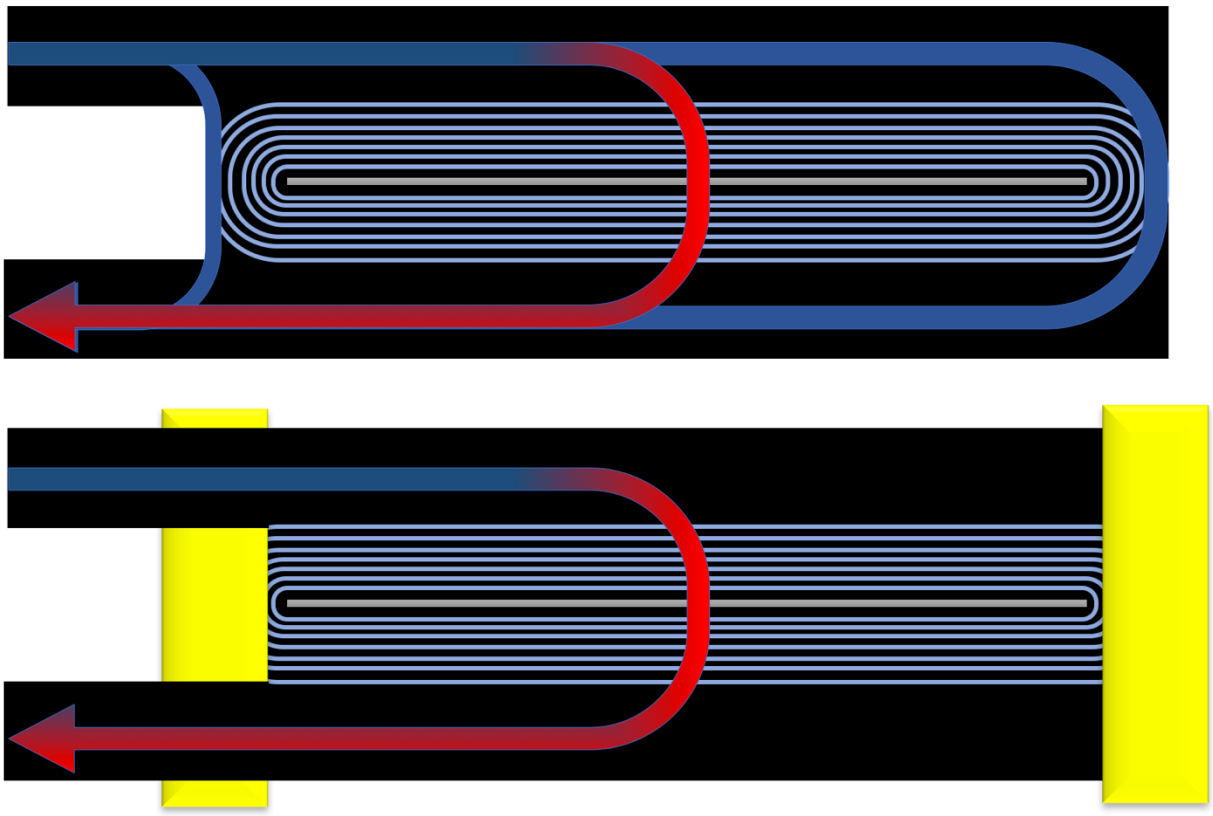

**Figure 4.10**: a) Current PAD design, which allows for blood to shunt around the fiber bundle, between the bundle and the housing; b) The new PAD design will add two additional areas of potting material to completely eliminate shunting.

### 4.4.2 Bloodflow Resistance Testing

The *in vitro* resistance testing of the PAD resulted in an average resistance of 2.06 mmHg/(L/min) at 2 L/min blood flow, which meets our performance goal of 2.5 mmHg/(L/min) at 2 L/min blood flow, although it is higher than was predicted by the computational model (1.5 mmHg/(L/min)). Although this meets our performance goals, there are ways in which the device could be optimized further.

i. *Fiber in the flow path*: When the devices were potted, the top layers of the fiber bundle bunched up (**Figure 4.11**). This puts these layers of fiber in the flow path, which may alter the predicted flow patterns (yellow arrows). Going forward, potting in four directions should mitigate this problem by better securing the bundle in four directions.

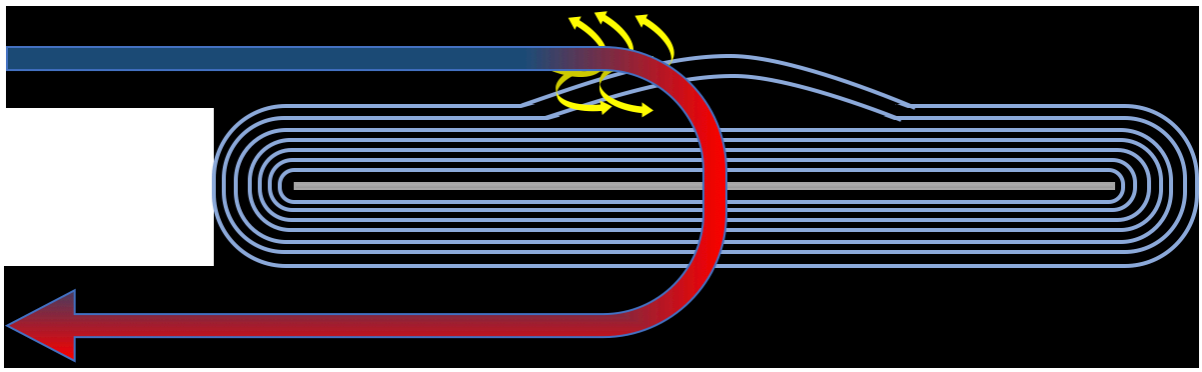

**Figure 4.11**: During the potting process, the top layer of the fiber bundles bunched up and were in the way of the blood flow path, disrupting flow (yellow arrows).

ii. *Model inaccuracies*: The computational modeling used the Darcy porous media model which does not account for the change in fiber direction at the rounded edges. Furthermore, the model assumes there is a consistent permeability in three dimensions with a constant pore size, but the permeability actually changes based on position within the bundle due to the fiber orientation. Additionally, this model assumes flow is traveling normal to the fiber bundle, but upon entering the device flow is actually parallel with the fiber bundle. This results in a rough surface being created by the fibers as the flow travels parallel with fiber bundle surface but perpendicularly with the individual fibers, which could cause additional minor losses. To improve the predictive value of the computational models, they must be improved.

Overall, the PAD met both our gas exchange and resistance goals. Its current resistance is approximately 25-50% of commercially available oxygenators, and two modules in parallel will have a resistance approaching the native lung. This is critical to our destination therapy concept for a number of reasons: i) a lower resistance through the device will result in less blood activation and damage, ii) in a pumped setting, the pump can be set on lower RPMs to generate the same flows, thereby decreasing pump-induced blood damage and activation, and iii) the device could be implanted in a PA-LA fashion without putting increased burden on the heart. Two of these devices in parallel would be particularly useful in patients with pulmonary hypertension and/or right heart insufficiency whose hearts are not strong enough to pump through the currently available devices. The next immediate step includes eliminating shunting by increasing bundle compression or potting the PAD in four directions. Following this, the device will be ready for *in vivo* testing in sheep. If successful, the PAD could revolutionize the way we manage respiratory failure.

## Chapter 5: Conclusion

This work focused on the development of technologies necessary for destination therapy. First, the limitations of currently available devices were investigated. It was determined that although CH last longer than Qx oxygenators, both still have a limited lifetime of 1-2 weeks due to thrombosis. Next, NO was investigated as a means of clot prevention in artificial lungs, and it was determined that 100 ppm NO provides the ideal balance of preventing platelet adsorption without causing toxicity in the form of metHb. Last, a new PAD was tested *in vitro* to determine its resistance and gas exchange capabilities. Ultimately, the PAD met all of our performance goals, saturating to 98.1% at 2 L/min blood flow and exchanging 141.9 mL/min of $CO_2$ at 5 L/min sweep gas flow rate, with a resistance of 2.06 mmHg/(L/min), when our goals were 95%, 100 mL/min, and <2.5 mmHg/(L/min), respectively.

### 5.1 Oxygenator Analysis

*This study demonstrated that overall, the Qx devices fail earlier and more frequently than CH devices, cause a significant decrease in platelet count not seen in CH patients, and have an early decrease in gas exchange capabilities.*

5.1.1 Although having no difference in their starting platelet count, by the end of the ECMO course, the CH group had an average percent change in platelet count of 7.19±15.45%, whereas the Qx group had a percent change of -33.87±10.26% ($p < 0.05$).

5.1.2 The Qx oxygenators have an immediate prominent increase in resistance over the initial 24 hours, whereas there is little change in resistance of the CH devices over the first 4 days.

5.1.3 Kaplan Meier survival data indicates that Qx devices meet the blood flow resistance failure criteria more quickly than CH oxygenators ($p < 0.05$).

5.1.4 Gas exchange performance, as measured by $\Delta C_{O2}$, declined earlier in the Qx group, with a significant decrease by day 2 ($p < 0.05$), which correlates with the increase in resistance also seen in this group. Together, these signify an increased early clot burden in the Qx oxygenators.

5.1.5 Probability densities of clot formation reveal that, as expected, clot formation is most significant at points most distal from the inlets and progresses with time. However, in the Qx devices clot is diffuse, whereas in the CH devices it is concentrated at the center of the device inlet. Interestingly, the two failed CH devices did not have much visible inlet surface clot.

5.1.6 The greater longevity of the CH oxygenators, as well as platelet and gas exchange preservation, suggest that a more distributed, four-inlet approach is better than a single-inlet.

**5.2 Nitric Oxide**

*This study demonstrates that 100 ppm NO appears to reduce platelet consumption and activation without causing toxicity and is thus optimal.*

5.2.1 100 ppm significantly reduced the amount of platelet consumption ($p < 0.05$), resulting in a marked improvement in the initial loss in platelets, whereas the 250 and 500 ppm groups did not differ significantly from the control ($p = 0.99$ and 0.75, respectively).

5.2.2 100 ppm had the smallest increase in device resistance.

5.2.3 The concentration of soluble p-selectin increases substantially in the first 30 minutes of each experiment, after which it tends to stabilize. However, 100 and 250 ppm NO reduce the initial increase ($p < 0.05$).

5.2.4 SEM images reveal clot formation on the gas exchange fibers, with the most significant amount on the 0 ppm fibers, and much less on all NO fibers. All groups had clot formation on the weaving fibers, however, which do not release NO.

5.2.5 The metHb concentrations in the 100 and 250 ppm groups did not increase significantly vs. the control ($p = 0.99$ for both), with less than a 0.1% difference with the 0 ppm group. The 500 ppm group was the only group to result in a statistically significant increase in metHb ($p < 0.01$).

5.2.6 As a result of increasing metHb concentration, the 500 ppm group demonstrated decreasing oxygen carrying capacity and thus significantly increasing serum lactate ($p < 10^{-9}$) and decreasing serum bicarbonate concentration ($p < 10^{-5}$). There was no significant difference between the control group and the 100 and 250 ppm groups ($p = 0.99$).

5.2.7 Overall, 100 ppm NO does not increase metHb concentrations significantly, appears to reduce platelet consumption more than 250 or 500 ppm, and is thus the ideal concentration for future experiments.

5.2.8 When used in conjunction with anti-adsorptive zwitterionic pCB coatings, we expect a synergistic relationship that will further prevent platelet activation and clotting of artificial lung devices.

**5.3 Pulmonary Assist Device**

*Overall, the PAD meets our performance goals of saturating blood to >95% and having a resistance less than 2.5 mmHg/(L/min) at 2 L/min blood flow rate, and removing >100 mL/min $CO_2$ at 5 L/min sweep gas flow rate.*

5.3.1 The devices saturated blood to an average of 98.1% at 2 L/min blood flow rate and an average of 141.9 mL/min $CO_2$ exchange was observed.

5.3.1.1 There was visible shunting in the devices. To eliminate this shunting, future devices could be compressed more on the bundle curvature or potted in 4 directions, which would enhance gas exchange even further.

5.3.2 All PAD devices met our goal of having a resistance less than 2.5 mmHg/(L/min) at 2 L/min blood flow rate, with an average resistance of 2.06 mmHg/(L/min).

5.3.2.1 The resulting average resistance was higher than predicted with computer modeling. This could be due to a combination of inaccuracies of the model, fiber in the flow path, and clot formation within the devices. In the future, potting the devices in four directions should help secure the fiber bundle and prevent bunching of the fiber.

5.3.3 Dimensionless analysis determined that the dimensionless gas transfer coefficients, *m* and Φ, were 0.776 and 0.5074, respectively. These numbers can be used to predict device performance under various conditions, as well as in computer modeling to design future devices.

## 5.4 Limitations and Future Work

### *5.4.1 Oxygenator Analysis*

One limitation of this study is that our images only evaluate the inlets and outlets of the device and do not indicate the clot formation patterns on the interior. Future studies should consider performing similar assessment of the internal aspects of the fiber bundle, either by cutting devices open or using non-invasive imaging techniques. Other useful future studies to help explain the observed differences would include analysis of the relative rates of platelet activation by the pumps

when isolated from their oxygenators and more detailed analysis of platelet coagulation, including both extent of platelet activation and function, and concentration of activated coagulation factors. One final limitation is that all information came from a single institution. Patient and circuit management differs based on institutional and clinician preference, which could influence the functional durability of the oxygenators.

### *5.4.2 Nitric Oxide*

Although the results indicate that NO flux is capable of reducing platelet binding and activation, the results also demonstrate some limitations. The SEM images clearly show that the beneficial effects of the NO flux are markedly less effective at limiting platelet adhesion and activation on the horizontal weaving fibers used to connect the gas exchanger fibers into a fiber mat for manufacturing. These weaving fibers are densely packed, contain areas of stasis, and do not carry and release NO. In standard mats, these areas typically occur every 0.5-1 cm, should be minimized if possible, and may, in particular, benefit from anti-adsorptive pCB coatings.

### *5.4.3 Pulmonary Assist Device*

The PAD work was limited by the effects of potting in two directions, namely shunting around the bundle and fiber bunching up into the flow path, as well as inaccuracies in computational models. However, the devices still met all of our performance goals. In the future, the PAD could be potted in four directions which will eliminate shunting and better-secure the fiber bundle, after which to the device will be ready for long-term *in vivo* testing in sheep.

**References**


1. American Lung Association, Lung Disease Data. 2008.
2. National Heart L, and Blood Institute. Morbidity and Mortality: 2012 Chart Book on Cardiovascular, Lung, and Blood Diseases. Bethesda, MD: National Institutes of Health.
3. Leopold JA. Redox Pioneer: Professor Joseph Loscalzo. Antioxid Redox Signal 2010;13:1125-32.
4. Organ Procurement and Transplant Network SRoTR. Annual Data Report. 2011.
5. National Heart L, and Blood Institute. Morbidity and Mortality: 2012 Chart Book on Cardiovascular, Lung, and Blood Diseases. Bethesda, MD: National Institutes of Health 2012.
6. Bermudez CA, Rocha RV, Zaldonis D, et al. Extracorporeal membrane oxygenation as a bridge to lung transplant: midterm outcomes. Ann Thorac Surg 2011;92:1226-31; discussion 31-2.
7. Anthony Seaton DS, A. Gordon Leitch. Crofton and Douglas's Respiratory Diseases, Fifth Edition: Wiley-Blackwell; 2008.
8. Martin L. Respiratory failure. Med Clin North Am 1977;61:1369-96.
9. Jacono FJ. Control of ventilation in COPD and lung injury. Respir Physiol Neurobiol 2013;189:371-6.
10. Kumar V, Robbins SL. Robbins basic pathology. 8th ed. Philadelphia, PA: Saunders/Elsevier; 2007.
11. Sabiston DC, Townsend CM. Sabiston textbook of surgery : the biological basis of modern surgical practice. 18th ed. Philadelphia, PA: Saunders/Elsevier; 2008.
12. Cove ME, MacLaren G, Federspiel WJ, Kellum JA. Bench to bedside review: Extracorporeal carbon dioxide removal, past present and future. Crit Care 2012;16:232.
13. Anzueto A, Frutos-Vivar F, Esteban A, et al. Incidence, risk factors and outcome of barotrauma in mechanically ventilated patients. Intensive Care Med 2004;30:612-9.
14. Peek GJ, Elbourne D, Mugford M, et al. Randomised controlled trial and parallel economic evaluation of conventional ventilatory support versus extracorporeal membrane oxygenation for severe adult respiratory failure (CESAR). Health Technol Assess 2010;14:1-46.
15. Simonis FD, Binnekade JM, Braber A, et al. PReVENT--protective ventilation in patients without ARDS at start of ventilation: study protocol for a randomized controlled trial. Trials 2015;16:226.
16. Network TARDS. Ventilation with Lower Tidal Volumes as Compared with Traditional Tidal Volumes for Acute Lung Injury and the Acute Respiratory Distress Syndrome. New England Journal of Medicine 2000;342:1301-8.
17. Slutsky AS, Tremblay LN. Multiple system organ failure. Is mechanical ventilation a contributing factor? Am J Respir Crit Care Med 1998;157:1721-5.
18. Putensen C, Theuerkauf N, Zinserling J, Wrigge H, Pelosi P. Meta-analysis: ventilation strategies and outcomes of the acute respiratory distress syndrome and acute lung injury. Ann Intern Med 2009;151:566-76.
19. Needham DM, Colantuoni E, Mendez-Tellez PA, et al. Lung protective mechanical ventilation and two year survival in patients with acute lung injury: prospective cohort study. BMJ 2012;344:e2124.
20. Serpa Neto A, Cardoso S, Manetta J, et al. Association between use of lung-protective ventilation with lower tidal volumes and clinical outcomes among patients without acute respiratory distress syndrome: A meta-analysis. JAMA 2012;308:1651-9.

21. Hickling KG, Walsh J, Henderson S, Jackson R. Low mortality rate in adult respiratory distress syndrome using low-volume, pressure-limited ventilation with permissive hypercapnia: a prospective study. Crit Care Med 1994;22:1568-78.
22. Gattinoni L, Kolobow T, Agostoni A, et al. Clinical application of low frequency positive pressure ventilation with extracorporeal CO2 removal (LFPPV-ECCO2R) in treatment of adult respiratory distress syndrome (ARDS). Int J Artif Organs 1979;2:282-3.
23. Brodie D, Bacchetta M. Extracorporeal membrane oxygenation for ARDS in adults. N Engl J Med 2011;365:1905-14.
24. Bein T, Weber-Carstens S, Goldmann A, et al. Lower tidal volume strategy ( approximately 3 ml/kg) combined with extracorporeal CO2 removal versus 'conventional' protective ventilation (6 ml/kg) in severe ARDS: the prospective randomized Xtravent-study. Intensive Care Med 2013;39:847-56.
25. Turner DA, Ofori-Amanfo G, Williford WL, Cheifetz IM. Lung protective ventilation: a summary of the current evidence from the 2012 American Association for Respiratory Care International Congress. Expert Rev Respir Med 2013;7:209-12.
26. Marhong JD, Munshi L, Detsky M, Telesnicki T, Fan E. Mechanical ventilation during extracorporeal life support (ECLS): a systematic review. Intensive Care Med 2015;41:994-1003.
27. Disease GIfCOL. Global Strategy for the Diagnosis, Management, and Prevention of Chronic Obstructive Pulmonary Disease. 2017;2017 Report.
28. Halbert RJ, Natoli JL, Gano A, Badamgarav E, Buist AS, Mannino DM. Global burden of COPD: systematic review and meta-analysis. Eur Respir J 2006;28:523-32.
29. Guarascio AJ, Ray SM, Finch CK, Self TH. The clinical and economic burden of chronic obstructive pulmonary disease in the USA. Clinicoecon Outcomes Res 2013;5:235-45.
30. Marchetti N, Criner GJ. Surgical Approaches to Treating Emphysema: Lung Volume Reduction Surgery, Bullectomy, and Lung Transplantation. Semin Respir Crit Care Med 2015;36:592-608.
31. Sawicki GS, Rasouliyan L, McMullen AH, et al. Longitudinal assessment of health-related quality of life in an observational cohort of patients with cystic fibrosis. Pediatr Pulmonol 2011;46:36-44.
32. Briesacher BA, Quittner AL, Fouayzi H, Zhang J, Swensen A. Nationwide trends in the medical care costs of privately insured patients with cystic fibrosis (CF), 2001-2007. Pediatr Pulmonol 2011;46:770-6.
33. Goss CH, Burns JL. Exacerbations in cystic fibrosis. 1: Epidemiology and pathogenesis. Thorax 2007;62:360-7.
34. Lechtzin N, West N, Allgood S, et al. Rationale and design of a randomized trial of home electronic symptom and lung function monitoring to detect cystic fibrosis pulmonary exacerbations: the early intervention in cystic fibrosis exacerbation (eICE) trial. Contemp Clin Trials 2013;36:460-9.
35. Registry CFFP. 2015 Annual Data Report Bethesda, Maryland;2016 Cystic Fibrosis Foundation.
36. Texereau J, Jamal D, Choukroun G, et al. Determinants of mortality for adults with cystic fibrosis admitted in Intensive Care Unit: a multicenter study. Respir Res 2006;7:14.
37. Madden BP, Kariyawasam H, Siddiqi AJ, Machin A, Pryor JA, Hodson ME. Noninvasive ventilation in cystic fibrosis patients with acute or chronic respiratory failure. Eur Respir J 2002;19:310-3.

38. Cadiergue V, Philit F, Langevin B, et al. [Outcome of adult patients with cystic fibrosis admitted to intensive care with respiratory failure: the role of non-invasive ventilation]. Rev Mal Respir 2002;19:425-30.
39. Dwyer TJ, Robbins L, Kelly P, Piper AJ, Bell SC, Bye PT. Non-invasive ventilation used as an adjunct to airway clearance treatments improves lung function during an acute exacerbation of cystic fibrosis: a randomised trial. J Physiother 2015;61:142-7.
40. Jones A, Bilton D, Evans TW, Finney SJ. Predictors of outcome in patients with cystic fibrosis requiring endotracheal intubation. Respirology 2013;18:630-6.
41. Bosch B, De Boeck K. Searching for a cure for cystic fibrosis. A 25-year quest in a nutshell. Eur J Pediatr 2016;175:1-8.
42. Quon BS, Rowe SM. New and emerging targeted therapies for cystic fibrosis. BMJ 2016;352:i859.
43. Caminati A, Harari S. IPF: New insight in diagnosis and prognosis. Respir Med 2010;104 Suppl 1:S2-10.
44. Trudzinski FC, Kaestner F, Schafers HJ, et al. Outcome of Patients with Interstitial Lung Disease Treated with Extracorporeal Membrane Oxygenation for Acute Respiratory Failure. Am J Respir Crit Care Med 2016;193:527-33.
45. Rangappa P, Moran JL. Outcomes of patients admitted to the intensive care unit with idiopathic pulmonary fibrosis. Crit Care Resusc 2009;11:102-9.
46. Rachmale S, Li G, Wilson G, Malinchoc M, Gajic O. Practice of excessive F(IO(2)) and effect on pulmonary outcomes in mechanically ventilated patients with acute lung injury. Respir Care 2012;57:1887-93.
47. Mollica C, Paone G, Conti V, et al. Mechanical ventilation in patients with end-stage idiopathic pulmonary fibrosis. Respiration 2010;79:209-15.
48. Alpard SK, Wang D, Deyo DJ, Smolarz CM, Chambers S, Zwischenberger JB. Optional active compliance chamber performance in a pulmonary artery-pulmonary artery configured paracorporeal artificial lung. Perfusion 2007;22:81-6.
49. Roberts WC, Shafii AE, Grayburn PA, et al. Clinical and morphologic features of acute, subacute and chronic cor pulmonale (pulmonary heart disease). Am J Cardiol 2015;115:697-703.
50. Weitzenblum E, Chaouat A. Cor pulmonale. Chron Respir Dis 2009;6:177-85.
51. Weitzenblum E, Hirth C, Ducolone A, Mirhom R, Rasaholinjanahary J, Ehrhart M. Prognostic value of pulmonary artery pressure in chronic obstructive pulmonary disease. Thorax 1981;36:752-8.
52. Heyland DK, Cook DJ, Griffith L, Keenan SP, Brun-Buisson C. The attributable morbidity and mortality of ventilator-associated pneumonia in the critically ill patient. The Canadian Critical Trials Group. Am J Respir Crit Care Med 1999;159:1249-56.
53. Safdar N, Dezfulian C, Collard HR, Saint S. Clinical and economic consequences of ventilator-associated pneumonia: a systematic review. Crit Care Med 2005;33:2184-93.
54. Rello J, Ollendorf DA, Oster G, et al. Epidemiology and outcomes of ventilator-associated pneumonia in a large US database. Chest 2002;122:2115-21.
55. Cook DJ, Walter SD, Cook RJ, et al. Incidence of and risk factors for ventilator-associated pneumonia in critically ill patients. Ann Intern Med 1998;129:433-40.
56. Nash G, Blennerhassett JB, Pontoppidan H. Pulmonary lesions associated with oxygen therapy and artifical ventilation. N Engl J Med 1967;276:368-74.

57. Boussarsar M, Thierry G, Jaber S, Roudot-Thoraval F, Lemaire F, Brochard L. Relationship between ventilatory settings and barotrauma in the acute respiratory distress syndrome. Intensive Care Med 2002;28:406-13.
58. Gammon RB, Shin MS, Buchalter SE. Pulmonary barotrauma in mechanical ventilation. Patterns and risk factors. Chest 1992;102:568-72.
59. Gattinoni L, Bombino M, Pelosi P, et al. Lung structure and function in different stages of severe adult respiratory distress syndrome. JAMA 1994;271:1772-9.
60. Amato MB, Barbas CS, Medeiros DM, et al. Effect of a protective-ventilation strategy on mortality in the acute respiratory distress syndrome. N Engl J Med 1998;338:347-54.
61. Canadian Critical Care Trials G. A randomized trial of diagnostic techniques for ventilator-associated pneumonia. N Engl J Med 2006;355:2619-30.
62. Lau AC, So HM, Tang SL, et al. Prevention of ventilator-associated pneumonia. Hong Kong Med J 2015;21:61-8.
63. Melsen WG, Rovers MM, Groenwold RH, et al. Attributable mortality of ventilator-associated pneumonia: a meta-analysis of individual patient data from randomised prevention studies. Lancet Infect Dis 2013;13:665-71.
64. Mehta S, Hill NS. Noninvasive ventilation. Am J Respir Crit Care Med 2001;163:540-77.
65. Mas A, Masip J. Noninvasive ventilation in acute respiratory failure. Int J Chron Obstruct Pulmon Dis 2014;9:837-52.
66. Zapol WM, Snider MT, Hill JD, et al. Extracorporeal membrane oxygenation in severe acute respiratory failure. A randomized prospective study. JAMA 1979;242:2193-6.
67. Lang G, Taghavi S, Aigner C, et al. Primary lung transplantation after bridge with extracorporeal membrane oxygenation: a plea for a shift in our paradigms for indications. Transplantation 2012;93:729-36.
68. Javidfar J, Brodie D, Iribarne A, et al. Extracorporeal membrane oxygenation as a bridge to lung transplantation and recovery. J Thorac Cardiovasc Surg 2012;144:716-21.
69. Shafii AE, Mason DP, Brown CR, et al. Growing experience with extracorporeal membrane oxygenation as a bridge to lung transplantation. ASAIO J 2012;58:526-9.
70. Nolan H, Wang D, Zwischenberger JB. Artificial lung basics: fundamental challenges, alternative designs and future innovations. Organogenesis 2011;7:23-7.
71. Bartlett RH. Extracorporeal Life Support Registry Report 1995. ASAIO J 1997;43:104-7.
72. Organization ELS. ECLS Registry Report, International Summary2016.
73. Marasco SF, Lukas G, McDonald M, McMillan J, Ihle B. Review of ECMO (extra corporeal membrane oxygenation) support in critically ill adult patients. Heart Lung Circ 2008;17 Suppl 4:S41-7.
74. Matheis G. New technologies for respiratory assist. Perfusion 2003;18:245-51.
75. Biscotti M, Bacchetta M. The "sport model": extracorporeal membrane oxygenation using the subclavian artery. Ann Thorac Surg 2014;98:1487-9.
76. Abrams D, Brodie D. Emerging indications for extracorporeal membrane oxygenation in adults with respiratory failure. Ann Am Thorac Soc 2013;10:371-7.
77. Needham DM, Korupolu R, Zanni JM, et al. Early physical medicine and rehabilitation for patients with acute respiratory failure: a quality improvement project. Arch Phys Med Rehabil 2010;91:536-42.
78. Needham DM, Korupolu R. Rehabilitation quality improvement in an intensive care unit setting: implementation of a quality improvement model. Top Stroke Rehabil 2010;17:271-81.

79. Abrams D, Javidfar J, Farrand E, et al. Early mobilization of patients receiving extracorporeal membrane oxygenation: a retrospective cohort study. Crit Care 2014;18:R38.
80. Javidfar J, Brodie D, Wang D, et al. Use of bicaval dual-lumen catheter for adult venovenous extracorporeal membrane oxygenation. Ann Thorac Surg 2011;91:1763-8; discussion 9.
81. Javidfar J, Brodie D, Costa J, et al. Subclavian artery cannulation for venoarterial extracorporeal membrane oxygenation. ASAIO J 2012;58:494-8.
82. Hoopes CW, Kukreja J, Golden J, Davenport DL, Diaz-Guzman E, Zwischenberger JB. Extracorporeal membrane oxygenation as a bridge to pulmonary transplantation. J Thorac Cardiovasc Surg 2013;145:862-7; discussion 7-8.
83. Rehder KJ, Turner DA, Hartwig MG, et al. Active rehabilitation during extracorporeal membrane oxygenation as a bridge to lung transplantation. Respir Care 2013;58:1291-8.
84. Cardenas VJ, Jr., Lynch JE, Ates R, Miller L, Zwischenberger JB. Venovenous carbon dioxide removal in chronic obstructive pulmonary disease: experience in one patient. ASAIO J 2009;55:420-2.
85. Morris AH, Wallace CJ, Menlove RL, et al. Randomized clinical trial of pressure-controlled inverse ratio ventilation and extracorporeal CO2 removal for adult respiratory distress syndrome. Am J Respir Crit Care Med 1994;149:295-305.
86. Jackson A, Cropper J, Pye R, Junius F, Malouf M, Glanville A. Use of extracorporeal membrane oxygenation as a bridge to primary lung transplant: 3 consecutive, successful cases and a review of the literature. J Heart Lung Transplant 2008;27:348-52.
87. Fischer S, Hoeper MM, Tomaszek S, et al. Bridge to lung transplantation with the extracorporeal membrane ventilator Novalung in the veno-venous mode: the initial Hannover experience. ASAIO J 2007;53:168-70.
88. Haneya A, Philipp A, Mueller T, et al. Extracorporeal circulatory systems as a bridge to lung transplantation at remote transplant centers. Ann Thorac Surg 2011;91:250-5.
89. Fischer S, Simon AR, Welte T, et al. Bridge to lung transplantation with the novel pumpless interventional lung assist device NovaLung. J Thorac Cardiovasc Surg 2006;131:719-23.
90. Zimmermann M, Bein T, Arlt M, et al. Pumpless extracorporeal interventional lung assist in patients with acute respiratory distress syndrome: a prospective pilot study. Crit Care 2009;13:R10.
91. Florchinger B, Philipp A, Klose A, et al. Pumpless extracorporeal lung assist: a 10-year institutional experience. Ann Thorac Surg 2008;86:410-7; discussion 7.
92. Zimmermann M, Bein T, Philipp A, et al. Interhospital transportation of patients with severe lung failure on pumpless extracorporeal lung assist. Br J Anaesth 2006;96:63-6.
93. Bein T, Weber F, Philipp A, et al. A new pumpless extracorporeal interventional lung assist in critical hypoxemia/hypercapnia. Crit Care Med 2006;34:1372-7.
94. Zwischenberger JB, Alpard SK. Artificial lungs: a new inspiration. Perfusion 2002;17:253-68.
95. Kopp R, Dembinski R, Kuhlen R. Role of extracorporeal lung assist in the treatment of acute respiratory failure. Minerva Anestesiol 2006;72:587-95.
96. Paden ML, Conrad SA, Rycus PT, Thiagarajan RR, Registry E. Extracorporeal Life Support Organization Registry Report 2012. ASAIO J 2013;59:202-10.
97. Agerstrand CL, Burkart KM, Abrams DC, Bacchetta MD, Brodie D. Blood conservation in extracorporeal membrane oxygenation for acute respiratory distress syndrome. Ann Thorac Surg 2015;99:590-5.

98. Plotz FB, van Oeveren W, Bartlett RH, Wildevuur CR. Blood activation during neonatal extracorporeal life support. J Thorac Cardiovasc Surg 1993;105:823-32.
99. Ang AL. Predictors of increased transfusion requirements and optimizing transfusional support in patients on Extracorporeal membrane oxygenation (ECMO). ISBT Science Series 2012;7:89–91.
100. Robinson TM, Kickler TS, Walker LK, Ness P, Bell W. Effect of extracorporeal membrane oxygenation on platelets in newborns. Crit Care Med 1993;21:1029-34.
101. Khoshbin E, Westrope C, Pooboni S, et al. Performance of polymethyl pentene oxygenators for neonatal extracorporeal membrane oxygenation: a comparison with silicone membrane oxygenators. Perfusion 2005;20:129-34.
102. Vincent JL AS, De Mendonca A, Haji-Michael P, Sprung C, Moreno R, et al. The epidemiology of acute respiratory failure in critically ill patients. Chest 2002;121:1602-9.
103. Del Sorbo K RV, and Keshavjee S. Extracorporeal Membrane Oxygenation as "Bridge" to Lung Transplantation: What Remains in Order to Make It Standard of Care? American Journal of Respiratory and Critical Care Medicine 2012;185:699-701.
104. Scipione CN, Schewe RE, Koch KL, Shaffer AW, Iyengar A, Cook KE. Use of a low-resistance compliant thoracic artificial lung in the pulmonary artery to pulmonary artery configuration. J Thorac Cardiovasc Surg 2013;145:1660-6.
105. Schewe RE, Khanafer KM, Arab A, Mitchell JA, Skoog DJ, Cook KE. Design and in vitro assessment of an improved, low-resistance compliant thoracic artificial lung. ASAIO J 2012;58:583-9.
106. Schewe RE, Scipione CN, Koch KL, Cook KE. In-parallel attachment of a low-resistance compliant thoracic artificial lung under rest and simulated exercise. Ann Thorac Surg 2012;94:1688-94.
107. Mockros LF CK. The Artificial Lung. Austin, TX: Landes Bioscience; 2002.
108. Cook KE ML. The Artificial Lung. Austin, TX: Landes Bioscience; 2002.
109. Sato H, Hall CM, Lafayette NG, et al. Thirty-day in-parallel artificial lung testing in sheep. Ann Thorac Surg 2007;84:1136-43; discussion 43.
110. Sato H, Griffith GW, Hall CM, et al. Seven-day artificial lung testing in an in-parallel configuration. Ann Thorac Surg 2007;84:988-94.
111. Cook KE, Maxhimer J, Leonard DJ, Mavroudis C, Backer CL, Mockros LF. Platelet and leukocyte activation and design consequences for thoracic artificial lungs. ASAIO J 2002;48:620-30.
112. Haft JW, Griffith BP, Hirschl RB, Bartlett RH. Results of an artificial-lung survey to lung transplant program directors. J Heart Lung Transplant 2002;21:467-73.
113. Gazit AZ, Sweet SC, Grady RM, Huddleston CB. First experience with a paracorporeal artificial lung in a small child with pulmonary hypertension. J Thorac Cardiovasc Surg 2011;141:e48-50.
114. Camboni D, Philipp A, Arlt M, Pfeiffer M, Hilker M, Schmid C. First experience with a paracorporeal artificial lung in humans. ASAIO J 2009;55:304-6.
115. Strueber M, Hoeper MM, Fischer S, et al. Bridge to thoracic organ transplantation in patients with pulmonary arterial hypertension using a pumpless lung assist device. Am J Transplant 2009;9:853-7.
116. Schmid C, Philipp A, Hilker M, et al. Bridge to lung transplantation through a pulmonary artery to left atrial oxygenator circuit. Ann Thorac Surg 2008;85:1202-5.

117. Muller T, Lubnow M, Philipp A, et al. Extracorporeal pumpless interventional lung assist in clinical practice: determinants of efficacy. Eur Respir J 2009;33:551-8.
118. Wiebe K, Poeling J, Arlt M, et al. Thoracic surgical procedures supported by a pumpless interventional lung assist. Ann Thorac Surg 2010;89:1782-7; discussion 8.
119. Bartosik W, Egan JJ, Wood AE. The Novalung interventional lung assist as bridge to lung transplantation for self-ventilating patients - initial experience. Interact Cardiovasc Thorac Surg 2011;13:198-200.
120. Valapour M, Skeans MA, Heubner BM, et al. OPTN/SRTR 2012 Annual Data Report: lung. Am J Transplant 2014;14 Suppl 1:139-65.
121. Anderson RN. Deaths: leading causes for 2000. Natl Vital Stat Rep 2002;50:1-85.
122. Kreider M, Kotloff RM. Selection of candidates for lung transplantation. Proc Am Thorac Soc 2009;6:20-7.
123. Chen H, Shiboski SC, Golden JA, et al. Impact of the lung allocation score on lung transplantation for pulmonary arterial hypertension. Am J Respir Crit Care Med 2009;180:468-74.
124. Christie JD, Edwards LB, Kucheryavaya AY, et al. The Registry of the International Society for Heart and Lung Transplantation: 29th adult lung and heart-lung transplant report-2012. J Heart Lung Transplant 2012;31:1073-86.
125. Stavem K, Bjortuft O, Borgan O, Geiran O, Boe J. Lung transplantation in patients with chronic obstructive pulmonary disease in a national cohort is without obvious survival benefit. J Heart Lung Transplant 2006;25:75-84.
126. Thabut G, Christie JD, Ravaud P, et al. Survival after bilateral versus single lung transplantation for patients with chronic obstructive pulmonary disease: a retrospective analysis of registry data. Lancet 2008;371:744-51.
127. Toyoda Y, Bhama JK, Shigemura N, et al. Efficacy of extracorporeal membrane oxygenation as a bridge to lung transplantation. J Thorac Cardiovasc Surg 2013;145:1065-70; discussion 70-1.
128. Mason DP, Thuita L, Nowicki ER, Murthy SC, Pettersson GB, Blackstone EH. Should lung transplantation be performed for patients on mechanical respiratory support? The US experience. J Thorac Cardiovasc Surg 2010;139:765-73 e1.
129. George TJ, Beaty CA, Kilic A, Shah PD, Merlo CA, Shah AS. Outcomes and temporal trends among high-risk patients after lung transplantation in the United States. J Heart Lung Transplant 2012;31:1182-91.
130. Abrams DC, Brodie D, Rosenzweig EB, Burkart KM, Agerstrand CL, Bacchetta MD. Upper-body extracorporeal membrane oxygenation as a strategy in decompensated pulmonary arterial hypertension. Pulm Circ 2013;3:432-5.
131. Xu LC, Bauer JW, Siedlecki CA. Proteins, platelets, and blood coagulation at biomaterial interfaces. Colloids Surf B Biointerfaces 2014;124:49-68.
132. Anderson JM, Rodriguez A, Chang DT. Foreign body reaction to biomaterials. Semin Immunol 2008;20:86-100.
133. Buscher H, Vukomanovic A, Benzimra M, Okada K, Nair P. Blood and Anticoagulation Management in Extracorporeal Membrane Oxygenation for Surgical and Nonsurgical Patients: A Single-Center Retrospective Review. J Cardiothorac Vasc Anesth 2016.
134. de Agostini AI, Watkins SC, Slayter HS, Youssoufian H, Rosenberg RD. Localization of anticoagulantly active heparan sulfate proteoglycans in vascular endothelium: antithrombin binding on cultured endothelial cells and perfused rat aorta. J Cell Biol 1990;111:1293-304.

135. Gray E, Hogwood J, Mulloy B. The anticoagulant and antithrombotic mechanisms of heparin. Handb Exp Pharmacol 2012:43-61.
136. Gott VL, Whiffen JD, Dutton RC. Heparin Bonding on Colloidal Graphite Surfaces. Science 1963;142:1297-8.
137. Biran R, Pond D. Heparin coatings for improving blood compatibility of medical devices. Adv Drug Deliv Rev 2016.
138. Warkentin TE, Kelton JG. Temporal aspects of heparin-induced thrombocytopenia. N Engl J Med 2001;344:1286-92.
139. Pasche B, Elgue G, Olsson P, Riesenfeld J, Rasmuson A. Binding of antithrombin to immobilized heparin under varying flow conditions. Artif Organs 1991;15:481-91.
140. Hosoyama K, Ito K, Kawamoto S, et al. Poly-2-methoxyethylacrylate-coated cardiopulmonary bypass circuit can reduce transfusion of platelet products compared to heparin-coated circuit during aortic arch surgery. J Artif Organs 2016;19:233-40.
141. Gupta S AK, Suhaib A , Cook KE. Multi-Modal, Surface-Focused Anticoagulation Using Poly-2-methoxyethylacrylate Polymer Grafts and Surface Nitric Oxide Release. Advanced Materials Interfaces 2014;1.
142. Sundaram HS HX, Nowinski AK, Brault ND, Li Y, Ella-Menye JR, Amoaka KA, Cook KE, Patrick M, Senecal K, Jiang S. . Achieving one-step surface coating of highly hydrophilic poly(carboxybetaine methacrylate) polymers on hydrophobic and hydrophilic surfaces. . Advanced Materials Interfaces 2014;1.
143. Amoako KA, Sundaram, H.S., Suhaib, A., Jiang, S., Cook, K.E. Multimodal, Biomaterial-Focused Anticoagulation via Superlow Fouling Zwitterionic Functional Groups Coupled with Anti-Platelet Nitric Oxide Release. Advanced Materials Interfaces 2016;3.
144. Kelm M. Nitric oxide metabolism and breakdown. Biochim Biophys Acta 1999;1411:273-89.
145. Borland C. Endothelium in control. Br Heart J 1991;66:405.
146. Moncada S, Palmer RM, Higgs EA. Nitric oxide: physiology, pathophysiology, and pharmacology. Pharmacol Rev 1991;43:109-42.
147. Tevaearai HT, Mueller XM, Tepic S, et al. Nitric oxide added to the sweep gas infusion reduces local clotting formation in adult blood oxygenators. ASAIO J 2000;46:719-22.
148. Amoako KA, Montoya PJ, Major TC, et al. Fabrication and in vivo thrombogenicity testing of nitric oxide generating artificial lungs. J Biomed Mater Res A 2013;101:3511-9.
149. Amoako KA, Cook KE. Nitric oxide-generating silicone as a blood-contacting biomaterial. ASAIO J 2011;57:539-44.
150. Major TC, Brant DO, Burney CP, et al. The hemocompatibility of a nitric oxide generating polymer that catalyzes S-nitrosothiol decomposition in an extracorporeal circulation model. Biomaterials 2011;32:5957-69.
151. Amoako K.A. S, H.S., Suhaib, A., Jiang, S., Cook, K.E. . Multimodal, Biomaterial-Focused Anticoagulation via Superlow Fouling Zwitterionic Functional Groups Coupled with Anti-Platelet Nitric Oxide Release. Advanced Materials Interfaces 2016;3.
152. Sly MK, Prager MD, Li J, et al. Platelet and neutrophil distributions in pump oxygenator circuits. III. Influence of nitric oxide gas infusion. ASAIO J 1996;42:M494-9.
153. Lowson SM, Hassan HM, Rich GF. The effect of nitric oxide on platelets when delivered to the cardiopulmonary bypass circuit. Anesth Analg 1999;89:1360-5.
154. Weinberger B, Laskin DL, Heck DE, Laskin JD. The toxicology of inhaled nitric oxide. Toxicol Sci 2001;59:5-16.

155. Taylor MB, Christian KG, Patel N, Churchwell KB. Methemoglobinemia: Toxicity of inhaled nitric oxide therapy. Pediatr Crit Care Med 2001;2:99-101.
156. Colman RW. Hemostasis and thrombosis : basic principles and clinical practice. 4th ed. Philadelphia: Lippincott Williams & Wilkins; 2001.
157. Bolliger D, Zenklusen U, Tanaka KA. Point-of-care coagulation management algorithms during ECMO support: are we there yet? Minerva Anestesiol 2016.
158. Lehle K, Philipp A, Muller T, et al. Flow dynamics of different adult ECMO systems: a clinical evaluation. Artif Organs 2014;38:391-8.
159. Dornia C, Philipp A, Bauer S, et al. D-dimers Are a Predictor of Clot Volume Inside Membrane Oxygenators During Extracorporeal Membrane Oxygenation. Artif Organs 2015;39:782-7.
160. Dornia C, Philipp A, Bauer S, et al. Analysis of thrombotic deposits in extracorporeal membrane oxygenators by multidetector computed tomography. ASAIO journal (American Society for Artificial Internal Organs : 1992) 2014;60:652-6.
161. Reynolds MM, Frost MC, Meyerhoff ME. Nitric oxide-releasing hydrophobic polymers: preparation, characterization, and potential biomedical applications. Free Radic Biol Med 2004;37:926-36.
162. Cook KE, Perlman CE, Seipelt R, Backer CL, Mavroudis C, Mockrost LF. Hemodynamic and gas transfer properties of a compliant thoracic artificial lung. ASAIO J 2005;51:404-11.
163. Cruz-Landeira A, Bal MJ, Quintela, Lopez-Rivadulla M. Determination of methemoglobin and total hemoglobin in toxicological studies by derivative spectrophotometry. J Anal Toxicol 2002;26:67-72.
164. Sly MK, Prager MD, Eberhart RC, Jessen ME, Kulkarni PV. Inhibition of surface-induced platelet activation by nitric oxide. ASAIO J 1995;41:M394-8.
165. Lantvit SM, Barrett BJ, Reynolds MM. Nitric oxide releasing material adsorbs more fibrinogen. J Biomed Mater Res A 2013;101:3201-10.
166. Major TC, Brant DO, Reynolds MM, et al. The attenuation of platelet and monocyte activation in a rabbit model of extracorporeal circulation by a nitric oxide releasing polymer. Biomaterials 2010;31:2736-45.
167. Fleser PS, Nuthakki VK, Malinzak LE, et al. Nitric oxide-releasing biopolymers inhibit thrombus formation in a sheep model of arteriovenous bridge grafts. J Vasc Surg 2004;40:803-11.
168. Mellgren K, Mellgren G, Lundin S, Wennmalm A, Wadenvik H. Effect of nitric oxide gas on platelets during open heart operations. Ann Thorac Surg 1998;65:1335-41.
169. Tsukiya T, Taenaka Y, Tatsumi E, Takano H. Performance of a newly developed implantable centrifugal blood pump. ASAIO J 2001;47:559-62.
170. Schewe RE, Khanafer KM, Orizondo RA, Cook KE. Thoracic artificial lung impedance studies using computational fluid dynamics and in vitro models. Ann Biomed Eng 2012;40:628-36.
171. Funakubo A, Taga I, McGillicuddy JW, Fukui Y, Hirschl RB, Bartlett RH. Flow vectorial analysis in an artificial implantable lung. ASAIO J 2003;49:383-7.
172. Gage KL, Gartner MJ, Burgreen GW, Wagner WR. Predicting membrane oxygenator pressure drop using computational fluid dynamics. Artif Organs 2002;26:600-7.
173. Matsuda N NM, Sakai K, Kuwana K, and Tahara K. Theoretical and experimental evaluation for blood pressure drop and oxygen transfer rate in outside blood flow membrane oxygenator. J Chem Eng Jpn 1999;32:752-59.

174. Taga I, Funakubo A, Fukui Y. Design and development of an artificial implantable lung using multiobjective genetic algorithm: evaluation of gas exchange performance. ASAIO J 2005;51:92-102.
175. KE C. Design and testing of intrathoracic artificial lungs [master's thesis]. : Northwestern University; 1996.
176. Federspiel WJ, Hattler BG. Sweep gas flowrate and CO2 exchange in artificial lungs. Artif Organs 1996;20:1050-2.
177. Vaslef S. Analysis and Design of an Intravascular Lung Assist Device. 1990.

**Appendix A: MATLAB Heat Map Generation Code**

```
FileTif='All survived devices OUTLET.tif';
InfoImage=imfinfo(FileTif);
mImage=InfoImage(1).Width;
nImage=InfoImage(1).Height;
NumberImages=length(InfoImage);

dep=zeros(nImage,mImage);
FinalImage=zeros(nImage,mImage,NumberImages,'uint16');
for i=1:NumberImages
  FinalImage(:,:,i)=imread(FileTif,'Index',i);

  for n=1:nImage
   for m=1:mImage
      if FinalImage(n,m,i)==0
         dep(n,m)=dep(n,m)+0;
      elseif FinalImage(n,m,i)==255
         dep(n,m)=dep(n,m)+1;
      end
   end
  end
end
```

```
normdep=dep./NumberImages;

max(max(normdep))


imshow(normdep,'DisplayRange',[]),colorbar('East');

impixelinfo

caxis([0,1])


colormap(jet)
```

## Appendix B: Device Fabrication

The fabrication process of the MAL and PAD are very similar with the exception of housing construction, which will be separated into two sections: MAL and PAD. *Note: All PDMS referred to below is Wacker Elastosil RT625 PDMS.*

### A. Fiber Bundle

1. Using a laser cutter, cut a properly sized core from a 3/32 inch thick sheet of acrylic (**Figure B.1**).
2. Sand all surfaces of the core that will come into contact with the potting material (blue areas on **Figure B.1**) using 320 grit sandpaper.
3. Clean the core using water then a small amount of isopropyl alcohol on a Kimwipe.
4. Prime all sanded surfaces with Nusil MED-163 following manufacturer instructions.

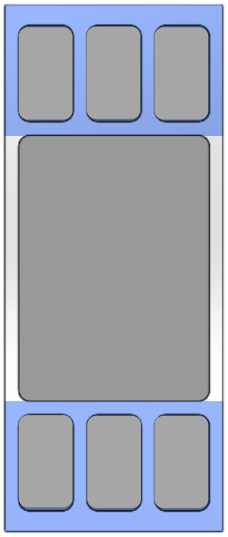

**Figure B.1**: MAL core drawing, blue regions to be sanded

5. After putting the core on a sheet of plastic, pour enough PDMS over the sanded surfaces to fully coat them. Lay another sheet of plastic on top, place a weight on top of the core to make the PDMS layer thin, and insert into the oven to cure overnight.
6. Peel off the plastic sheets from the core, and trim all excess PDMS, leaving a very thin layer on all sanded surfaces.
7. Heat seal an appropriate length of fiber depending on the desired surface area and fiber mat width, and cut off the excess.

8. Attach the fiber to the core using a small amount of PDMS on the core where the potting material will later contact (**Figure B.2a**).
9. Place the fiber and core into the oven and allow it to cure for at least 4 hours before handling.
10. Flip the core over 29 times to roll the fiber bundle. *Note: 51 times for the PAD*.
11. Measure the thickness and width of the fiber bundle using a caliper. Use the thickness measurement and core thickness to ensure that spacing between layers of fiber is 5-20 micrometers, and use the width to ensure the bundle is 20-40 micrometers larger than the housing width.
    i. Re-roll the bundle as needed until the sizing specifications are met.
12. Heat seal across the width of the fiber where it rolls over the side of the bundle and cut off the excess.
13. Using a small amount of PDMS, connect the flap to the bundle (**Figure B.2b**).

a) 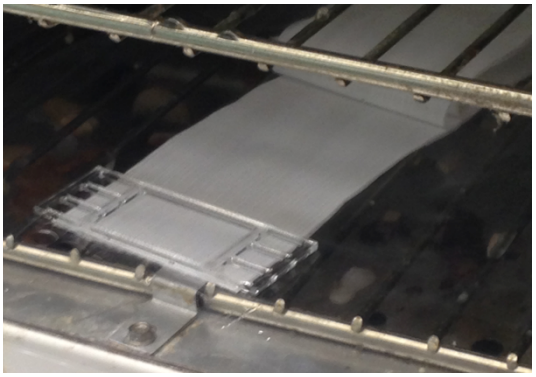 b) 

**Figure B.2**: a) fiber attached to core, b) final bundle

14. Place the rolled fiber bundle in the oven and allow to cure for at least 4 hours before handing.
15. Apply PDMS liberally to each side of the fiber bundle, where the fiber will be encapsulated in potting, to connect the layers of fiber together.

16. Place the fiber bundle in the oven and allow to cure for at least 4 hours before handing.

**B. Housing Preparation**

1. MAL
    i. Cut a 2.4" length of clear polyethylene terephthalate (PETG) tube with 1.75" OD and 0.025" thickness.
    ii. Sand both cut edges of the housing using 320 grit sandpaper, ensuring all surfaces that will come into contact with the potting material are sanded.
    iii. Clean the housing using water then a small amount of isopropyl alcohol on a Kimwipe.
2. PAD
    i. Sand all surfaces of the 3-D printed housing that will come into contact with potting material, as well as the faces of the two halves that will come into contact with each other using 320 grit sand paper.
    ii. Clean the housing using water then a small amount of isopropyl alcohol on a Kimwipe.
    iii. Prime all sanded surfaces that will contact potting material with Nusil MED-163 primer according to manufacturer instructions.
    iv. Paint PDMS onto the primed surfaces of the housing.
    v. Place housing into the oven and allow to cure overnight.
    vi. Prime the faces of the two halves that will come into contact with each other with Nusil MED-163 primer according to manufacturer instructions.

vii. Paint PDMS onto the newly primed faces of the housing, making sure to avoid excessive PDMS that could contact the fiber bundle when the two halves of the housing are compressed together.

viii. Insert fiber bundle into one half of the housing.

ix. Carefully attach the two halves of the housing together to avoid PDMS contacting the fiber bundle.

x. Clamp the housing lightly with C-clamps and place the housing-fiber bundle assembly into the oven and allow to cure for at least 1 hour.

C. Potting

1. Clean all Teflon potting molds with isopropyl alcohol and dry thoroughly.
2. Secure the housing and fiber bundle into the potting molds, ensuring the core of the fiber bundle slides into the slot on the mold.
3. Tighten all nuts and bolts are adequately. Apply low strength thread-locker to all bolts that secure Teflon.
4. Insert the assembled potting fixtures into the centrifuge, and secure each to one end of the centrifuge arm.
5. Attach silicone tubing from the center potting boat to the potting molds and secure with cable ties.
6. Review the "Potting Safety Checklist" while preparing the centrifuge. Be prepared to hit the emergency stop button on the centrifuge at any time. Operate the centrifuge according to current lab safety protocols, and only operate the centrifuge

once you have been trained. See **Figure B.3** for fully assembled potting setup secured in centrifuge.

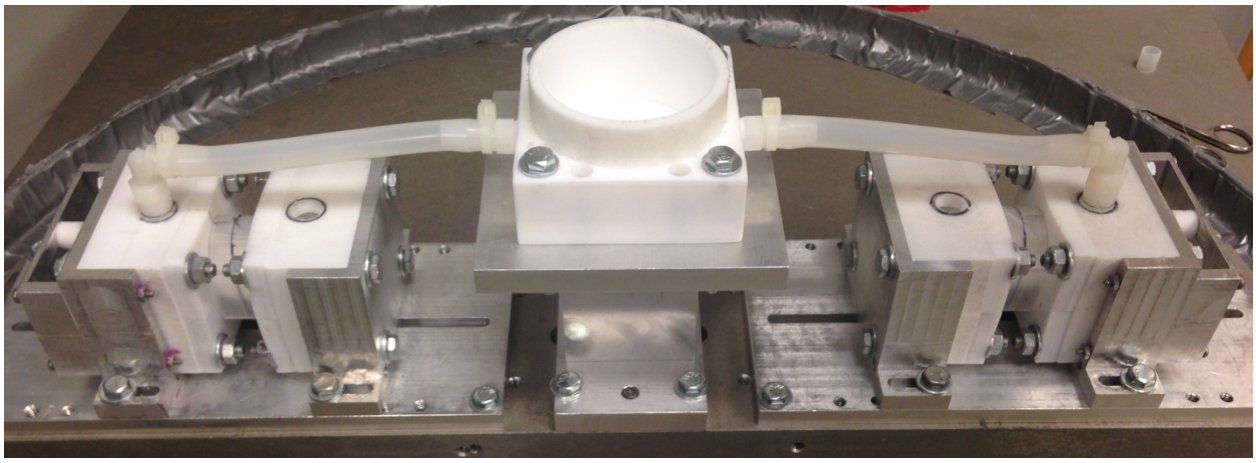

**Figure B.3**: Completed potting setup, secured in centrifuge.

7. Prepare the PDMS according to manufacturer instructions and insert into potting syringe-guns.
8. Turn on centrifuge and turn speed up to 707 rpms.
9. Slowly inject PDMS into the center of the potting boat.
10. Turn on heat gun at highest settings, monitor centrifuge temperature, and start a timer.
11. When the timer reaches 24 minutes or the temperature is 120˚F, turn down the centrifuge speed to approximately 200 rpm until the total centrifuging time reaches 1 hour while monitoring the temperature to ensure that it does not exceed 130˚F.
12. When the 1 hour centrifuge cycle is complete, allow the molds to cool for 1 hour.
13. Flip the fixtures around to pot the other side of the devices.
14. Clean out the potting boat, and remove all tubing and tubing connectors from the previously potted molds.

15. Attach new silicone tubing from the potting boat to the un-potted molds and repeat the above procedure to pot the second side of the devices.
16. Upon completion of the second round of potting, remove the fixtures from the centrifuge and insert into the oven to post cure the PDMS potting for at least a day.
17. De-mold the devices and place back into the oven to post cure for at least 2 more days.

D. Device Cutting

Follow all safety precautions and protocols when cutting, since the saw has the potential to cause injury when used improperly. Cut only according to current cutting protocols, as the cutting procedure is continuously improving and varies depending on equipment. Only senior staff members are permitted to cut devices, and they are never permitted to cut alone.

1. Plug/cover the blood inlet and outlet conduits.
2. Insert the device into the cutting fixture and secure properly.
3. Follow current lab cutting safety protocols.
4. Cut a thin slice of potting material away with the saw.
5. Repeat cuts until you have approximately 3/8 of an inch of potting material remaining.
6. Flip the device around and repeat the above procedure.
7. Remove from the device from the cutting fixture.
8. Inspect the last slice from each side of device by holding the slice up to the light to ensure the lumen of the fibers are not plugged with potting material.
9. If plugging exists, cut further slices from the device and check again.

E. Leak Testing the Potted Silicone

1. Fill the device with deionized water.
2. Attach tubing to the inlet and outlet blood conduits.
3. Attach a barbed tubing connector with a side luer to each tube.
4. Connect another section of tubing to the other end of barbed tubing connection.
5. Fill all tubes and connectors with deionized water and clamp the terminal tubing ends with tubing clamps.
6. Attach a pressure transducer to the luer lock on one barbed tubing connection, and attach a syringe filled with deionized water to the luer lock on the other barbed tubing connection.
7. Inject fluid with the syringe to pressurize the device to 60 mmHg.
8. Inspect the potted regions for leaks.
9. If there are leaks, mark them for patching with a fine tipped permanent marker.
10. Empty the device and dry it with filtered air for at least 8 hours.
11. Apply a small dot of PDMS to the marked leaks using a blunt applicator needle.
12. Place the device in the oven for at least one day to cure.
13. Repeat the above procedure until the device is leak free.

F. Gas Cap Attachment

1. Clean the gas caps with water.
2. Slide the gas cap onto the cut potting end of the device.
3. Apply a thick layer of silicone RTV gasket maker.
4. Force the silicone RTV into any gaps using a gloved finger, and smooth the silicone RTV out.

5. Allow the silicone RTV to dry in the fume hood according to manufacturer instructions.

G. Gas Cap Leak Testing

1. Attach tubing to the blood inlet and outlet conduits, and clamp these off with tubing clamps.
2. Attach tubing to the gas inlet and outlets on the gas caps.
3. Flow oxygen through the gas inlet at a rate of at least 3 L/min.
4. Submerge the device in a bucket of water while making sure that the gas outlet tube does not kink.
5. Inspect the seams between the gas caps and the housing for air leaks.
6. If there is a leak, mark it with a permanent marker for later patching.
7. Dry the device thoroughly before patching.
8. Force silicone RTV into any leaking areas with a glove finger.
9. Allow the silicone RTV to cure in the fume hood per manufacturer instructions.
10. Repeat the above procedure until no leaks are present.
11. The device is now ready for *in vitro* testing. However, the blood contacting surfaces should be rinsed with deionized water for a day before *in vivo* use. See **Figure B.4** for a completed MAL and PAD.

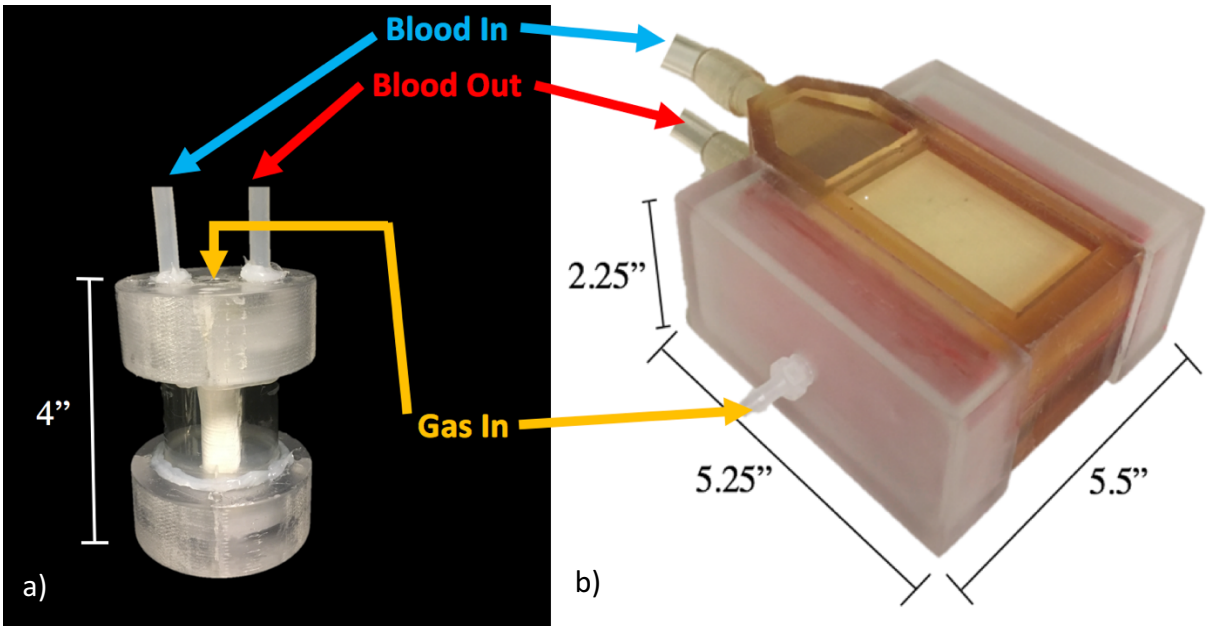


**Figure B.4**: a) Completed MAL, b) Completed PAD.